AN ABSTRACT OF THE THESIS OF

Thomas Holbeck Thomas (Name of student) for the Master of Science (Degree)

in Geology (Major) presented on February 2, 1981 (Date)

Title: GEOLOGY AND MINERAL DEPOSITS OF THE COYOTE HILLS MINING DISTRICT, LAKE COUNTY, OREGON

ABSTRACT APPROVED: Cyrus W. Field

The Coyote Hills are located about 46 kilometers north-northwest of Lakeview, Oregon, within the Basin and Range physiographic province. These hills represent a complex volcanic center of bimodal calc-alkaline igneous activity.

The oldest rocks recorded in the Tertiary succession are hornblende-bearing andesite and aphanitic basalt flows, laharic breccias, conglomerates, tuffaceous sandstones, and lithic wackes of the late Eocene to early Oligocene Lower Andesite formation. During middle to early late Oligocene time, voluminous eruptions of predominately basaltic andesite formed a large shield volcano. This unit, the Upper Basalt formation, was followed, after a short hiatus, by the Coyote Hills rhyolite of late Oligocene to early Miocene age. The Coyote Hills rhyolite represents a complex spectrum of multi-phase silicic volcanism and comagmatic near-surface plutonism. Magma compositions varied from dacite to rhyolite and include lava flows, volcanic plugs, a flow dome complex, and a hypabyssal quartz monzo-

nite intrusion. Volcanic activity that post-dates formation of the bimodal Coyote Hills complex culminated with the lower slopes of the shield volcano onlapped by the middle Miocene Steens Basalt, the late middle to early late Miocene Plush tuff, and the late Miocene to early Pliocene Upper basalt.

A prominent northwest and northeast-trending fault and fracture system formed after emplacement of the Coyote Hills rhyolite, and as early as late Oligocene to early Miocene in time. Basin and Range faults post-date the Steens Basalt and have caused some minor displacement of the younger rocks.

Penecontemporaneous with silicic volcanism of the Coyote Hills rhyolite was a period of hydrothermal activity. Fluids ascended favorable structures, altered the surrounding country rocks, and deposited minor quantities of epithermal gold-silver-copper-mercury-molybdenum(?)-lead(?), and zinc(?) in structurally controlled quartz-pyrite veinlets and as disseminations. Because of the association of mineralization with silicic volcanics in time and space, it is concluded that the two processes were genetically related.

The hydrothermal system in the Coyote Hills is related to the late stages of silicic volcanism. Evidence for a genetic relation includes the close association of rock type, and chemical and mineral zonations within the district. Geological and geochemical evidence that includes rock type and alteration patterns, and mineral and trace element zonations, collectively suggest that only the highest level of the hydrothermal system has been exposed. It is entirely possible that a large vein or disseminated-type deposit containing

both base and precious metals is present at depth.

Geology and Mineral Deposits of the Coyote Hills Mining District, Lake County, Oregon

by

Thomas Holbeck Thomas

A THESIS

submitted to

Oregon State University

in partial fulfillment of
the requirements for the
degree of

Master of Science

June 1981

Approved:

Redacted for Privacy

Professor of Geology in charge of major

Redacted for Privacy

Chairman of the Department of Geology

Redacted for Privacy

Dean of Graduate School

Date thesis is presented February 2, 1981

Typed by Sonja Cox for Thomas Holbeck Thomas

ACKNOWLEDGMENTS

The writer wishes to express his sincere appreciation to his major professor, Cyrus W. Field, for suggesting the thesis area, for his encouragement, guidance, and especially patience, and for critically reading the manuscript. Thanks are also extended to professors William H. Taubeneck, Edward M. Taylor, and Harold E. Enlows for helpful discussions.

The Bureau of Land Management is acknowledged for financial assistance, providing support during the field investigation and funding for major oxide and trace element analysis, and thin section preparation.

Thanks are extended to Western Nuclear, Inc. and Callahan Mining Corp. for allowing time on the job to complete the writing of this thesis.

Finally, the writer is indebted to his father, Bruce R. Thomas, for allowing the use of his pickup truck during the field season of 1977.

TABLE OF CONTENTS

LIST OF FIGURES

LIST OF TABLES

GEOLOGY AND MINERAL DEPOSITS OF THE COYOTE HILLS MINING DISTRICT LAKE COUNTY, OREGON

INTRODUCTION

The Coyote Hills are approximately 81 kilometers by road north-northeast of Lakeview (pop. 2820), the county seat of Lake County (pop. 6450) in south-central Oregon (Figure 1). The thesis area consists of 228 square kilometers in secs. 25-26 & 35-36, T.34S., R.22E.; secs. 25-36, T.34S., R.23E.; sec. 28-33, T.34S., R.24E.; the eastern one-third T.35S., R.22E.; and the western one-half T.35S., R.24E., Willamette Base and Meridian. The area is readily accessible by driving 9.7 kilometers north from Lakeview on U.S. 395; then east via State 140 for 24 kilometers; then north for 31 kilometers on a county secondary road to the hamlet of Plush; and then 16 kilometers further north on the gravel Hogback Road. Local access is attained by a network of unimproved dirt roads and primitive jeep trails maintained, in part, by the U.S. Bureau of Land Management. Road travel is generally restricted to four-wheel drive vehicles.

Topography and Exposure

The Coyote Hills are within the Basin and Range physiographic province of Oregon (Figure 2). In Oregon, this province is characterized by Tertiary volcanics that have been intricately off-set by three prominent fault sets. The dominant set trends northwest, whereas the subordinate sets trend north and northeast. This structural pattern, coupled with the relatively youthful age of the province, has resulted

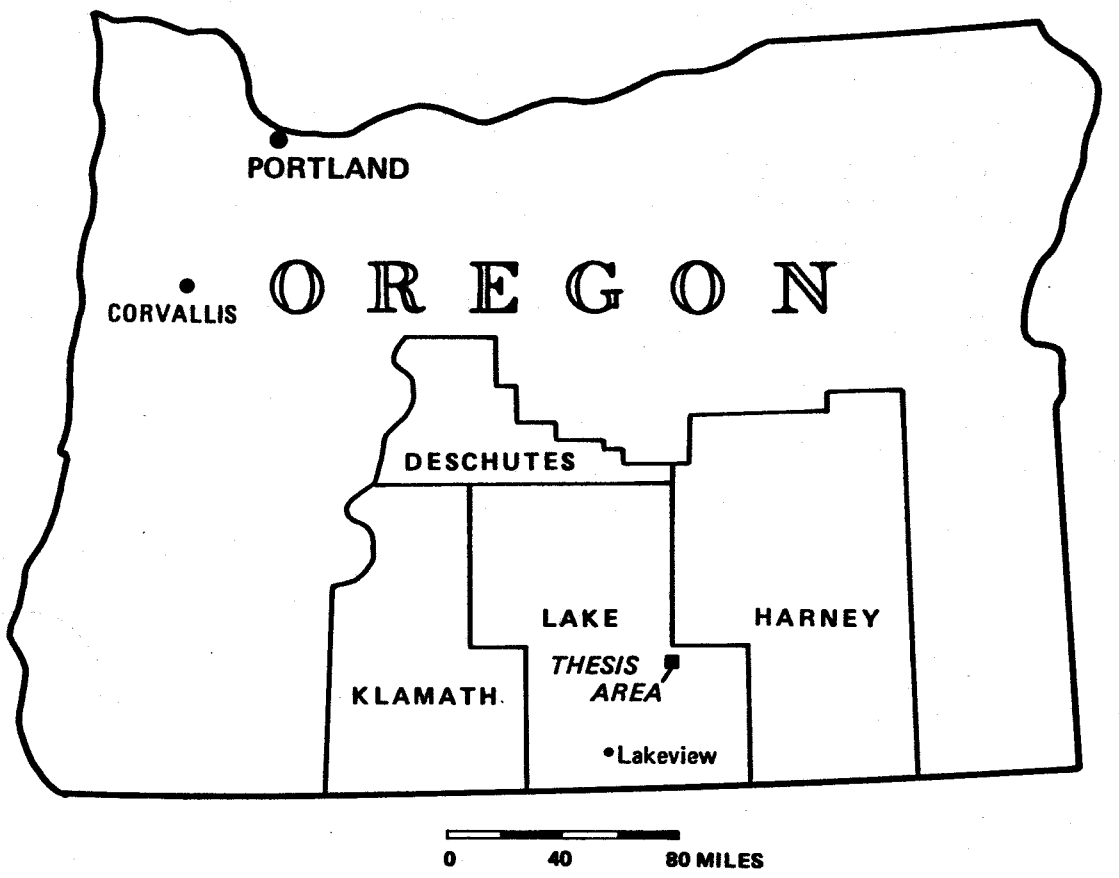

FIGURE 1. Index map of the Coyote Hills area, Oregon.

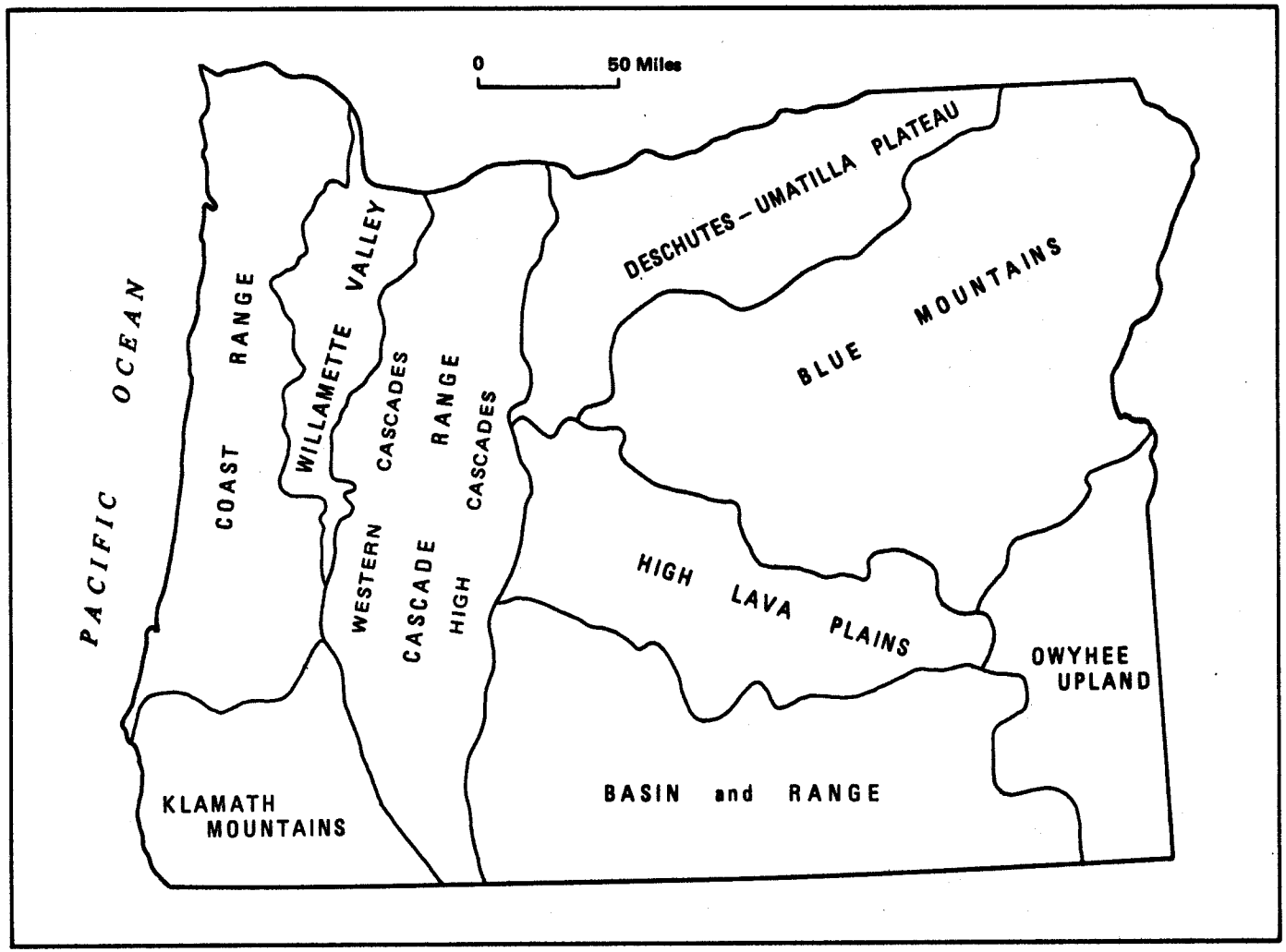

FIGURE 2. Physiographic divisions of Oregon (after Dicken, 1965).

in the formation of a largely undissected terrain consisting of elongate north-trending fault-block mountains and basins.

The Coyote Hills are on the North Warner Mountain block, a land surface that slopes gently to the east and northeast. This block is bounded on the west by Abert Rim, a precipitous scarp of about 640 meters, and on the east by Warner Valley.

Maximum elevation in the Coyote Hills is 2084 meters in sec. 9, T.35S., R.23E., whereas the minimum is about 1372 meters along the Hogback Road. Locally, the structurally modified radial drainage has resulted in numerous draws and valleys providing adequate exposures with approximately 712 meters of relief.

Climate and Vegetation

The climate of south-central Oregon is semi-arid. This climate results primarily from the rain shadow effect of the Cascade Mountains (Patton, 1976). These barrier mountains hinder eastward migration of the Pacific maritime air masses, and thus weaken their moderating influences east of the Cascade Range. The resulting climate is characterized by a wide range in diurnal and seasonal temperatures, moderate to low rainfall, and low humidity. Average January temperatures are below freezing, whereas July averages range from 15° to 20° celsius, depending on the altitude. Annual precipitation east of the Cascade Mountains averages only 25 to 50 centimeters. This precipitation is not entirely seasonal as 55 to 75 percent falls between October 1 and March 1. Furthermore, a high proportion of the annual precipitation falls as snow. As a result, most streams are ephemeral, whereas the numerous internally drained basins often contain shallow pluvial

Figure 3. Warner Valley, looking southeast from the south flank of the Coyote Hills.

saline lakes. The following table exemplifies the climatic conditions of the Hart Mountain weather station located about 117 kilometers northeast of the Coyote Hills.

Table 1. Climatic data for the Hart Mountain and Coyote Hills regions of southeast Oregon

	Elevation (m.)	Location		Ave. Temp. (°C.)		Ave. Pp. (cm.)	
				Jan.	July	Jan.	July
Hart Mt.	1712	lat.:	43°33'	-1.85	17.9	2.54	0.99
		long. :	119°39'				
Coyote Hills	1718*	lat.:	42°33'				
		long.:	120°00'				

* Average elevation
Data for period 1967 - 1976, from Climatological Data, U. S. Dept. of Commerce, National Oceanic and Atmospheric Administration, Environmental Data Service Annual Summary

The vegetation in the Coyote Hills is characteristic of that found in the shrub-steppe environments as described by Franklin and Dyrness (1973). For the most part, the vegetation is dominated by various types of sagebrush, Artesmesia tridentata and A. arbuscula, rabbitbrush, Chrysothamnus nauseous, and several varieties of bunchgrasses. Locally, near springs and perennial streams and especially in the southwest quarter of the Coyote Hills, greater Western Junipers, Juniperous occidentails, are present.

Previous Work

A moderate amount of general and reconnaissance geologic information is available for the area of study and the surrounding region. The earliest report that describes the general geology of south-central Oregon are those of I. C. Russell (1884). In his pioneering reconnaissance of the Quaternary geology of the northwest Great Basin he described the general features of south-central Oregon as follows:

> "The desert portion of southern Oregon has the same general type of mountain topography as gives character to the greater part of the entire area of interior drainage, and has the Basin Range type of mountain structure even more clearly defined than in Nevada and Utah. The great fault-scarps forming the mountain faces in many instances nearly vertical walls, hundreds of feet in height, of such recent date that they have scarcely been notched by erosion, and have but small, if any, alluvial cones at their bases.
>
> Here, as in all the area of the Great Basin thus far explored, the structural elements are long and narrow orographic blocks, bounded by profound faults. The mountains are sculptured from the unpraised edges of the tilted blocks, while the valleys and plains occupy the depressed portions, which have been deeply buried beneath alluvium and lake sediments. The ranges are bold serrate ridges, trending approximately north and south, with one face presenting an abrupt palisade, while the opposite slope conforms with the dip of the beds, and is comparatively gentle in its inclination. The desert plains, separating the narrow mountain ridges, are frequently white with drifting alkalies, or are occupied by shallow alkaline lakes or absolutely barren playas."

This original work was later amplified and extended by I. C. Russell (1903a and 1903b) and Waring (1908 and 1909) in their geologic and hydrologic investigations of the region. Waring (1908) constructed the first topographic and geologic maps for much of south-central Oregon. Other important early contributions to the stratigraphy of the region were made by Russell (1928) in the Warner Mountains of northeast

California, and by Fuller (1931) for the Steens Mountain of southeast Oregon.

Fuller and Waters (1929) summarized the geologic structure of south-central Oregon based on their investigations of Steens Mountain. More recent contributions to the interpretation and origin of Basin and Range structure in Oregon have been made by Donath (1962), Larson (1965), and Lawrence (1976).

Walker (1963) and Walker and Repenning (1965), under the auspices of the U.S. Geological Survey and in cooperation with the State of Oregon, Department of Geology, have completed some of the most recent geologic reconnaissance mapping in much of southern Oregon east of the Cascade Mountains. The Geologic Map of Oregon East of the 121st Meridian (1:500,000) by Walker (1977) is the most up-to-date map of the region.

Paleomagnetic studies of the mid-Miocene flood basalts in this region have been conducted by Watkins (1963, 1964, & 1965), and Watkins and Larsen (1966). The magnetostratigraphy of the flood basalts has been summarized by Watkins and Baksi (1974).

Investigations by Peterson (1959), Brooks (1963), and Peterson and McIntyre (1970) provide an excellent source of background information concerning the economic potential of this area.

Recent thesis work in areas near the Coyote Hills include a reconnaissance study of the structure, stratigraphy, and paleomagnetics of the Plush area by Larson (1965) and a detailed investigation of the Drake Peak rhyolite complex by Wells (1975).

Purpose

The purpose of this investigation is to provide a better geologic understanding of the Coyote Hills. Particular emphasis was given to the stratigraphy and structural relations within the area, petrography of the volcanic rocks, and to the type, extent, and controls of mineralization and alteration.

Methods of Investigation

Approximately seven weeks were spent in the field during the summer of 1977. The thesis area was mapped at a scale of 1:24,000 on appropriate sections of the Plush, Rabbit Hills SW, Cooper Draw, and Drake Peak NE $7\frac{1}{2}$ minute topographic quadrangle maps. Aerial photographs with scales of 1:24,000, and approximately 1:35,400 were utilized as an aid in the mapping processes. Lithologies, structure, alteration, and mineralization were mapped in as much detail as the map scale would permit.

A suite of approximately 400 rocks were collected in the field, of which 50 were subsequently examined petrographically in the laboratory. Modal analysis of 20 representative rock samples were obtained from the study of thin sections utilizing a mechanical stage and point counter; 500 points were counted per slide. Plagioclase feldspar compositions were determined by both the Michel-Levy method and by the combined carlsbad-albite twin method where applicable. Plagioclase microlite compositions were determined using the microlite method.

Twenty selected rock samples were petrochemically analyzed for major oxide components. X-ray fluorescence spectrometry was employed to determine the values for Al_2O_3, FeO, TiO_2, CaO, and K_2O, whereas

those of MgO and Na_2O were determined by atomic absorption spectrophotometry. SiO_2 was determined by both x-ray fluorescence and visible light spectrometry. Total ferric and ferrous iron was recorded as FeO. The analyses were performed on polished buttons fused from pulverized rock samples. Thus, H_2O determinations were not made. All analytical determinations for the major oxides were undertaken at Oregon State University by Dr. E. M. Taylor and R. L. Lightfoot of the Department of Geology, Oregon State University.

The 80 mesh fractions of 18 rock and 45 soil samples were analyzed for trace element concentrations of Cu, Mo, Pb, An, Au, Ag, and Hg. All trace element analyses were performed by Chemical and Mineralogical Services, Salt Lake City, Utah.

Nomenclature

Nomenclature and classification systems either used and/or discussed by the following authors was, unless otherwise stated, adhered to in this thesis. The volcanic rocks were classified primarily on the basis of percent SiO_2 (Nockolds, 1954; Taylor, 1978, personal communication), percent SiO_2 versus percent K_2O (Mackenzie and Chappell, 1972), and secondarily on the mineralogical classification of Streckeisen (1967, in Hyndman, 1972, p. 35). Textural descriptions were based on those described by Jackson (1970). Volcaniclasitc nomenclature was based on classifications by Fisher (1961 & 1966). Color descriptions of all rock samples both fresh and weathered, were described according to the Rock Color Chart published by the Geological Society of American (1970).

GEOLOGIC AND TECTONIC SETTING

Stratigraphy

The Basin and Range Province of Oregon is characterized by great thicknesses of volcanic flows and pyroclastic rocks of middle to late Tertiary age. Little is known concerning the pre-Tertiary basement throughout the province except for a small window of Mesozoic and older rocks that crop out in the Pueblo and Trout Creek Mountains of southeast Oregon. Pre-Tertiary rocks are not exposed in other localities in south central Oregon by the major range faults, nor have they been penetrated by exploratory wells as much as 3.66 kilometers in depth. This is unusual in that all the major divisions of geologic time are represented by rocks in the Basin and Range province to the south as in Nevada (Nolan, 1943).

The oldest Tertiary rocks in the province include deformed flows of dacite and andesite, breccias, and some interbedded tuffaceous sedimentary rocks of pre middle Oligocene age. Locally, these rocks are unconformably overlain by rhyolitic tuffs and tuffaceous sedimentary rocks that contain vertebrate fossils of late Oligocene or early Miocene age (Walker, 1969b). These volcanics have been intruded by a small plutonic complex in the Paisley Hills that has been radiometrically dated at 33 m.y. (Muntzert and Field, 1969).

During middle (?) and late Miocene time, flood basalts and some andesite flows blanketed much of the province. In the eastern half of the province the name Steens Basalt (Fuller, 1931) has been applied to this sequence of flows. The flood basalts have been dated at about

15 m.y. (Baksi et al., 1967) and correlated with the middle to lower Yakima Basalts of the Columbia River Plateau (Watkins and Baksi, 1974). High alumnia basalt appears to be the dominant petrochemical type in the sequence, although alkali olivine basalt flows are also common (Walker, 1963). In the western half of the province unnamed but similar basalts have been correlated with the Steens Basalt on the basis of lithology and stratigraphic position. These flood basalts emerged as fissure eruptions localized primarily along faults.

During late Miocene time the flood basalts were overlain, for the most part, by ash-flow tuffs and tuffaceous flood plain deposits that locally interfinger with the basalts. Radiometric dating of the upper flows of the flood basalts and paleontological dating of the tuffaceous deposits indicates an age of 13 to 15 m.y. (Walker, 1969a).

Late Miocene or early Pliocene flows of olivine basalt overlie the Miocene tuffaceous rocks and commonly cap many of the fault blocks. The source areas for these flows have been traced to cinder and lava cones, shield volcanoes, and fissures (Peterson and McIntyre, 1970).

Ash-flow tuffs of Pliocene age 3.6 to 9.7 m.y., blanket large segments of the province north of Lake Abert and Warner and Catlow Valleys. These tuffs were extruded from fissures in the Brothers Fault zone (Green et al., 1972) and have been correlated as southward extensions of the Danforth Formation (Piper et al., 1939).

Large centers of silicic volcanic rocks containing domes, flows, and ash-flow tuffs of Miocene to Holocene age (MacLeod et al., 1975) are widely distributed throughout the province and adjacent areas. The domal centers are principally in two broad linear belts that

that trend about N.50° to 80°W. The northern belt is in the High Lava Plains and Owyhee Uplands and corresponds to the trend of the Brothers Fault Zone, whereas the southern belt is in the Basin and Range Province and roughly corresponds to the trend of the Eugene-Denio Fault Zone.

During Pleistocene time volcanic activity was restricted to small basaltic eruptions related to cinder cone activity in the Klamath and Fort Rock basins. Glaciation during Pleistocene time modified the morphology of the province by producing cirques, moraines, and glacial striations on such peaks as Steens Mountain (Bentley, 1974), Gearhart Mountain (Crandall, 1965), and Drakes Peak (Wells, 1975). The more humid conditions relating to the Pleistocene glacial stages resulted in the formation of large pluvial lakes that filled structural basins such as Warner Valley, and Goose Lake Basin. Shoreline features, including wave-built terraces, wave-cut benches, and gravel bars, a few tens of meters above the present valley floors, characterize the maximum depth reached by these Pleistocene glacial lakes.

Structure

Differential high-angle block faults resulting in tilted horsts with intervening grabens form the principal structure in south-central Oregon. This horst and graben structure is characteristic of the Basin and Range physiographic province that extends over Nevada, and parts of California, Idaho, Oregon, New Mexico, and Utah. Within Oregon, the Basin and Range Province is bounded on the north by the

High Lava Plains, on the west by the High Cascade Subprovince, and on the east by the Owyhee Uplands. The principal faults, along which several hundreds of meters of dip-slip movement has occurred, generally trend slightly east of north and divide the area into a series of structurally delineated blocks that consist of alternating elongate basins and ranges. Seven prominent structural basins and numerous minor ones are present within this province. The major tectonic depressions, from west to east, are the Klamath, Goose Lake Valley, the composite Summer Lake-Abert Lake, Warner Valley, Guano Valley, Catlow Valley, and the Alvord grabens. Visible displacement on the major fault blocks ranges from a maximum of about 1.7 kilometers (Fuller, 1931) on Steens Mountain, through 0.6-0.9 kilometers for such blocks as Abert Rim, Hart Mountain, and Poker Jim Ridge, to several tens of meters for the smaller faults. The valleys or grabens are characterized by internal drainage and are variably filled with alluvial and lacustrine material. Estimates by Larson (1965) and geophysical investigations by Travis and Gettings (1974) indicate the valley fill to be several hundreds of meters to two kilometers in thickness.

Two major fault systems are present within south central Oregon. One of the two major systems is comprised of a rhombold conjugate set of faults. The dominate set strikes N.20° to 50°W. and the other N.20° to 40°E. (Donath, 1962; Larson, 1965; Lawrence, 1976). These faults are characterized by relatively minor dip-slip movement in the range of a few tens of meters (Larson, 1965; Peterson and McIntyre, 1970) along high-angle scarps, close en echelon spacing, consistency

in the strike pattern, and short lengths of approximately 10 kilometers or less. The members of each fault set are remarkably subparallel. However, faults of the northwest set extend over longer distances than do those on the northeast set, which also are fewer in number and tend to be more widely separated. Because each set is either offset (Donath, 1962) or terminated (Larson, 1965) by the other, it is assumed that both sets formed essentially contemporaneously.

Included within this first category of faults are four major right-lateral en echleon strike slip fault zones trending N.50° to 60°W. with about 10 to 20 kilometers of displacement separating blocks broken by normal faults. These zones form the transition between the main Basin and Range Province of Nevada and the largely unfaulted Columbia River Plateau of north-central Oregon. The four zones, from south to north, are the McLoughlin, Eugene-Denio, Brothers, and Vale Fault zones (Lawrence, 1976).

The second of the two major fault systems consists of range faults that trend in a north to north-northeast direction (Larson, 1965; Peterson and McIntyre, 1970). The major range blocks or horsts have been tilted as a consequence of differential movement along these bounding range faults. Characteristically, the range faults exhibit irregular but continuous traces that extend over distances of greater than 10 kilometers, lack conspicuous en echelon arrangements, and have large dip-slip movements measured in hundreds of meters. Minimum displacements of about 1677, 915, 610, and 183 meters have been measured at Steens Mountain, Hart Mountain, Surprise Valley, and West Guano Valley, respectively.

Investigations, by Donath (1962), Larson (1965), Peterson and McIntyre (1970) in Oregon, and Zoback and Thompson (1978) in Nevada, have shown that movement along the rhomboid conjugate fault set commenced by late Miocene to early Pliocene time and ceased, for the most part, by early Pleistocene time with some minor movement probably continuing to early Holocene time. The earliest movement along the range faults occurred in post-late middle Pliocene to early Pleistocene time.

Seismic and historical records indicate that few earthquakes have occurred in the Basin and Range Province of Oregon during the last 150 years. Throughout the period 1841 to 1958 (Berg and Baker, 1963), 16 earthquakes have been recorded in this region with assigned intensities of II to VI on the Modified Mercalli scale. In 1968, 13 earthquakes, with focal depths averaging 20 to 25 kilometers, occurred in Warner Valley near Plush (Couch and Johnson, 1968). The magnitude of the largest earthquake was 5.1 on the Richter scale. First motion studies for eight of the quakes indicated north-south normal movement. However, strike-slip motion with a dip-slip component was indicated for two of the earthquakes. Solutions for the strike-slip faults indicated either right-lateral displacement of N.80^{o}W. or left-lateral displacement of N.10^{o}E. The former solution is consistent with the right-lateral movement proposed by Lawrence (1976) for the Eugene-Denio fault trend.

Folds in the Basin and Range Province of Oregon are restricted to minor structures locally associated with intrusive domes and major faults (Larson, 1965).

Tectonic Setting

The Basin and Range Province in Oregon is located within the Columbia Arc (Taubeneck, 1966) section of the Nevadan Orogenic Belt (Blackwelder, 1914) of middle to late Jurassic age (Lanphere et al., 1968) (Figure 4). This arc is characterized by a complex tectonic structure, a varied metamorphic history, and a great thickness of diverse lithologies, including both normal (calc-alkaline) and spilitic (keratophyres) volcanic flows, pyroclastic deposits, and epiclastic derivatives interbedded with shallow marine sediements (Anderson, 1930; Cook, 1954; Albers and Robertson, 1961; and Hamilton, 1963 & Hamilton and Myers, 1966). These features are indicative of an island arc-trench eugeoclinal type environment that was present throughout much of the Mesozoic Era (Hamilton, 1963; Burchfiel and Davis, 1972).

Pre-Tertiary rocks, with the exception of two small outcrops of Mesozoic rocks in southeast Oregon, are not present in the Basin and Range Province of Oregon. However, the pre-Tertiary rocks of the Columbia Arc may underlie this terrain if it is assumed that the Nevadan Orogenic Belt of southwest and northeast Oregon is continuous and underlies the extensive Cenozoic volcanic pile of this region. This inference is not accepted by Hamilton and Myers (1966), who postulated that a rift system separated the Klamath Mountains in southwest Oregon from equivalent rocks in northeast Oregon during late Miocene time.

The elongate Tertiary horst and graben structures of the Basin and Range Province are the result of east-west extension. This extension commenced in late Cenozoic time when the North American

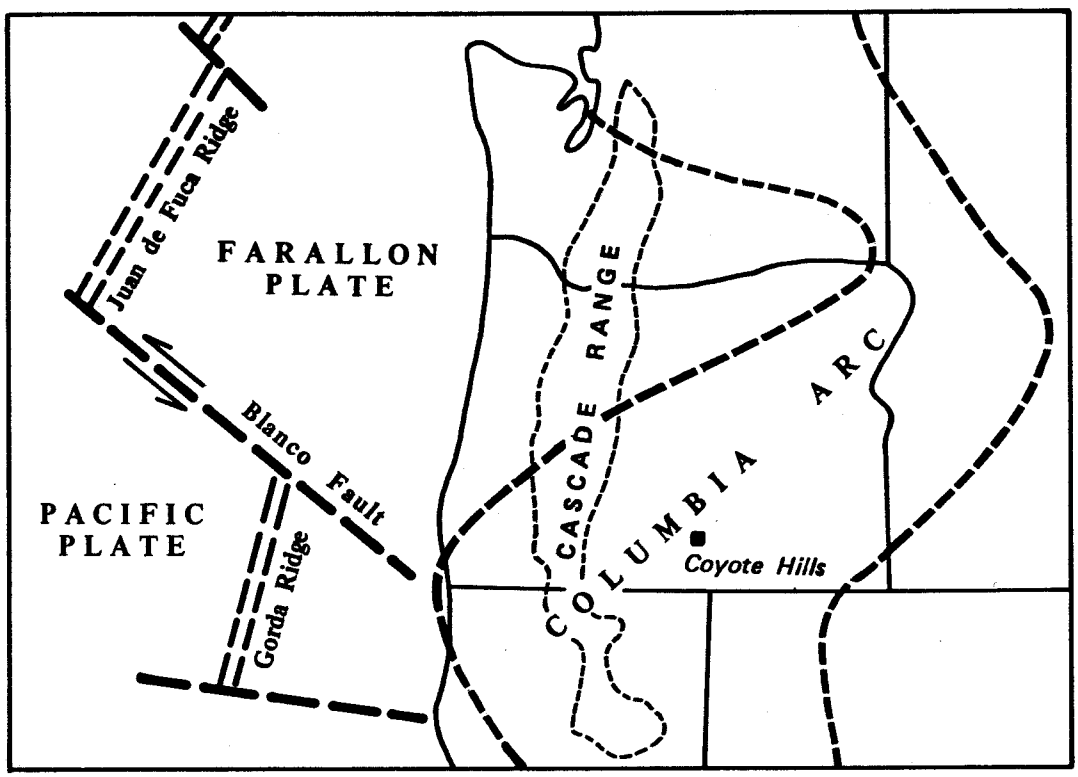

FIGURE 4. Tectonic setting of Pacific Northwest. Columbia Arc section of the Nevadan orogenic belt after Taubeneck (1966) and Burchfiel and Davis (1972); mid-oceanic ridges and transform faults after Atwater (1970); and modified after Hammit (1976).

and Pacific plates collided and thus initiated a progressive termination of subduction along western North America (Atwater, 1970; Lipman et al., 1971). Various models have been proposed for the tectonics of this province. They include those by Atwater (1970) who inferred that western North America represented a soft plate boundary responding to right-lateral shear along the San Andreas Fault, whereas Wilson (1970) and Kistler et al., (1971) proposed a center of subcrustal spreading in the province. Scholz et al., (1971) and Henyey and Lee (1976) have suggested that the Basin and Range extensional province represents an ensialic interarc basin that developed in response to the relaxation of compressional stress along the western margin of North America at the time of cessation of subduction and initiation of strike-slip faulting about 30 m.y. ago and with the contemporaneous development of a diapiric plume(s). Bimodal volcanism is characteristic of this type of orogenic regime, of which the basalts and rhyolites of the Coyote Hills may be local representatives.

STRATIGRAPHY OF THE COYOTE HILLS

Rocks in the Coyote Hills range in age from late Eocene(?) to Recent. Essentially they are all near surface to surface volcanic rocks or epiclastic derivatives (Figure 5).

The dominant geomorphic features of the Coyote Hills is a low but broad shield volcano. The rocks of this shield volcano are here informally named the Coyote Hills Foundation group. This group has been subdivided into the Lower Andesite and Upper Basalt formations. Characteristically, rocks of these two formations are radically variable, both in lateral lithologic continuity and in thickness.

Intruding and overlying this shield volcano are numerous volcanic plugs and flows of intermediate to silicic composition. These features are designated the Coyote Hills rhyolite.

Rock units younger than the Coyote Hills rhyolite primarily include flood basalts; however, lahars, tuffs, and tuffaceous sediments are present locally.

Quaternary strata are primarily comprised of alluvial, lacustrine, and eolian sediments, derived from the older formations and deposited locally.

Addendum. During the period between the initiation, and completion of this thesis the geologic time column has undergone considerable refinement. In particular, the time boundaries between the Oligocene-Miocene and Miocene-Pliocene Epochs have been redefined as 22 from 26 and 5 from 12 m.y. respectively. A consequence of this refinement necessitates an alteration to the time designations of

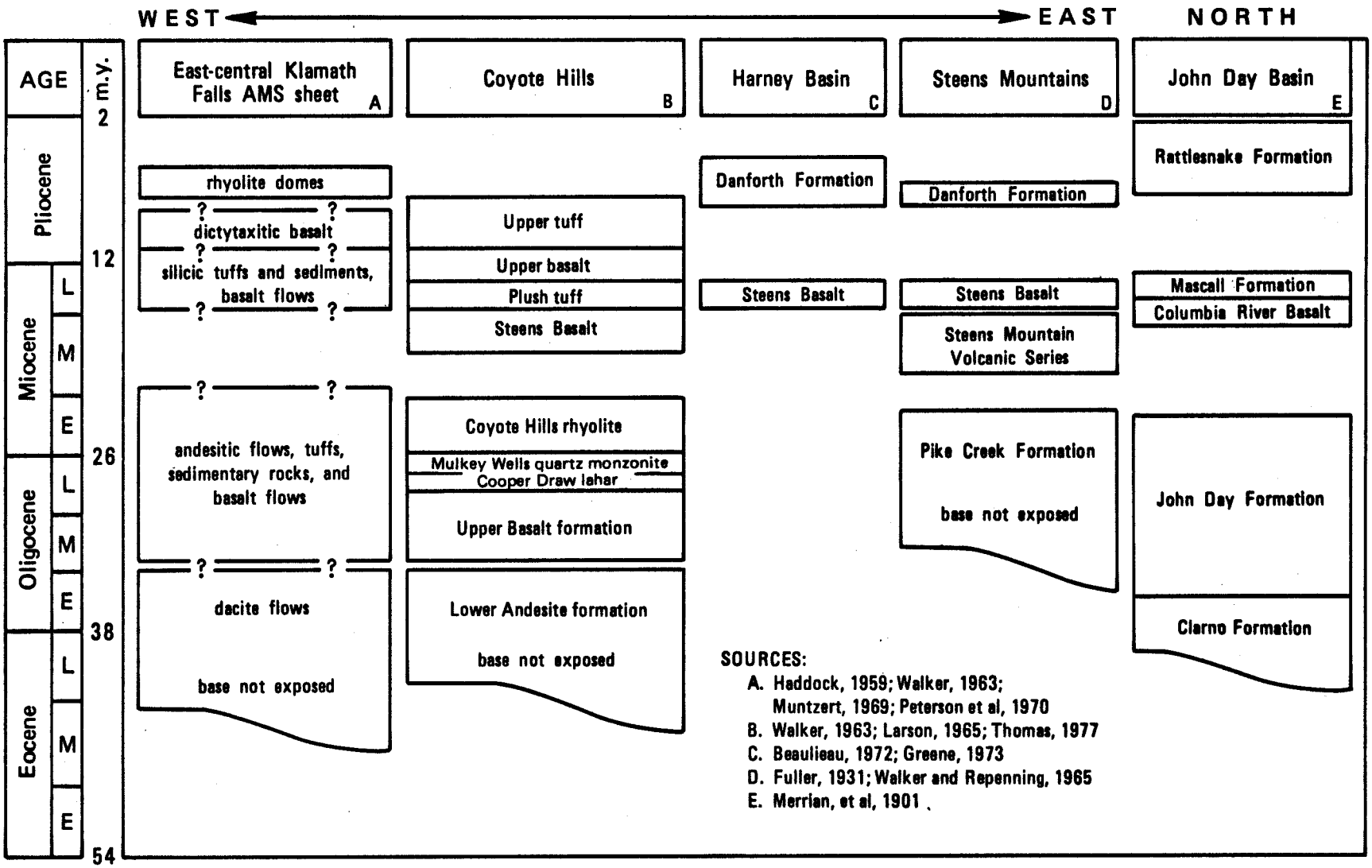

Figure 5. Correlation chart of central and south-central Oregon (Vertical dimensions indicates time rather than thickness).

the rock units in the Coyote Hills. Particular attention should be made by the reader to note these changes as they are not made in the text of the thesis.

The Coyote Hills rhyolite and the Steens Basalt previously considered to be upper Oligocene to lower Miocene, and middle to late middle Miocene, respectively, are now more correctly early late Oligocene, and late early to early middle Miocene in age. All other modifications in the time designations can readily be tied into this new scheme using the above two transformations.

COYOTE HILLS FOUNDATION GROUP

The foundation group includes, for the purpose of this discussion, those formations which form the erosional remnants of a large shield volcano of late Eocene to early Miocene age. Exposure of these formations varies from moderate to good and constitutes approximately 95 percent of the Coyote Hills stratigraphic sequence.

The foundation group consists primarily of flow rocks with subordinate amounts of breccia, tuffs, lahars, and other epiclastic derivatives. The composition of the rocks varies from basalt to andesite. Individual members of this volcanic sequence characteristically exhibit variations in thickness, lateral continuity, and mineralogical composition and thus possess little stratigraphic significance. Consequently, these mapped formations commonly consist of lithologic assemblages having considerable variability.

The foundation group has been subdivided into two formations and have been informally named the Lower Andesite formation and the Upper Basalt formation. The Lower Andesite formation consists primarily of andesite flows and volcaniclastic rocks of similar composition. The overlying Upper Basalt formation consists primarily of basalt flows, flow breccia, and epiclastic derivatives.

Lower Andesite Formation

Rocks of the Lower Andesite formation crop out along the inner margin of the remnant shield volcano. As such, this formation represents the oldest rocks that crop out in the Coyote Hills. They

typically form subdued slopes, of which the best exposures are found at the junction of Windy Hollow and an unnamed draw in sec. 6, T.35S., R.23E. (Figure 6).

The lowest exposed strata of this sequence include an undifferentiated series of rocks primarily of andesitic character. These include volcaniclastic lithic wackes, tuffaceous sandstones, pebble to boulder conglomerates, and laharic breccias. Intercalated within these strata are a few aphanitic basalt flows. Overlying this predominately volcaniclastic sedimentary sequence and locally interfingering with it are hornblende-bearing andesite flows.

Color variations of the sedimentary members are limited and range from grayish red (5R 4/2), to very light and light gray (N8, N7), to medium gray (N5). Grain size of these volcaniclastic rocks varies from 0.3 to about 25 cm. The thin basalt flows vary in color from dark reddish brown (10R 3/4) to medium dark black (N4), and typically are aphanitic. The andesite flows grade in color from grayish red (5R 4/2) to light brownish gray (5YR 6/1), and normally are porphyritic.

Lithology and Petrology

The conglomerate and laharic members of the Lower Andesite formation contain subangular to subrounded clasts of dark to medium gray andesite of varied texture. The clasts range in size from a few centimeters to 25 cm. in a matrix of argillaceous to tuffaceous material. Individual beds, 2 to 3 meters thick, are poorly sorted and graded. However, grading is better developed in the conglomerate beds. Interstratified within these members are thin light gray

Figure 6. Typical outcrop of the Lower Andesite formation.

lithic wackes. The primary constituents of the wackes are plagioclase feldspar, hornblende, and subangular lithic fragments varying in size from 0.3 to 1.3 cm. The intercalated basalt flows are thin, usually less than 1.5 meters, and are characterized by dark reddish brown top and bottom rubble zones, and medium dark black central massive sections containing a few flow-aligned feldspar phenocrysts. Overlying, and partly interfingering with the above members, are predominately grayish red hornblende-bearing andesites. These flows range from 3 to 4.5 meters in thickness.

Petrographic examination of a representative clast from a laharic member indicates that it is a hornblende-bearing andesite. The clast exhibits pilotaxitic texture; thus, indicating it was originally from a flow. The primary phenocrysts are andesine (An_{40-49}), hornblende, and augite of which the latter two are numerically subordinate.

Examination of a selected sample from the andesite flows indicates that it is relatively unaltered, fine to medium grained, and seriate porphyritic. The plagioclase microlites and phenocrysts are both andesine with compositions of An_{40-45} and An_{34-38}, respectively. The phenocrysts, none larger than 2 mm, consitute 30 percent of the rock. They are moderately aligned and include andesine (79.6%), hornblende (7.2%), augite (4.6%), hypersthene (2.6%), and magnetite (5.9%). The cores of the normally zoned crystals of plagioclase feldspare are commonly altered to dustings of clay, calcite, and rarely white mica. The rims of the hornblende phenocrysts are altered to chlorite, magnetite, and pyroxene.

Stratigraphic Relationship and Thickness

The lower contact does not crop out, thus obscuring the basal stratigraphic relations of this formation. However, the upper contact is exposed and is delineated by an angular unconformity. This unconformity separates the overlying Upper Basalt formation from the Lower Andesite formation.

These rocks have been faulted primarily by Basin and Range tectonics. This faulting, in combination with the absence of an exhumed lower contact, and the rapid lateral variation of the individual members, makes determination of the total thickness of this group impossible. Field estimates indicate a minimum thickness of about 62 meters.

Source

An andesitic provenance is indicated by the intermediate composition of the predominant flow type and of the clasts in the volcaniclastic members. The poor sorting, angularity of the clasts, variable grain size, and steep radial outward dip of the flows and beds suggest that they were deposited in close proximity to their source area(s). It is postulated that these rocks probably represent the erosional remnants of a much smaller volcanic edifice that was the precursor to the larger basaltic shield volcano.

Age and Correlation

R. J. Russell (1928), in his investigation of the Warner Range in northeastern California, described 1121 meters of andesitic agglomerate, tuffs, intercalated flows, and minor nonvolcanic sediments. Russell

named these rocks the Lower Series of the Cedarville Formation. This series has been dated at 32 m.y. (Duffield and McKee, 1974). In the Paisley Mountains, approximately 48 kilometers northwest of the Coyote Hills, rocks of a similar andesitic character are present. These rocks have been intruded by a plutonic complex radiometrically dated at 33 m.y. (Muntzert and Field, 1969). Additionally, volcanic rocks similar to those present in the Coyote Hills outcrop at Steens Mountain, the Pike Creek Formation, about 120 kilometers to the east, and at Drake Peak, about 22 kilometers south of the Coyote Hills. The Pike Creek Formation has been tentatively dated as Oligocene to early Miocene in age (Walker and Repenning, 1965). The andesitic rocks at Drake Peak have tentatvvely been dated as Oligocene an age (Wells, 1975).

Without the benefit of either a radiometric age determination or stratigraphic continuity with other known occurrences, the age of the Lower Andesite formation cannot be determined precisely. However, based on similarities in lithology and stratigraphic position with the above-mentioned formations and on the limiting age of about 26.5 m.y. (MacLeod, 1978, personal communication) for an overlying unit, the Lower Andesite formation is considered to be late Eocene to early Oligocene in age.

The Lower Andesite formation is time equivalent and probably correlative, in-part, with the Clarno and John Day Formations of central Oregon and the Lower Series of the Cedarville Formation of northeast California. These Formations are dated at 46 to 32 m.y., 36 to 32 m.y., and latest Oligocene to middle Miocene, respectively.

(Enlows and Parker, 1972; Walker et al., 1974; Russell, 1928).

Upper Basalt Formation

The Upper Basalt formation is comprised of a series of flows and flow breccia, dike swarms, and other epiclastic rocks of mafic to intermediate composition. This formation unconformably overlies the Lower Andesite formation and represents the stratigraphic bulk of the exposed shield volcano.

The most continuous and stratigraphically complete section of the basalt flows is located west of the jeep trail in sec. 6, T.35S., R.23E. (Figure 7). The topographic expression of these rocks varies from gentle to moderately steep slopes. Characteristically, the flows attain a thickness of 3 to 6 meters. The lateral thickness of individual flows varies markedly, making correlation difficult over great distances. Furthemmore, definition of specific flows is many times masked by merging interflow breccias or zones of rubble.

The basalts are massive, fine-grained, and primarily non-vesicular. The percentage of phenocrysts varies from the extremes of non-porphyritic to porphyres. These rocks are medium gray (N5) to medium dark gray (N4), and they weather to a range of colors varying from dark gray (N3) to dark greenish gray (5GY 4/1), to yellowish brown (10 YR 2/2).

The effects of weathering on these rocks are influenced both by fractures and by glass content. Where fractures are abundant, as in the thinner flows, platy colluvium is formed. Conversely, where the fracture density is less intense and (or) the glass content is high, a very uneven to semi-conchoidal surface develops on the erosional debris.

Figure 7. View northwest at a thick section of the Upper Basalt formation (left background). A portion of a dike swarm is located in the foreground.

Intercalated within this sequence of basalt flows are volcaniclastic lithic wackes of minor extent. The wackes are moderately well-graded with fragment size ranging from fine to coarse sand.

Petrology

The dominant textural types include pilotaxitic, intersertal, hyalo-ophitic, and occasionally intergranuaar. The primary phenocrysts are plagioclase feldspar (An_{55-72}), with labradorite (An_{64}) the most prevalent. The feldspars are euhedral, except where broken or where incipient resorbtion has taken place. Albite twins are most common, carlsbad twins less common, and pericline twins least common. The average length of the feldspars is 0.75 cm; however, feldspars up to 2 cm in length are found in the basalt porphyries. Microlites of plagioclase feldspar (An_{45-65}) are abundant in all sections examined, with labradorite (An_{52}) the most prevalent. Characteristically, the microlites are less than 0.5 mm in length.

Both clinopyroxene and orthopyroxene are present as phenocrysts and as groundmass crystals. Typically, euhedral to subhedral phenocrysts of augite up to 1 mm in size are found throughout the basaltic rocks. Smaller subhedral to anhedral crystals of augite are present, either interstitially or in the groundmass. Numerically subordinate crystals of hypersthene are normally present as groundmass constituents; however, a few phenocrysts are present. The textural mode of the pyroxenes is subhedral to anhedral. The few phenocrysts of hypersthene are altered to iddingsite, whereas adjacent clinopyroxenes are not. The size of the groundmass pyroxenes is normally less than

0.3 mm.

Subhedral crystals of olivine are present, but they are subordinate to those of the pyroxenes. These crystals normally are present as phenocrysts up to 1 mm in size. Most phenocrysts are altered to iddingsite, magnetite, and chlorite.

Magnetite is present as a minor consituent in the groundmass and rarely as phenocrysts. Crystal form varies from primary euhedral, to skeletal, to secondary fine-grained granular varieties.

Basaltic glass, ranging in color from brown-black to brown to red, is present in every sample. Commonly, the glass contains unidentifiable opaques.

The basaltic flow rocks are compositionally classified as basaltic andesites, as determined primarily from the optical properties of the plagioclase microlites and, secondarily from An-contents of the plagioclase phenocrysts. However, they are high aluminum basalts as deduced from the unusually large concentrations of alumina obtained from major oxide analyses of two samples (Table 2). The chemical data for these and other samples will be discussed more fully in a later section concerning petrochemistry.

Feeder Dikes

Basaltic feeder dike swarms are present in three large centers in sec. 4, T.35S., R.23E. Columnar jointing is well-developed, giving outcrops the appearance of stacked cord wood. Individual dikes are nearly vertical in attitude, cross-cut one another, and vary in width from about 1.5 to 4.6 meters (Figure 8).

Table 2

Modal Composition of Selected Rocks from the Upper Basalt Formation

Sample No.	13	71	127	210	218	144
Phenocrysts						
plagioclase	33.0	38.4	27.0	20.6	12.8	8.2
clinopyroxene	-	4.0	5.0	5.0	4.4	0.8
orthopyroxene	-	1.0	-	0.5	0.2	-
olivine	-	2.0	3.0	3.0	2.6	-
quartz	-	-	-	-	-	-
opaques	1.0	2.0	2.0	1.0	1.0	-
Groundmass						
plagioclase	20.0'	26.0	25.0'	39.0'	41.0'	46.4'
clinopyroxene	3.0'	8.6	T	5.0'	3.0'	2.0'
orthopyroxene	-	0.8	-	-	1.0'	1.0'
olivine	3.0'	2.0	T	1.0'	2.0'	-
opaques	4.0'	7.4	8.0'	9.0'	8.0'	6.4'
glass	30.0'	4.0	20.0'	15.0'	25.0'	30.0'
other	5.0'	T	1.0'	T	T	1.0'
voids	1.4'	3.8	10.0	-	-	3.8
Total	100.4	100.0	101.0	99.1	101.0	101.4

Major Element Composition of Selected Rocks from the Upper Basalt Formation

Sample No.	13	144
SiO_2	52.00	62.00
Al_2O_3	19.20	19.10
FeO	9.00	4.90
MgO	3.00	3.00
CaO	10.10	6.00
Na_2O	4.00	3.90
K_2O	0.75	2.30
TiO_2	2.15	0.45
Total	100.20	101.65

' visual estimate

Table 2 (contd.)

Sample No.	Rock Name Petrographic Determination Chemical Determination	Location/Elevation
13	porphyritic basaltic andesite high aluminum basalt	SE¼, SE¼, sec. 24, T.35., R.23E 5120 feet (1516m.)
71	porphyritic basaltic andesite --	NE¼, SW¼, sec. 8, T.35S., R.24E 5120 feet (1561m.)
127	porphyritic basaltic andesite --	SE¼, SE¼, sec. 36, T.34 S., R.22E 6640 feet (2024 m.)
210	porphyritic basaltic andesite --	NW, NW¼, sec. 30, T.35 S., R.23E. 5740 feet (1750 m.)
218	porphyritic basaltic andesite --	SE¼, SE¼, sec. 23, T.35 S., R.22E. 5600 feet (1707 m.)
144	andesite high potassium andesite	NE¼, NW¼, sec. 8, T.35 S., R.23E. 6460 feet (1969 m.)

In the field these rocks have a textural and compositional appearance of a melanodiorite or fine-grained gabbro.

The three dike swarm centers form a nealy concentric pattern approximately centered on a large volcanic neck. This neck is now preserved by a dacitic plug (refer to p. 52). The spatial relations between the dikes and the volcanic neck and the overall central location of this area with respect to the shield volcano indicates that this locale which encompasses nearly 2.6 square kilometers, represents the primary vent area for the large shield volcano that comprises the Coyote Hills.

Figure 8. Dike complex.

Stratigraphic Relationship and Thickness

The Upper Basalt formation unconformably overlies the Lower Andesite formation. This unconformity, which crops out only locally, is inferred to be represented by an irregular or undulating topography of moderate relief.

In the northwest quarter of the Coyote Hills a minimum thickness of 366 meters is indicated for the most continous section of the Upper Basalt formation.

Source

The irregularity of the flows, the large amount of flow breccia, the high glass content of the rocks, and the presence of a centrally located feeder dike system collectively indicate that the lava erupted from a local source vent(s), flowed with difficulty, and quenched quickly.

Age

Smith (1927), based on his field investigation and interpretation of Warings' (1908) work in south-central Oregon, concluded that the rocks of the Coyote Hills were of pre-flood basalt age and possibly as old as Eocene. Fuller (1931), in his report on the geology of Steens Mountain, described a sequence of pre-Steens Basalt rocks as the Upper Andesite Series, which appear from his description to be similar to those of the Upper Basalt formation. The base of the Upper Andesite Series has been dated at 21.3 m.y. (Evernden and

James, 1964).

Larson (1965), in a reconnaissance investigation of southeastern Lake County, has tentatively correlated the rocks, here informally named the Upper Basalt formation, with sections of pre-Steens Basalt which are found sporadically throughout this area. This tentative conclusion is based on stratigraphic relations, comparative petrology, and apparent age based on relative geomorphic features. Authors who disagree with this contention are Walker (1963 and 1977) and Walker and Repenning (1965). They have tentatively dated the Coyote Hills volcanics as contemporaneous with or slightly post-Steens Basalt in age; about 14 to 15 m.y. However, recent radiometric dating of a "phyric rhyolite or rhyodacite" by E.H. McKee of the U.S. Geological Survey has established a minimum age of 26.5 m.y. (Macleod, 1978, personal communication) for the Upper Basalt formation. These silicic rocks intrude and overlie both formations of the foundation group.

My field investigations revealed no evidence of a well-developed soil profile at the unconformity between the Lower Andesite formation and the Upper Basalt formation. Thus, for the Upper Basalt formation, a time bracket of about middle to early late Oligocene is established. The Upper Basalt formation is tentatively assigned an age of early late Oligocene.

COOPER DRAW LAHAR

The term lahar indicates a mudflow or landslide of broken volcanic debris; it may contain a subordinate admixture of nonvolcanic material, may be hot or of "ordinary" temperature, and may be wet or dry (Lydon, 1968).

A polylithic sequence of lahars of moderate areal extent is present in the north-central section of the Coyote Hills. Topographically, this unit forms subdued slopes and low-standing hills. Representative exposures are found along Windy Hollow in sec. 6, T.35S., R.23E. (Figure 9 and 10). This unit is here referred to and informally named the Cooper Draw lahar.

The individual lahars consist of subangular fragments of both basaltic and andesitic compositions in crudely graded to massive or nongraded beds. The subangular fragments range from cobble to boulder in size and are contained in a matrix of argillaceous ash and lapilli sized fragments. Clasts of basalt vary widely in texture, whereas those of andesite are more uniform. Distinctive varieties, such as a basalt porphyry, can be tentatively correlated with similar rocks that crop out in the surrounding areas of higher elevations.

Intercalated within this sequence of lahars, and of minor extent, are volcaniclastic lithic wackes. The wackes are moderately well-graded with fragment sizes ranging from fine to coarse sand.

Stratigraphy, Origin, and Age

The lahars unconformably overlie the flows of the Upper Basalt formation and thin rapidly northward. This sequence of lahars has a

Figure 9. Close-up of a typical lahar.

Figure 10. Low standing hill made up of a series of lahar.

minimum thickness of 46 meters.

It is inferred that the volcanic plug and related intrusive features centered in and adjacent to sec. 4, T.35S., R.23E. provided the initial generating influence or event that destabilized the area and caused this thick sequence of mud flows to form. Indirect evidence indicates that resurgence was penecontemporaneous with or slightly later than consolidation of the plug. It is postulated that positive, or possibly fluctuating pressure was maintained on this plug by the underlying parental magma chamber. Upon commencement of resurgence, this and adjacent areas became unstable and susceptible to very rapid rates of mechanical erosion. The Cooper Draw lahar that consists entirely of clasts from the Upper Basalt Group was a consequence of this resurgence and rapid erosion. This unit is inferred to represent laharic and fluvial debris that was preserved in erosional channels located along the breached side of the shield volcano. No silicic fragments were found in the individual lahars. Thus, this event is inferred to have occurred after the emplacement of the Upper Basalt formation, but before the Coyote Hills rhyolite actively breached the surface. A tentative age of late Oligocene is assigned to this unit.

MULKEY WELLS QUARTZ MONZONITE

A poorly defined hypabyssal intrusion of porphyritic quartz monzonite is in the S½ sec. 11, T.35S., R.23E. The morphological expression of this intrusion is a subdued domal-shaped hill sub-circular in plan and with dimensions of about 820 by 1060 meters. The surface of the intrusion is mantled by a cobble-sized stone field of quartz monzonite rubble and debris from the overlying volcanic rocks rather than in-place outcrop which indicates the juvenile stage of erosion for this feature. This intrusion is informally named the Mulkey Wells quartz monzonite.

Lithology and Petrology

The porphyritic quartz monzonite is fine to medium-grained and holocrystalline allotrimorphic granular. Exposures are a variegated assemblage of very light gray (N8) and light bluish gray (5B 7/1) colors that weather to a brownish gray (5YR 4/1).

Mineralogically, the quartz monzonite is comprised primarily of orthoclase feldspar (49%), quartz, (15%), plagioclase feldspar (12%), and plagioclase feldspar phenocrysts (5%). Accessory minerals include biotite (2%), augite (1%), epidote (1%), calcite (1%), pyrite (2%), magnetite (1%), and apatite and sphene (1%). In addition, miarolitic cavities are common with an abundance of about 10 percent by volume. The feldspar phenocrysts are 7 mm in length or approximately 3.5 to 7 times larger than the constituent groundmass crystals.

The compositional range for the oligolase and andesine feldspar is An_{22-28} and An_{34-38}, respectively. These crystals are subhedral,

moderately zoned, and are commonly twinned. Incipient alteration has preceeded to dustings of clay, minor white mica, epidote and calcite.

Crystals of quartz and orthoclase were probably the last minerals to crystallize as they are present interstitially as anhedra. Additionally, micrographic intergrowths of quartz and orthoclase are common. The crystals of orthoclase have been insipiently altered to dustings of clay and white mica.

Biotite and augite are subhedral to anhedral in form. They tend to be smaller in size than the plagioclase feldspars. Both ferromagnesium minerals have been altered to chlorite.

Relation to the Volcanic Rocks

"Stratigraphically" overlying and somewhat offset to the southwest of the quartz monzonite intrusion is a volcanic plug (see p. 49 for a description of this plug) of nearly identical chemistry (Table 3). Additionally, numerous nearly vertical disjointed silicic dikes with obsidian selvages are present along an arcuate ridge located above the intrusion and immediately east of the volcanic plug. The ridge itself is made up of numerous flows of silicic composition.

The close spatial proximity and chemical similarities between the overlying rhyodacitic plug, dikes, and flows with the underlying quartz monzonite suggest a genetic intrusive/extrusive relationship rather than a spatially fortuitous event. The presence of this high-level plutonic phase and the abundance of silicic plugs and domes in the immediate area indicate the probable presence of a much larger plutonic body in the general vicinity of the Coyote Hills and at a probable

depth of 1 to 2 kilometers.

Table 3

Major Element Compositions of the Mulkey Wells quartz monzonite (#302) and an Overlying Volcanic Plug (#309)

Sample No.	302	309
SiO_2	69.6	71.0
Al_2O_3	17.0	16.0
FeO	1.6	3.3
MgO	0.0	0.0
CaO	1.0	1.1
Na_2O	5.0	5.1
K_2O	3.75	3.95
TiO_2	0.65	0.4
Total	100.5	100.75

Age

A tentative age of latest Oligocene is assigned to this hypabyssal intrusion on the basis of a nearly continuous lithologic sequence from quartz monzonite to an overlying rhyodacitic plug, a K-Ar date of 26.5 m.y. (refer to p. 65) for a nearby rhyodacitic flow, and the assumption that the intrusion was a precursor or comagmatic associate of the overlying volcanics.

COYOTE HILLS RHYOLITE

The Coyote Hills rhyolite represents a spectrum of silicic intrusive and extrusive rock types. This spectrum varies in composition from dacite to rhyolite and includes such features as volcanic plugs, flow domes, ring intrusions, laccoliths, and related flows and tuffs. As a whole, these volcanic features mantle large areas of the southwest, central, and eastern sections of the area mapped. It is apparent from the lithology, areal extent, and spatial relations that these rocks comprising the informally named Coyote Hills rhyolite were emplaced during a limited time interval of intrusive and extrusive activity.

Williams (1932) described three categories of volcanic domes: (1) plug domes formed as upheaved conduit fillings; (2) endogenous domes constructed by addition of new material from within; and (3) exogenous domes built by surface eruptions. Category (1) will be modified for the purpose of this thesis to separate the resultant feature from the emplacement event. MacDonald (1972) defined volcanic plugs as more or less cylindrical masses of congealed magma or tephra. This term, volcanic plug, will be utilized in lieu of plug dome to describe a volcanic feature, such as volcanic neck, rather than the mode of emplacement. However, where field evidence is sufficient to demonstrate that forcefull injection was the mode of emplacement then the term piston intrusion (Taylor, 1977, personal communication) will be used. The term piston intrusion will denote a forcefully injected cylindrical mass of semi-congealed magma. Category (2) will be expanded to include the term flow dome. A flow dome is here defined

as an exogenous dome that through whatever mechanism (tectonic, fluctuating magma pressure, etc.) a breach formed in the domal carapice. This breach results in the immediate flowage of the otherwise contained viscous magma beyond the carapice.

Volcanic Plugs A, B, and C

Three small volcanic plugs are located on a N.70°W. linear trend in the east one-half of the area. These plugs, from east to west, are in the middle of the NE¼ sec., 19, T.35S., R.24E., the NE¼ sec. 24, and the SW¼, NW¼, sec. 14T.35S., R.23E. and are labled A through C, respectively. They are approximately cylindrical in cross-section and sub-circular in plain, with the longest horizontal axis no greater than 60 meters. A fourth plug (D) is in the center of sec. 4 T.35S., R.23E. This plug is conical in shape and has dimensions that are approximately twice that of any of the preceeding plugs.

The volcanic plug (A) located in section 19 is massive and comprised almost exclusively of inclined imperfectly formed hexagonal columns approximately 20 cm in width (Figure 11). The rocks are light bluish gray (5B 7/1) to pale blue (5PB 7/2) and weather to a grayish orange (10YR 7/4) and brownish gray (5YR 4/1) assemblage.

Mineralogically, this plug is relatively uniform and simple. The rocks are composed principally of phenocrysts of sanidine in a mesostasis of partly devitrified glass. The phenocrysts of sanidine are primarily euhedral except where broken or merge with adjacent crystals. They are present as both crystalline aggregates and single crystals, and vary in length from 2 to 3 mm. Also present, but of

Figure 11. Volcanic plug A located in the NE¼, sec. 19, T.35S., R.24E.

Figure 12. Volcanic plug B located in the NE¼, NE¼, sec. 24, T.35S., R.23E. Plug is just below the sky line in left corner.

both subordinate quantity and size, are subhedral crystals of plagioclase feldspar, quartz, and opaques. The devitrified matrix contains randomly orientated to radiating microlites of feldspar and quartz. This plug is classified compositionally as a trachite on the basis of modal analysis. However, chemically is is a rhyolite (Table 4, #346).

The volcanic plug (B) in section 24 (Figure 12 p.47) is approximately 165 meters higher in elevation than the previous one. It is massive and composed of a few silicic fragments in a matrix of alkali feldspars and devitrified glass. An exception to the rather massive nature of this plug is the presence of small scale columnar jointing at the base. Only the tops of the columns crop out over a vertical distance of about 1.2 meters.

This plug is pinkish gray (5YR 8/1) to pale blue (5PB 7/2) on fresh surfaces. It weathers to grayish orange (10YR 7/4) and brownish gray (5YR 4/1). This plug is a rhyolite on the basis of chemical composition (Table 4, #46).

Indirect field evidence suggests that this plug may have actively breached the surface. Evidence suggestive of this event includes: (1) the overall massive and blocky character of the plug; (2) the irregularity of the apical carapice; (3) a small outcrop of lithified crumble(?) breccia in the draw below the plug; and (4) the higher altitude (by 165 m.) above plug (A). Evidence to the contrary is the absence of a glassy or perlitic selvage sheathing the plug, the presence of columnar jointing at the base of the plug, and the absence of a contiguous flow or tuff of similar composition. Further-

Table 4

Modal and Major Element Compositions of Volcanic Plugs A and B from the Coyote Hills rhyolite

	(A)		(A)	(B)
Sample No.	346		346	46
Phenocrysts				
sanidine	13.6	SiO_2	76.5	75.9
plagioclase	8.0	Al_2O_3	13.2	15.0
quartz	6.4	FeO	2.1	1.3
opaques	0.2	MgO	0.0	0.0
Groundmass[1]	72.5	CaO	0.2	0.4
Voids	0.4	Na_2O	5.1	5.0
		K_2O	4.5	4.75
		TiO_2	0.05	0.15
Total	101.1		101.65	102.5

Note: 1 - groundmass includes feldspar microlites, crystallites, opaques, and glass.

more, it is possible that the crumble(?) breccia is lithified talus material that post-dates the exhumation event.

Volcanic plug (C) in section 14 (Figure 13) is about 60 meters higher in elevation than plug (B) in section 24. This body consists of a nearly monolithic breccia that geomorphically forms a crudely columnar and orthogonally jointed sub-conical plug.

Exposures of this feature are light bluish gray (5B 7/1) to pinkish gray (5YR 8/1). They alter to a variegated assemblage of medium bluish gray (5B 5/1) and brownish gray (5YR 4/1) colors.

Mineralogicaly, this plug consists of isolated subhedral phenocrysts of sanidine and, in order of decreasing abundance, smaller crystals of opaques, quartz, hornblende, and plagioclase. These

smaller phenocrysts are anhedral to subhedral and randomly orientated. The phenocrysts are contained in a devitrified matrix of randomly oriented microlites and crystallites of feldspar, opaques, and quartz. Based on modal analysis this plug is a trachite, whereas chemically it is a rhyodacite (Table 5, #309).

Microbrecciation and incipient alteration are characteristic of this volcanic plug. Hornblende has altered to hematite, magnetite, epidote, and quartz; sandidine to dustings of clay and white mica. The devitrified glass has altered to an undetermined alteration mineral/mineraloid, probably a member of the smectite clay group, that imparts a light green tinge to the glass.

Origin of Volcanic Plugs A through C

These three volcanic plugs are inferred to represent exhumed masses of igneous rock that solidified in a volcanic conduit beneath an insulating cover of varying thickness of either its own ejecta or rocks of the Upper Basalt formation. This insulating cover has subsequently been removed by erosional processes. However, the lack of well developed columnar jointing in the plugs labeled B and C indicates that they either breached the surface or were emplaced near the surface. Emplacement at shallow depth would preclude slow cooling and formation of well-developed columnar jointing as is present in the plug labeled A.

The mode of emplacement of these three plugs is concluded to have been passive rather than forceful based on the following observations; absence of (1) concentric growth lines of viscous flow stri-

Figure 13. Volcanic plug C located in the SW¼, NW¼, sec. 14, T.35S., R.23E. The plug is found in the center of the frame.

Table 5

Modal and Major Element Compositions of Volcanic Plug C from the Coyote Hills rhyolite

Sample No.	(C) 309		(C) 309
Phenocrysts		SiO_2	71.0
sanidine	13.7	Al_2O_3	16.0
plagioclase	3.5	FeO	3.3
quartz	3.0	MgO	0.0
hornblende	2.2	CaO	1.1
opaques	4.4	Na_2O	5.0
Groundmass[1]	67.0	K_2O	3.95
Voids	6.2	TiO_2	0.4
Total	100.0		100.75

Note: 1 - groundmass includes feldspar, microlites, crystallites, opaques, and glass.

ations; (2) laminar or pilotaxitic texture; (3) breach flows; and (4) structual adjustment of adjacent rocks.

Volcanic Plug D

Located in the center of sec. 4, T.35S., R.23E. is a large volcanic neck preserved by the intrusion of volcanic plug (D) of intermediate composition. This plug is approximately 35 meters in height and about 120 meters in width at the base (Figure 14). A subdued and nearly closed fan structure is present in this otherwise structureless and massive plug. A small apron of large talus blocks is present at the base of the plug.

This intrusive is a relatively unaltered fine to medium grained seriate glomeroporphyritic dacite (Table 6, #92). Exposures display a variegated dusky blue (5PB 3/2) and grayish purple (5P 4/2) color that weathers to a varicolored brownish gray (5YR 2/1) to medium gray (N5).

The dominant textures are glomeroporphyritic and sub-pilotaxitic. The primary plagioclase phenocryst is andesine (An_{39-45}). These subhedra of andesine are approximately 2 mm in length. Smaller in size, and numerically subordinate, are subhedral to anhedral crystals of quartz, alkali feldspar, opaques, hypersthene, and augite. The plagioclase phenocrysts and the smaller crystals are in a groundmass of glass containing microlites and crystallites. The cores of the larger normally zoned plagioclase feldspars are altered to dustings of clay, calcite, and rarely white mica. The rims of both augite and hornblende are slightly altered to chlorite and magnetite.

Figure 14. Volcanic plug D located in the center of sec. 4, T.35S., R.23E. A laccolith is located in the center of the frame.

Table 6

Modal and Major Element Compositions of Volcanic Plug D from the Coyote Hills rhyolite

Sample No.	(D) 92		(D) 92
Phenocrysts		SiO_2	63.2
plagioclase	34.3	Al_2O_3	17.3
anorthoclase	3.0	FeO	6.0
quartz	2.0	MgO	1.1
hypersthene	1.6	CaO	4.0
augite	0.61	Na_2O	5.3
opaques	2.2	K_2O	2.65
Groundmass[1]	56.3	TiO_2	0.75
Total	100.01		100.3

Note: 1 - groundmass includes feldspar microlites, crystallites, opaques, and glass.

Origin of Volcanic Plug D

The closed fan structure superimposed on this seemingly massive volcanic neck is interpreted to represent near vertical viscous flow banding. This is, in part, confirmed by the sub-pilotaxitic texture of the rocks. Textural evidence in conjunction with the absence of both crumble breccia and the apparent structural displacement of adjacent rocks, indicates that the magma was passively injected into a previously existing volcanic conduit.

Laccolith

Associated with the volcanic plug (D), previously discussed, are proximal satellite apophysis. The most notable is a laccolith located about 910 meters east of the volcanic plug and 120 meters lower in elevation (see Figure 14, p. 53). This mushroom-shaped laccolith is characterized by moderately well-developed vertical columnar jointing. From the perfection of these vertical columns it is inferred that this feature represents a hypabyssal intrusion now only partially exhumed by erosional processes.

Flow Dome

Located in sec. 18, T.35S., R.23E. are the remnants of a very large collapsed endogenous dome of rhyodacitic composition (Table 7, #201-A). Morphologically, this dome is approximately 1.2 kilometers in diameter and is defined by a blocky dismembered annular wall up to 12 meters in height by about 3 meters in width. Rocks from the collapsed dome are light brownish gray (5YR 6/1) to pinkish gray

(5YR 8/1) and weather to slightly darker shades of the same colors. The dominant textural types are sub-pilotaxitic and seriate porphyritic; although phenocrysts constitute only about 12 percent of the rock. The phenocrysts include alkali feldsparup to 8 mm in length (5%); quartz, 2-3 mm in diameter (3%); hornblende, up to 2 mm in length (2%); and biotite, less than 1 mm across (1%). These phenocrysts are set in a massive, flow-banded, aphanitic matrix.

Accumulations of talus are moderate on either flank of the remnant walls. This talus is unconsolidated and texturally equivalent to the standing walls, and is inferred to have resulted from weathering and not from extrusive or explosive activity. Thus, the available evidence suggests that the broad apical carapice of this dome collapsed inward rather than exploded outward. This collapse resulted in a cauldron-like subsidence crater. Collapse of the dome is inferred to be due to a breach in the southeast flank that resulted in a lobate breach flow. The flow is crystal-rich (greater than 70 percent) versus the crystal-poor walls of the dome (less than 15 percent). The flow traveled in an essentially southeast direction for approximately 4 kilometers.

Rocks from the breach flow are a combination of colors ranging from dusky blue (5PB 3/2) to grayish purple (5P 4/2). They weather to a medium dark gray (N4) to pinkish gray (5YR 8/1) assemblage. Texturally, the rocks are fine to medium grained hypocrystalline hiatial porphyritic. The predominant crystals are alkali feldspar, followed in abundance by quartz, hornblende, and biotite. The alkali feldspars are "crystal clear", vary in size up to 5 mm, and are mostly

Table 7

Major Element Compositions of a Selected Intrusive Rock from the Coyote Hills rhyolite

Sample No.	201-A
SiO_2	70.2
Al_2O_3	16.9
FeO	2.7
MgO	0.0
CaO	2.8
Na_2O	5.0
K_2O	2.9
TiO_2	0.3
Total	100.8

broken. The mafic minerals have altered to chlorite and magnetite in contrast to the unaltered appearance of the feldspars.

Ring Intrusion and Piston Intrusion

Approximately 610 meters south of the collapsed endogenous dome are too small satellite bodies that, because of spatial proximity, are inferred tohave emanated from the same source as the flow dome complex. These two features, a ring intrusion and a piston intrusion (Figure 15 and 16), are in the center of sec. 19, T.35S., R.23E.

The ring intrusion is dissected and nearly circular in plain with a northwest-southeast dimension of 254 meters and a northeast-southwest dimension of 305 meters. A few fragments of the intruded Upper Basalt formation have been incorporated into the nearly vertical inward-dipping walls of platy rhyodacite.

Ring intrusions, first described by Harker (1904), consist of two types which are generally associated with one another in central

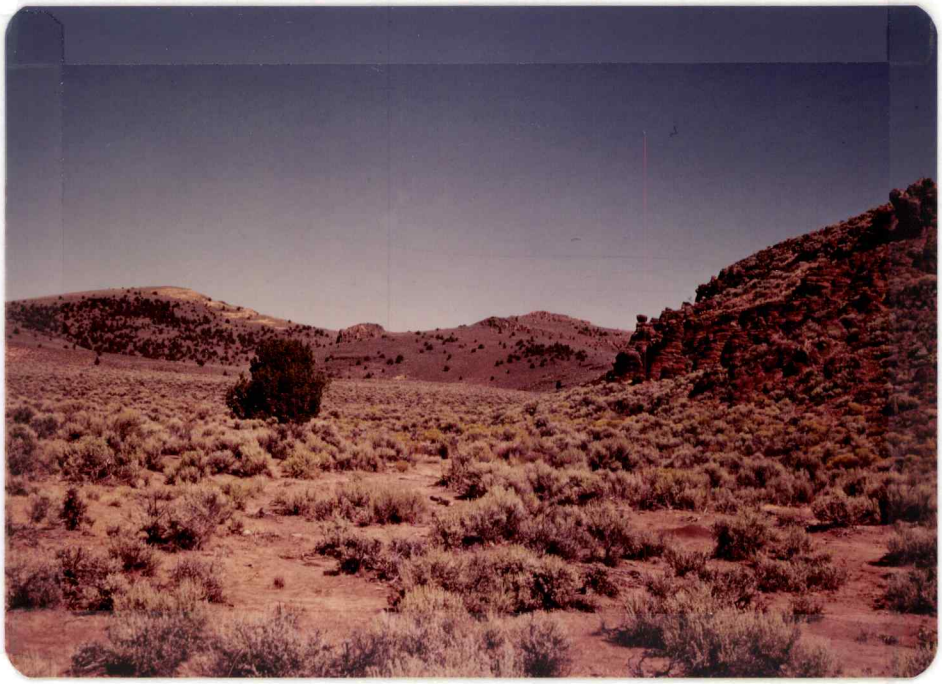

Figure 15. Ring Intrusion and plug intrusion, located in the center of sec. 19, T.35S., R.23E., and found in the center mid-ground of the frame.

Figure 16. Close-up of ring intrusion.

igneous complexes. Cone sheets are inward-dipping conical sheets that focus at a shallow depth over the supposed magma chamber. At the Ardnamurchan complex, Scotland, dips of the average cone sheet range from 35° at the edge of the complex to 75° near the center (MacDonald, 1972). Cone sheets are restricted to a concentric zone above the chamber and are usually not found beyond a limiting lateral distance from the chamber. Cone sheets are generally thin (less than 5 meters) and basaltic in composition. Ring dikes are circular to elliptical in plain, they may be up to several kilometers across and 1.5 kilometers in thickness, and sometimes they are found in concentric groups. They are generally coarse-grained and range from peridotite to granite in composition. The best known example of a ring dike is at Loch Ba on the Island of Mull (Bailey et al., 1924); it is an oval 5.8 by 8.5 kilometers in diameter with a maximum thickness of 310 meters. The dip of the ring dike walls is often outward at steep angles (75°), but may also dip vertically or inward at angles approaching 60°.

The standard explanation for cone sheets and ring dikes is that they have formed in response to tensile failure and shear failure, respectively, above a magma chamber as a result of fluctuations in magma pressure. Most ring dikes are in fact associated with cauldron subsidence of several hundred meters (Smith and Bailey, 1968; Roberts, 1970). Some ring dikes that apparently have been emplaced at a high level (through the volcanic pile) show steep inward dips in contradiction to the expected attitudes predicted from theoretical results (Roberts, 1970). Roberts has suggested that such ring dikes occupy tensional fractures resulting from excess magma pressure, and that

the fractures have been enlarged by marginal distortion of the country rock or by explosive venting magma to the surface.

It is inferred that the ring dike intrusion in the Coyote Hills was emplaced along shear fractures due to fluctuating pressures in the large flow dome complex to the north rather than by explosive venting of magma to the surface.

The small piston intrusion is 130 meters southwest of the ring intrusion. This intrusion is massive and irregularly fractured with vertical groves or slickensides common on the outer walls of the carapice (Figure 17). Based on the abundance of the vertical slickensides, it is apparent that intrusion of this body was forcefull or piston like.

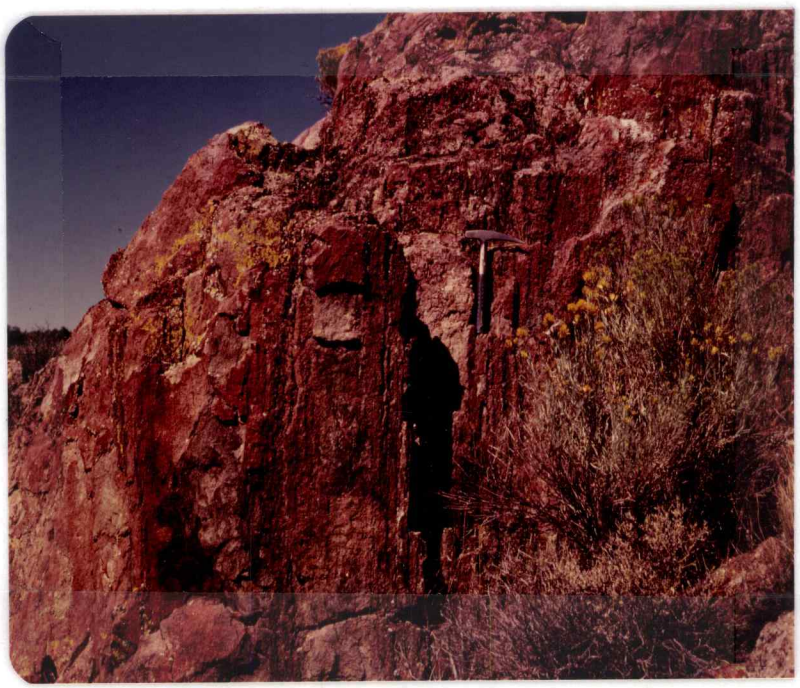

Figure 17. Vertical slickensides on carapice of the piston intrusion.

Dikes

Located along the arcuate ridge in parts of secs. 13 and 14, T.35S., R.23E. and along the upper reaches of Miners Draw, are the remnants of a few near vertical silicic dikes. These dikes, 1 to 2 meters in width, increase in density adjacent to a rhyodacite volcanic plug located in the NW¼ sec. 14. Localized sporadically along the borders of the dikes is a selvage of obsidian. These dikes are inferred to represent one of the feeder systems for the numerous flows on and adjacent to the ridge and Miners Draw.

Flows and Tuffs

Intermediate and silicic flows and numerically subordinate intercalated tuffs unconformably mantle large areas of the Coyote Hills. The flows attain thicknesses of 1.5 to 3 meters with a few as thick as 6 meters. Individual flows are short, discontinuous, and difficult to trace over any appreciable distance. They vary in color from pale red purple (5RP 6/2) to grayish red purple (5RP 4/2), and weather to slightly darker shades. The massive flows are fine-grained, normally porphyritic with the phenocrysts commonly exhibiting pilotaxitic texture, and occasionally have flow-aligned or stretched vesicular flow tops. Small zeolites commonly are present in the vesicules. Refer to Table 8 for the modal analysis of six silicic lava flows.

Intercalated between the flows are tuffs of similar composition. Commonly they are partially welded crystal-bearing tuffs. However, in sec. 21, T.35S., R.23E. remnants of a more firmly welded tuff outcrop. This tuff is characterized by a thin vitrophyric base and

Table 8

Modal Compositions of Selected Extrusive Rocks from the Coyote Hills rhyolite

Sample No.	25	28	183	251	341	363
Phenocrysts						
plagioclase	8.8	9.6	7.2	6.4	2.0	0.8
(An-phenocrysts)	(24-28)	(25-30)	(32-38)	(20-23)	(23-28)	(8-16)
(An-microlites)	(16-22)			(16-20)	(15-20)	
alkali feldspar*	2.3	1.8	2.6	T	8.0	10.5
quartz	2.0	2.2	T	1.0	0.4	1.8
augite	1.6	1.0	1.2	4.8	-	-
opaques	0.6	1.4	0.8	1.2	1.4	0.5
voids	0.6	0.8	4.6	0.4	1.8	2.0
Groundmass'	84.4	83.2	83.6	86.2	86.4	84.4
Total	100.3	100.	100.+	100.+	100.+	100.

Nore: *includes both sanidine and anorthoclase.
'in each sample the approximate breakdown of groundmass constituents is: microlites (60%), crystallites (30%), and residum (10%).

Table 8 (contd.)

Sample No.	Rock Name Petrographic Determination	Location/Elevation
25	rhyodacite	SW¼, NW¼, sec. 19, T.35S., R.24E. 5600 feet (1707 m.)
28	dacite	NW¼, NW¼, sec. 19, T.35S., R.24E. 5880 feet (1792 m.)
183	dacite	NE¼, SW¼, sec. 21, T.35S., R.23E. 6300 feet (1920 m.)
251	rhyodacite	NE¼, NW¼, sec. 28, T.35S., R.23E. 6040 feet (1841 m.)
341	rhyodacite	SW¼, SW¼, sec. 24, T.35S., R.23E. 5240 feet (1597 m.)
363	rhyolite	SW¼, SW¼, sec. 25, T.35S., R.23E. 5320 feet (1622 m.)

minor amounts of semi-collapsed pumice above the base.

The large number of individual flows indicates that effusive activity occurred over a period of undertermined length; however, the period between activity was not so long as to expose individual flows to the processes of degradation.

Source of the Flows and Tuffs

On the basis of the attitudes of the flows, which generally dip radially outward from the NW¼, sec. 15, T.35S., R.23E.; the direction of vesicular stretching; and the flow-alignment of the feldspars it is apparent that the source area for these flows and tuffs is located within the Coyote Hills. Moreover, the abundance of silicic dikes and other potential volcanic vents, and the mixed chemistry of the flows indicate that they issued from more than one vent. The exact number and location of these vents could not be determined from this investigation.

Lithic Wacke

A distinctive volcaniclastic lithic wacke is located in the southeast part of the Coyote Hills. This wacke erodes easily and forms gentle slopes or slight hollows in the topography. The best exposures are just north of Miners Draw in sec. 30, T.35S., R.24E. (Figure 18).

Exposures of the lithic wacke are dark yellowish brown (10YR 6/6) and weather to a moderate yellowish brown (10YR 5/4). The host is well-sorted and normally graded. However, it exhibits reverse size grading. Where uncollapsed pumice fragments, 0.6 to 1 cm in diameter, are present they are localized "stratigraphically" higher than lithic fragments of comparable size. Clasts in the lithic wacke range from 0.3 to 10 cm in size and include angular to subangular fragments of basalt, andesite, and pumice. They are supported in an argillaceous matrix. Individual beds vary in thickness from 3 to 40 cms.

Intercalated within the wacke is a light gray (5Y 6/1) fine-grained volcaniclastic sandstone. Bedding ranges from about 1 to 2 cm in thickness. Normal grading on a fine scale is indicated by faint alternating light and dark bands. Small scale scour and fill features and very local unconformities are present throughout both volcaniclastic members. The base of the lithic wacke does not crop out; however, projected structural attitudes suggest that the wacke unconformably overlies the underlying rocks of the Upper Basalt formation.

Figure 18. Lithic wacke and intercalated volcaniclastic sandstone.

Origin of the Lithic Wacke

The high content and subangularity of the pumice clasts demonstrates that the wacke was derived locally and was deposited shortly after the initial eruptive event of the Coyote Hills rhyolite.

Age and Correlation

The Coyote Hills are located along a linear belt of rhyolitic domal centers. This linear belt, which in part corresponds to the mid-Miocene to early Pliocene Eugene-Denio fault zone, extends from approximately Beatys Butte, about 60 kilometers southeast of the Coyote Hills, to the Yamsey Mountains-Black Hills area, located northeast of Klamath Falls, Oregon. These two endpoints are dated at

10.4 m.y., and 4.7 and 5.6 m.y. respectively. Numerous age determinations by the U.S. Geological Survey and others have established that there exists along this linear trend a systematic east to west progressive monotonic decrease in the ages of these domal centers. MacLeod et al. (1975) have constructed isochrons perpendicular to this linear trend that, when judiciously utilized, allow the predicition of ages for the intervening undated rhyolitic domes. The position of the Coyote Hills with respect to the isochrons indicates an age of 8 to 9 m.y. This age range of 8 to 9 m.y. is in good agreement with the tentative date of late Miocene for the silicic rocks of the Coyote Hills as postulated by Walker (1963 and 1977). However, recent K-Ar dating of a "phyric rhyolite or rhyodacite", located at the "extreme north sec. line 22-23, T.35S., R.23E.; north side of Miners Draw, elev. 5450 feet", indicates an age of 26.5 m.y. (MacLeod, 1978, personal communication). Thus, an age of late Oligocene to early Miocene will be assigned to these rocks informally named the Coyote Hills rhyolite. It is possible that the silicic domes and flows of the Coyote Hills are temporal equivalents to similar rocks of the upper Oligocene to lower Miocene John Day Formation (Peck, 1961).

STEENS BASALT

A thick sequence of basalt flows at Steens Mountain, southeast Oregon, was originally described in detail by Fuller (1931). Fuller formally designated this basalt sequence as the Steens Mountain Basalt. Piper et al., (1939) shortened the name to Steens Basalt.

The basalt flows along the southwest margin of the Coyote Hills topographically define a surface that dips gently southward. Exceptions are found where the rocks are displaced by faults or incised by fluvial channels, in which case steep cliffs are present. Representative exposures are found on either side of Snyder Creek in sec. 26, T.35S.,R.22E.

Individual flows are approximately 3 meters in thickness. Flow breccia is conspicuously absent. Occasionally, ropy pahoehoe features are preserved on the flow tops (Figure 19). Vesicles are present throughout individual flows, but their greatest concentration is near the upper most portion of the flows, and, to a lesser degree, along the base.

Primary columnar jointing is absent. However, weathering along a discontinuous subvertical system of joints about 0.3 meters apart gives the impression of crude columnar jointing. Additionally, a nearly horizontal system of partings superimposed on the latter system, and accentuated by weathering, confers the impression of stacked disks (Figure 20).

Figure 19. Pahoehoe texture on a Steens Basalt flow.

Figure 20. Typical exposure of Steens Basalt.

Lithology and Petrology

Megascopically, the rocks are medium grained and have a felty to diktytaxitic texture. They are medium dark gray (N4) on fresh surfaces and weather to a grayish brown (5YR 3/2). Petrographically, the dominant textural types are ophitic, subophitic, and diktytaxitic with intergranular less common. The primary phenocrysts consist of plagioclase feldspar, clinopyroxene, olivine, and minor opaques.

The plagioclase feldspars range in composition from An_{55-68}, with labradorite (An_{62}) the most prevalent. The crystals are present as laths about 0.5 mm in length. They are normally euhedral, except where incipient resorption or corrosion has taken place, and they may occur as interlocking laths. Simple twinning is the norm; compositional zoning was not observed.

Phenocrysts of clinopyroxene, augite, are present as anhedral plates about four times the size of the feldspar laths. These crystals typically enclose the feldspar laths and less so the crystals of olivine forming an ophitic to subophitic texture. The degree of enclosure grades from partial to complete.

Euhedral phenocrysts of olivine up to 1 mm in size are present. However, the more common mode of occurrence is in the groundmass as anhedral crystals approximately 0.25 mm in size. The olivine is predominantly altered to iddingsite.

The opaques, primarily magnetite, are normally found in the groundmass, but a few equant phenocrysts are also present. The crystal form of the groundmass opaques varies from skeletal grains

Table 9

Modal Analysis and Comparison of Rocks from the Steens Basalt

Sample No.	369	Waters (1961)	Larson (1965)
plagioclase	52.5	51.3	53.6
clinopyroxene	20.0	20.1	20.8
olivine	12.5	18.0	13.6
opaques	4.7	5.7	5.4
apatite	0.5'	0.6	-
glass and microlites	5.6	4.2	6.6
voids	4.2		
Total	100.0	100.0	100.0

Sample No.	Rock Name	Location/Elevation
		SW¼, SW¼, sec. 26, T.35S., R.22E. 5500 feet (1667 m.)

' visual estimate
Waters average of 56 samples
Larson average of 15 samples

to irregular. Crystallites of apatite and blebs of dark brown glass are present in minor amounts throughout the thin sections examined.

Stratigraphic Relationship and Thickness

These basalt flows are nearly flat-lying with a gentle dip to the south, even where they have been off-set by a northwest-trending normal fault. The down-dropped block is overlain, in part, by the Plush tuff; whereas the tuff unit on the upthrown block has been removed by erosion.

Larson (1965) reported that the Steens Basalt in the Plush area attains a maximum thickness of 610 meters. However, the flood basalts locally have unconformably on-lapped onto topographic highs, such as the Coyote Hills, resulting in out crop thicknesses much less than the maximum. Along the southern margin of the Coyote Hills the basalt flows attain a minimum thickness of about 48 meters.

Age and Correlation

Rocks from the Steens Basalt type-locality have been radiometrically dated at 14.6 to 15 m.y. (Evernden et al., 1964; Evernden and James, 1964). Additionally, paleomagnetic investigations have been conducted on the Steens Basalt throughout this region (Watkins, 1963; Larson, 1965; Watkins and Baksi, 1974). With few local exceptions (Larson, 1965), these rocks are all reversely magnetized. Watkins has demonstrated the existence of a major polarity transition from reverse to normal in the rocks at Steens Mountain. This transition has been dated at 15.1 m.y. by Baksi et al., (1967).

Locally, the basalt flows that are tentatively correlated as equivalent to Steens Basalt are overlain by a tuffaceous unit designated the Plush tuff. The Plush tuff has been dated as late Miocene (Walker, 1963) on the basis of paleontological evidence. Therefore, these basalt flows are tentatively dated as middle to late Miocene in age, and equivalent to the Steens Basalt, based on a petrographic equivalency between the rocks present along the southwest flank of the Coyote Hills and the Steens Basalt and the limiting age of the Plush tuff.

PLUSH TUFF

Larson (1965) published a geological reconnaissance of an area approximately centered on Plush, Oregon, in which he mapped and informally named a tuffaceous sedimentary unit the Plush tuff. This name is retained to avoid confusion and to facilitate correlations with the work of other authors and to avoid the proliferation of formational names.

This unit is along the south and southwest margin of the Coyote Hills. Its topographic expression is that of gently rolling to nearly flat lying hills with moderate relief. The best exposures are found along and north of the unimproved dirt road in sec. 31, T.35S., R.23E.

The color of these rocks is moderate yellowish brown (10YR 5/4) which weather characteristically to pale yellowish brown (10YR 6/2). The rocks are comprised of fine to medium-grained silicic pyroclastic and lithic fragments.

Medium grained subrounded clasts of pumice are found throughout this unit. The host is massive and the individual strata are poorly defined, but are moderately well sorted (Figure 21).

Stratigraphic Relationship and Thickness

The Plush tuff disconformably overlies the Steens Basalt and unconformably overlies the foundation group where the tuff onlaps these older rocks. Locally, the Steens Basalt - Plush tuff contact dips gently southward. The base of this unit crops out in the N½, sec. 26, T.35S.,R.22E. (Figure 22). The unit attains a thickness of 52 meters in a remnant erosional bluff located in sec. 31,T.35S., R.23E.

Figure 21. Typical outcrop of Plush Tuff.

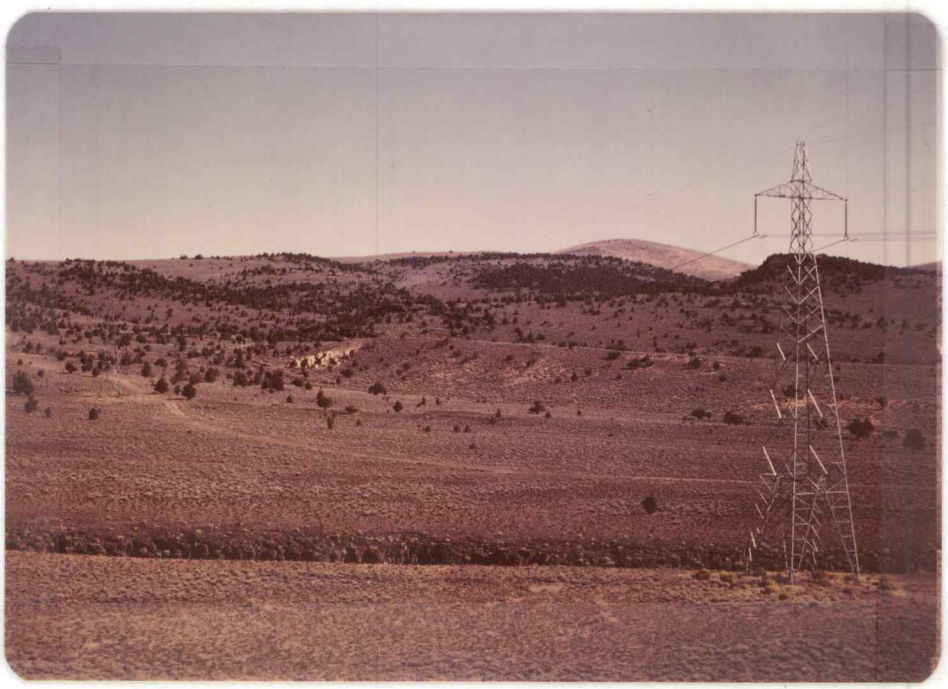

Figure 22. View northeast from the SW¼, SW¼ sec. 26, T.35S., R.22E. of Plush Tuff, the buff colored unit, overlying the nearly flat lying Steens Basalt.

Origin

Within the Coyote Hills the Plush tuff represents tuffaceous epiclastic rocks that were deposited in a fluviolacustrine environment. In other nearby localities, these rocks commonly contain carbonaceous fragments which Larson (1965) interprets as having been deposited in a flood-plain environment.

Age and Correlation

Walker (1960 and 1963) has established the age of the Plush tuff as Barstovian (late to early late-middle Miocene) on the basis of vertebrate fossils. Radiometric dating of an intercalated basalt flow near Beatys Butte, about 60 kilometers southeast of the Coyote Hills, has established a date of 14.5 m.y. (Evernden and James, 1964) for the Plush tuff. No field evidence was found that might modify the dates established by the above authors. Similar lithologic and temporarily equivalent units are found throughout the Basin and Range province of Oregon (Larson, 1965; Walker, 1977).

UPPER BASALT

A series of basalt flows that stratigraphically overlie the Plush tuff are along the southeast margin of the Coyote Hills. Walker and Repenning (1965), in their reconnaissance map (I 446) of the Adel Quadrangle, mapped these volcanics as unnamed, nearly flat lying rim-forming basalt flows. Shortly thereafter, Larson (1965) informally named these flows the Upper basalt. The name, Upper basalt is retained in this thesis. These flows are of limited areal extent within the boundaries of the mapped area. Topographically, this unit is expressed as a nearly flat-lying surface dipping gently southward. Exceptions are found where fluvial action or faults have dissected this unit. These flows are best exposed in Miners Draw in the center of sec. 32, T.35S.,R.24E.

The color on unweathered surfaces is medium to medium dark gray (N5-N4). These rocks are commonly stained a dark reddish brown (10R 3/4) to grayish brown (5YR 3/2) on weathered surfaces. Crystal size grades from fine to medium. The flows range in thickness from 3 to about 6 meters. They are moderately vesicular primarily along the flow tops, lack abundant flow breccia, and are orthogonally jointed. The joint pattern is irregularly spaced and gives rise to a stacked slab-pattern.

Petrology

The dominant textural types include ophitic to subophitic, diktytaxitic, and moderately intergranular. The primary minerals are plagioclase feldspar, clinopyroxene, olivine, and opaques. The

plagioclase feldspars range in composition from An_{55-70}, with labradorite (An_{62}) the most abundant. The feldspar crystals are less than 0.5 mm in length, euhedral, unzoned, and are found as randomly orientated interlocking laths. The primary twins are albite and carlsbad. Crystals of clinopyroxene are found as euhedral to subhedral blocky laths approximately 0.25 to 0.5 mm in size. They are often fractured, embayed, and altered in varying degrees to iddingsite. Opaque minerals, primarily magnetite, are present as phenocrysts and as intergranular fine dustings, and with crystal form varying from equant to irregular blebs.

Table 10

Modal Analysis and Comparison of Rocks from the Upper basalt

Sample No.	359	Larson[1] (1965)
plagioclase	52.0	51.5
pyroxene	20.6	21.6
olivine	15.2	16.9
opaques	5.0	5.6
glass and crystallites	3.6	4.4
apatite	T	T
voids	5.4	
Total	101.8	100.0

Sample No.	Rock Name	Location/Elevation
	Petrographic Determination Chemical Determination	
359	basalt high aluminum basalt	SW¼, NE¼, sec. 32, T.35S., R.24E. 4750 feet (1448 m.)

1 - modal analysis of 36 samples from the Upper basalt.

Stratigraphic Relationship and Thickness

Locally, the base of this unit crops out in a draw located in sec. 32, T.35S., R.24E. Projected attitudes of this contact indicate that the unconformity between the Upper basalt and the underlying Plush tuff is nearly concordant. The Upper basalt thins rapidly to the west and northwest. However, in the vicinity of Miners Draw this unit attains a maximum thickness of about 45 meters in the opposite direction.

Age and Correlation

The Upper basalt overlies the Plush tuff and, thus, can be no older than early Miocene. However, as it is present as a capping unit, a minimum age is difficult to determine. Pediment gravels locally overlie a small outcrop of these flows in sec. 29, T.35S., R.24E. and indicate that the unit is no younger than upper Pleistocene.

These basalts are equivalent to those mapped by Walker (1963) as Tb of late Miocene to early Pliocene age, and those mapped by Larson (1965) as Upper basalt and Young Upper basalt of late-middle Miocene to Recent(?) age. The two basalt units mapped by Larson (1965) are nearly indistinguishable except where the Danford Welded Tuff-Breccia (Piper et al., 1939) is found intercalated between them. Locally, the tuff breccia is absent along the southern margin of the Coyote Hills.

UPPER TUFF

Remnants of a moderately well-welded tuff are in the northeast portion of the mapped area. The topographic expression of this tuff is approximately neutral with very little contrast in relief between the tuff and the surrounding unconsolidated Holocene alluvium. The outcrop pattern is sporadic, thus the over-all distribution is inferred from the float distribution. The best exposure is found in Mulkey Wells Draw along the section line 31 - 32, T.34S., R.24E.

The color of this tuff is pale red (5R 6/2) on fresh surfaces, whereas, it is grayish red (5Y 4/2) on weathered surfaces. This unit is massive and unlaminated. It contains uncollapsed pumice fragments in subparallel alignment, in addition to subordinate amounts of collapsed glassy pumice fragments, broken crystals, and subangular lithic fragments.

Stratigraphic Relationship and Thickness

A partial exposure, about 2.5 meters, of this nearly flat-lying tuff is found in a shallow draw along the section line 31-32, T.34S., R.24E. No basalt flows crop out near the tuff unit, nor are there any other stratigraphic or structural features evident at this locality.

Origin, Age and Correlation

Outcrop patterns based on float indicate that the source area for this tuff flow was north of the Coyote Hills. It flowed in a southerly direction along slight depressions in the topography and

entrapped lithic and collapsed pumice fragments from inferred underlying tuffs along its course of passage.

Descriptions by Larson (1965) suggest that the Upper tuff is correlative with the "partially to densely welded rhyolitic tuff-breccia" that is present in the northern one-half of the Plush area. He tentatively correlated this tuff with the upper tuff-breccia member of the Danforth Formation. The Danforth Formation, consisting predominately of tuffaceous sediments and tuffs, was first described and named by Piper et al., (1939) from outcrops on the Danforth Ranch, near Burns, Oregon. Evernden et al., (1964) have radiometrically dated the Danforth Tuff-Breccia at 6.4 m.y.

BLOCKY FLOWS

Two small block flows are in sec. 7, T.35S., R.23E. They are approximately 300 meters in length, 30 meters in width, and about 3.5 meters thick (Figure 23). No central, non-blocky or massive section of the flows was found. As such, the flows consist completely of a jumbled collection of blocks. Individual blocks are massive, angular in form and shaped as crude cubes, and encrusted by smooth, dark glassy rinds. Associated with and largely encompassing the flows is a thin layer of moderately indurated light brown ash. Compositions of the flows and ash are inferred to be basaltic andesite rather than basalt. This inference is based primarily on the very short (or viscous) nature of the two flows.

Age

The overall appearance of these flows suggests they have formed recently. Glassy rinds on the blocks have neither an oxidized nor hydrated texture. Additionally, the blocks are well-defined by sharp edges and are not rounded by processes of weathering. Because of the pristine nature of the flows and the large amount of remnant ash, they are assigned an age of late Pleistocene to early Holocene.

Figure 23. Long range view of blocky flows formed by low dark ridge in mid-ground, with the Rabbit Hills in the background.

QUATERNARY DEPOSITS

Land surfaces, primarily along the southeast margin of the Coyote Hills above the present stream level are relatively flat and covered to a shallow depth (4.5 to 6 meters) with conglomeratic alluvial material (Figure 24). These poorly sorted, poorly consolidated deposits represent pediment material deposited on a surface cut by streams flowing from the Coyote Hills. In support of this hypothesis, the deposits are composed of rocks common to the local area. The surface is presently undergoing dissection by Recent streams, such as in Miners Draw, which have incised their courses 30 to 45 meters into this surface. The age of this pediment material is unknown, but presumably it was deposited during the Pleistocene.

Undifferentiated and unconsolidated Quaternary material found along the east and north margins of the Coyote Hills has accumulated by various processes. Portions of the sediment have been deposited in a lacustrine environment, probably during the Pleistocene when standing water was present for lengthy periods. Other portions are principally alluvial in origin or are primarily eolian in character.

Figure 24. Quaternary pediment gravels exposed in a quarry (NW$\frac{1}{4}$, SW$\frac{1}{4}$, sec. 33T.35S., R.24E).

STRUCTURE

The structural style of the Tertiary volcanic rocks comprising the Coyote Hills may be characterized as gently deformed. This deformation is controlled, for the most part, by normal faults. The volcanic units, as a whole, dip radially outward from the approximate geographic center of the Coyote Hills, but locally they are unreliable as the dips may be related to irregularities below unconformities between major units.

Unconformities and Folds

Unconformities of varying types and magnitude are common within the Coyote Hills. They range from major angular unconformities, as between the Lower Andesite and Upper Basalt formations through disconformities as found between the Plush tuff and the Upper basalt, to minor unconformities of local extent as found within the lithic wacke of the Coyote Hills rhyolite.

No evidence of tectonic fold structures was found within the Coyote Hills.

Faults

Faults having a significant displacement were not recognized anywhere within the mapped area. In general, the faults contained within the major units are difficult to recognize because of the homogeneity of the volcanic rocks, absence of marker beds, and paucity of continuous bedrock exposure.

A series of small northeast-trending faults of limited displace-

ment located in secs. 17 and 20, T.35S., R.23E., the northwest alignment of the three volcanic plugs (A-C), in the east one-half of the area, and the northwest-trend of quartz pyrite veinlets in sec. 14 and 15, T.35S., R.23E. form the primary basis for identifying the predominate N.30°-70°W, and subordinate N.30°E. structural trends within the Coyote Hills. Coincident with these two trends are numerous draws and gullys that are inferred to be consequent erosional features.

Structural Development in Relation to Intrusive Events

The spatial coincidence of the three volcanic plugs (A-C) and their alignment along a N.70°W. linear trend implies a sympathatic relationship. The sequence of events is interpreted to be (1) normal faulting, and (2) intrusion of the volcanic plugs with their orientation controlled by the pre-existing basement structure.

Age

Donath (1962), Larson (1965), Lawrence (1976), and others have identified en echelon fault systems that trend N.40°-60°W. and N.40°-50°E. in south-central Oregon. The earliest age of movement along either of these fault systems is thought to be late to latest Miocene. However, field evidence in the Coyote Hills indicates that movement along these trends commenced much earlier. The alignment of the three northwest-trending volcanic plugs argues that structural conduits existed prior to their emplacement. Thus, the earliest dislocation along this northwest trend is considered to be late Oligocene or prior to about 26.5 m.y., the age of the Coyote Hills

rhyolite.

Structurally controlled lithologic relationships in secs. 17 and 20, T.35S., R.23E. indicate that the earliest movement along these northeast-trending faults post-dates consolidation of the Coyote Hills rhyolite. The Plush tuff, located southwest of and along the trend of these faults, shows no displacement or disturbance along the projected trends; thus, a probable age bracket of early to middle Miocene is indicated for these faults.

Evidence that discontinuous movement along both trends continued up to early Pliocene is found in sec. 30, T.35S., R.24E. Located in the approximate center of this section is a dissected vent of the Upper Basalt. Faults that parallel both trends crop out in this area.

A northwest-trending fault, located in sec. 26, T.35S., R.22E., offsets the Steens Basalt by approximately 15 meters. The age of this fault post-dates the Steens Basalt and pre-dates the undisturbed Plush tuff.

PETROCHEMISTRY

Chemical analysis is one of the primary methods by which igneous rocks, and especially volcanic rocks, can be compared with one another. In contrast, the main use of petrography is in the naming of rocks and the assigning of varietal names. Furthermore, petrographic comparisons of volcanic rocks can be unreliable due to quenching effects, mode of emplacement and differing partial pressures of water and oxygen (Manson, 1967; Hamilton and Anderson, 1967).

Ideally, by chemical analysis, volcanic rocks can be segregated into groups based upon the composition of the magma at the time of emplacement. However, subsequent alteration of these rocks, whether it be by deuteric, hydrothermal, or supergene processes may cause changes in composition that can be difficult to chemically interpret.

Twenty samples were selected for major oxide (partial) and specific trace element analyses. They were collected at random; however, a certain bias was probably introduced because they were chosen from the finer-grain less porphyritic lithologies. Nonetheless, the chemical analyses should be representative of the various rock types found in the Coyote Hills. Major oxide and normative minerals are summarized in Table 11 and 12, respectively. Comparisons of the analyses for samples from the Coyote Hills to those of representative rock types from other localities are given in Tables 13 and 14. Trace element chemistry will be discussed in a later section.

The rock names as portrayed in Figure 25 are based on a modified classification scheme of Mackenzie and Chappell (1972). The parameters for this scheme are weight percent K_2O versus weight percent

Table 11

Major Element Chemistry of Igneous Rocks from the Coyote Hills

	13	131	162	212	359	92	144	72	89	183
SiO_2	52.0	49.6	48.0	50.9	48.2	63.2	62.0	71.8	65.0	66.5
Al_2O_3	19.2	18.4	14.2	14.2	16.3	17.3	19.1	15.2	16.9	17.4
FeO	9.0	10.7	14.1	12.2	10.4	6.0	4.9	3.2	5.1	4.1
MgO	3.0	4.7	4.7	4.2	8.6	1.1	3.0	0.4	1.4	0.0
CaO	10.1	9.85	10.2	8.2	10.8	4.0	6.0	1.7	3.9	2.4
Na_2O	4.0	3.7	4.2	4.3	2.9	5.3	3.9	4.7	5.1	6.3
K_2O	0.75	0.85	1.35	1.3	0.2	2.65	2.3	4.5	2.9	3.35
TiO_2	2.15	1.55	3.1	3.0	0.9	0.75	0.45	0.3	0.65	1.5
Total	100.2	99.35	99.85	98.3	98.3	100.3	101.65	101.8	100.95	101.55
	201-A	37	40	46	251	275	302	309	346	426
SiO_2	70.2	68.2	68.2	75.9	68.2	74.8	69.6	71.0	76.5	69.2
Al_2O_3	16.9	16.2	15.8	15.0	16.4	13.2	17.0	16.0	13.2	16.8
FeO	2.7	4.3	4.9	1.3	3.5	4.0	1.6	3.3	2.1	2.7
MgO	0.0	0.2	0.0	0.0	0.2	0.0	0.0	0.0	0.0	0.2
CaO	2.8	0.7	0.9	0.4	1.2	1.7	1.0	1.1	0.2	1.0
Na_2O	5.0	6.2	6.9	5.0	6.3	4.9	6.9	5.0	5.1	6.7
K_2O	2.9	4.45	3.35	4.75	3.35	2.95	3.75	3.95	4.5	4.0
TiO_2	0.3	0.65	0.5	0.15	0.85	0.7	0.65	0.4	0.05	0.45
Total	100.8	100.90	100.55	102.50	100.00	102.25	100.50	100.75	101.65	101.05

Table 11 (contd)

Sample No.	Location/Elevation
72	SW¼ NW¼ sec.T.35S., R.24E. 5100 feet (155 m.)
89	SW¼ NE¼ sec. 4,T.35S., R.23E. 5900 feet (1798 m.)
183	NE¼ SW¼ sec. 21, T.35S.,R.23E. 6300 feet (1920 m.)
201-A	SE¼ NW¼ sec. 18, T.35S.,R.23E. 6280 feet (1914 m.)
37	NW¼ SE¼ sec. 18, T.35S.,R.24E. 5640 feet (1719 m.)
40	SW¼ SE¼ sec. 18, T.35S.,R.24E. 5460 feet (1664 m.)
46	NE¼ NE¼ sec. 24, T.35S.,R.23E. 5740 feet (1750 m.)
13	SE¼ SE¼ sec. 24, T.35S.,R.23E. 5120 feet (1561 m.)
131	NE¼ NW¼ sec. 12, T.35S.,R.22E. 6160 feet (1878 m.)
162	NW¼ SW¼ sec. 13, T.35S.,R.22E. 6340 feet (1932 m.)
212	NE¼ SE¼ sec. 24, T.35S.,R.22E. 6040 feet (1841 m.)
359	SW¼ NE¼ sec. 32, T.35S.,R.24E. 4750 feet (1457 m.)
92	SE¼ NW¼ sec. 4, T.35S.,R.23E. 6200 feet (1890 m.)
144	NE¼ NW¼ sec. 8, T.35S.,R.23E. 6460 feet (1969 m.)
251	NE¼ NW¼ sec. 28, T.35S.,R.23E. 6040 feet (1841 m.)
275	NW¼ SE¼ sec. 2, T.35S.,R.23E. 5640 feet (1719 m.)
302	SW¼ SE¼ sec. 11, T.35S.,R.23E. 5500 feet (1676 m.)
309	SW¼ NW¼ sec. 14, T.35S.,R.23E. 5920 feet (1804 m.)
346	middle NE¼ sec. 19, T.35S., R.24E. 5220 feet (1591 m.)
426	NE¼ NW¼ sec. 23, T.35S.,R.23E. 5400 feet (1646 m.)

Table 12

Normative Mineral Analyses* of Igneous Rocks from the Coyote Hills

	13	131	162	212	359	92	144	72	89	183
Q	0.00	0.00	0.00	0.00	0.00	9.38	10.43	20.94	11.70	10.61
C	0.00	0.00	0.00	0.00	0.00	0.00	0.00	0.00	0.00	0.00
OR	4.42	5.05	7.98	7.81	1.20	15.61	13.37	26.13	16.98	19.50
AB	33.73	29.44	20.60	36.72	24.92	44.67	32.44	39.04	42.71	52.46
AN	32.12	31.25	15.90	15.85	31.37	15.53	27.35	6.95	14.51	9.16
NE	0.00	1.09	8.08	0.12	0.00	0.00	0.00	0.00	0.00	0.00
AC	0.00	0.00	0.00	0.00	0.00	0.00	0.00	0.00	0.00	0.00
DI	6.92	7.43	13.26	10.09	11.98	1.05	0.89	0.24	1.49	0.00
HE	7.98	7.42	15.73	11.15	6.85	2.58	0.69	0.91	2.44	2.29
HY	6.41	0.00	0.00	0.00	1.01	8.56	13.02	4.58	7.94	2.37
OL	2.55	13.19	9.72	9.98	18.81	0.00	0.00	0.00	0.00	0.00
MT	1.80	2.16	2.83	2.49	2.12	1.20	0.97	0.63	1.02	1.02
IL	4.07	2.96	5.88	5.79	1.74	1.42	0.84	0.56	1.22	1.22

	201-A	37	40	46	251	275	302	309	346	426
Q	22.21	10.81	10.76	26.33	14.11	29.17	12.43	22.31	27.57	11.07
C	0.00	0.00	0.00	0.88	0.23	0.00	0.00	1.48	0.00	0.00
OR	17.01	26.07	19.69	27.41	19.81	17.06	22.07	23.18	26.18	23.41
AB	41.95	51.96	58.02	41.26	53.28	40.52	58.08	41.97	42.11	56.08
AN	13.78	3.19	2.23	1.94	5.95	5.19	4.31	5.42	0.00	3.90
NE	0.00	0.00	0.00	0.00	0.00	0.00	0.00	0.00	0.00	0.00
AC	0.00	0.00	0.00	0.00	0.00	0.00	0.00	0.00	0.29	0.00
DI	0.00	0.02	0.00	0.00	0.00	0.00	0.00	0.00	0.00	0.13
HE	0.00	0.20	1.97	0.00	0.00	2.73	0.56	0.00	0.87	0.75
HY	3.51	5.67	5.40	1.65	4.32	3.26	1.01	4.23	2.62	3.29
OL	0.00	0.00	0.00	0.00	0.00	0.00	0.00	0.00	0.00	0.00
MT	0.54	0.86	0.98	0.26	0.70	0.79	0.32	0.66	0.27	0.54
IL	0.57	1.22	0.94	0.28	1.61	1.30	1.23	0.75	0.09	0.85

*Adjusted to 100 percent

Table 13

A Comparison of the Major Oxide Chemistry of Basalts from the Coyote Hills to those from Other Areas

	A	b	c	d	e	f	g	h	i	J
SiO_2	50.1	49.85	45.2	46.8	48.4	48.5	48.28	48.5	48.	48.2
Al_2O_3	16.5	16.96	16.0	13.86	16.7	15.1	16.84	15.6	16.	16.3
Fe_2O_3		4.48	6.5	2.59	4.3	2.9	4.36	5.2		
FeO	11.5	5.57	8.1	9.52	7.5	6.9	6.17	6.1	11.	10.4
MnO		0.15	0.17	0.12	0.2	0.15	0.17	0.2		
MgO	4.2	4.00	7.6	9.74	5.8	7.45	7.73	6.2	6.4	8.6
CaO	9.6	8.01	9.3	10.38	9.0	9.50	11.24	9.0	8.4	10.8
Na_2O	4.1	4.22	3.2	2.82	3.0	3.52	2.58	3.0	4.5	2.9
K_2O	1.1	1.95	0.81	0.67	1.0	1.48	0.23	1.0	2.1	0.2
H_2O+		0.76	1.0	0.59	1.5	2.0	0.72			
H_2O-				0.24			0.82			
TiO_2	2.5	2.50	2.3	2.70	2.2	1.77	0.87	1.9	2.7	0.9
P_2O_5		0.98	0.39	0.35	0.4	0.50	0.07	0.5		
Total	99.6	99.43	100.60	100.06	100.0	99.77	100.08	97.2	99.1	98.3

A -Average of 4 analysis of basalt from the Coyote Hills of late Oligocene(?) age (13, 131, 162, 212).
b -Average of 2 analysis of Hawaiite from Nandewar Volcano, N.S.W., Australia of Miocene Age (Abbott,1969).
c -Analysis of 1 olivine-basalt from Moroto, eastern Uganda (Varne, 1968).
d -Average of 7 alkali olivine-basalts from the Hawaiian Islands (Kuno et al. 1957).
e -Average of 18 analysis of basalts from southeastern Oregon of late middle or late Miocene age (Walker, 1969a).
f -Average of 36 analysis of Basin and Range basalts (Leeman and Rodgers, 1970).
g -Analysis (1) from chilled base of Warner Basalt (high-alumina type) of Pleistocene(?) age (Kuno, 1965).
h -Average of 10 analysis of Steens Basalt (Avent, 1969).
i -Average trachybasalt (personal communication, Taylor, 1978).
j -Analysis of 1 basalt from the Coyote Hills of late Miocene age (359).

Table 14

A Comparison of the Major Oxide Chemistry of Rhyodacites and Rhyolites from the Coyote Hills to those from Other Areas

	A	b	c	d	e	f	g	h	i	J
SiO_2	69.5	69.27	73.	72.92	75.	75.50	76.20	76.53	77.05	76.02
Al_2O_3	16.3	14.34	13.	14.01	13.	12.80	13.34	13.58	12.58	14.1
Fe_2O_3		2.51		0.82		0.34	0.80	0.38	0.31	
FeO	3.2		2.8	1.78	2.0	0.60	--		0.45	1.7
MnO		0.07		0.04		0.11	0.13	0.04	0.04	
MgO	0.3	0.88	0.6	0.14	0.3	0.05	0.30	0.21	0.03	0.0
CaO	1.3	1.88	2.2	1.23	1.5	0.62	0.75	0.81	0.44	0.3
Na_2O	5.9	3.75	3.9	4.80	3.6	3.70	3.77	3.92	3.96	5.1
K_2O	3.7	4.59	3.7	3.45	4.0	5.10	3.40	4.70	4.68	4.6
H_2O+		2.16		0.50		0.85	1.24	0.56	0.19	
TiO_2	0.1	0.40	0.3	0.35	0.2	0.03	0.07	0.10	0.07	0.1
P_2O_5		0.13		0.06		0.10		0.00	0.01	
Total	100.3	99.98	99.95	99.60	99.6	100.00	100.00	100.83	99.95	102.1

A - Average of 8 analysis of rhyodacite from the Coyote Hills.
b - Analysis of 1 rhyolite (DP-109AD) from Drakes Peak (Wells, 1975).
c - Average calc-alkaline rhyodacite (personal communication, Taylor, 1978).
d - Average South Sister and Newberry rhyolites (Higgins, 1968; McBirney, 1968).
e - Average calc-alkaline rhyolite (personal communication, Taylor, 1978).
f - Mono Crater's rhyolite (Loney, 1968).
g - Rhyolite dome near Cox Flat, south-central Oregon (Peterson and McIntyre, 1970).
h - Analysis of 1 rhyolite from Drakes Peak (Wells, 1975).
i - Glass Mountain Rhyolite, California (Noble et al., 1972).
J - Average of 2 analysis of rhyolite from the Coyote Hills.

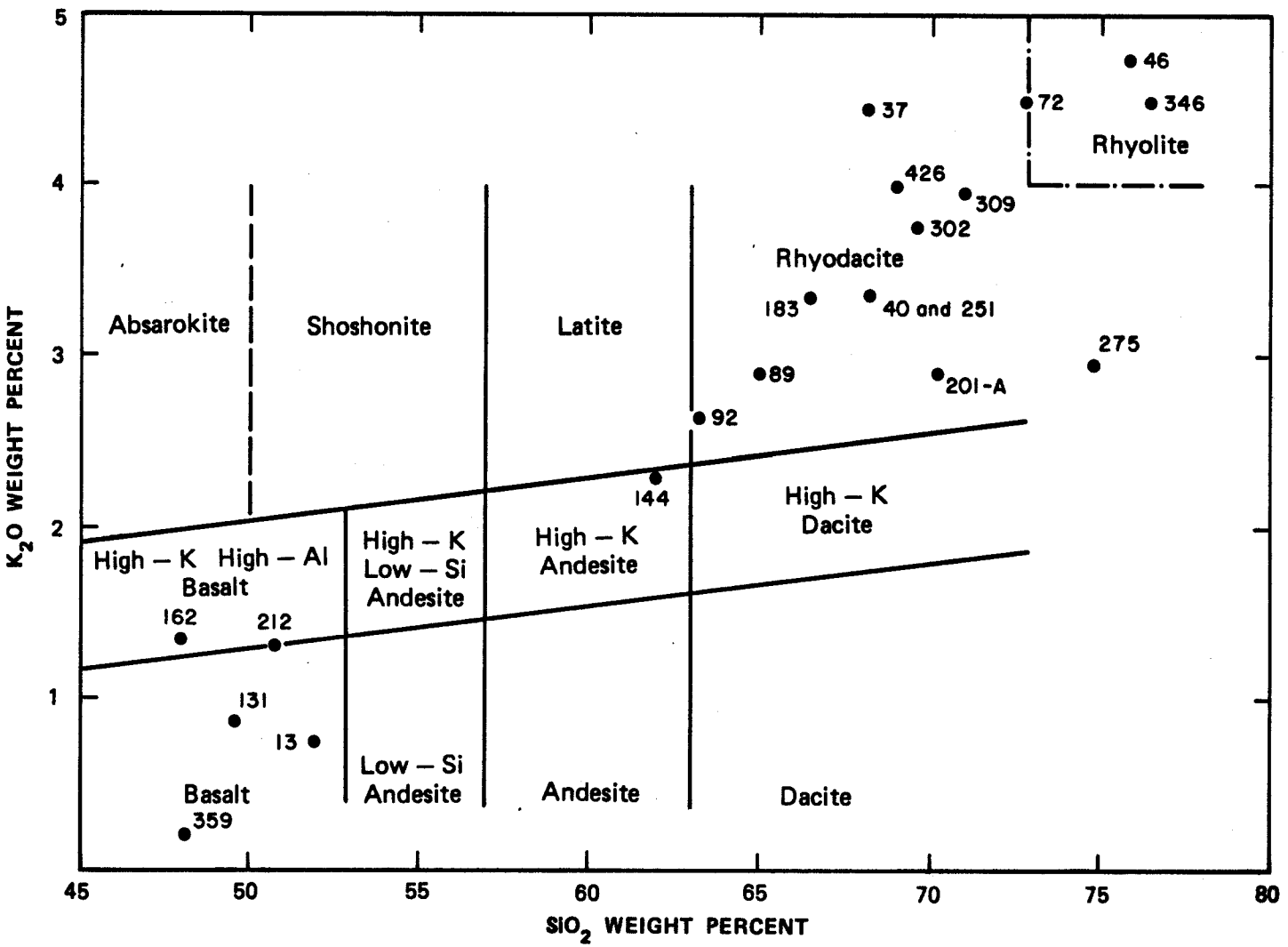

FIGURE 25. Chemical classification of the volcanic rocks from the Coyote Hills (diagram modified after Mackenzie and Chappell, 1972).

SiO_2. This author has added an additional field to the Mackenzie and Chappell scheme to discriminate between rocks of rhyolitic and rhyodacitic compositions. This additional field is defined by K_2O greater than 4 weight percent and SiO_2 greater than 73 weight percent (Taylor, 1978, personal communication). The primary rock types depicted by this scheme are basalts, rhyodacites, and rhyolites. Rocks between 53 and 63 weight percent SiO_2, with one exception, are absent.

The volcanic rocks of the Coyote Hills are calc-alkaline in character as indicated by the Peacock (1931) alkali-lime index (Figure 26). The alkali-lime index, defined as the SiO_2 value at which the sum of $Na_2O + K_2O$ equals the value of CaO, is 58 percent. This value is within the calc-alkaline boundaries of 56 to 61 weight percent SiO_2. However, the data are definitely skewed towards the lower, more alkaline boundary of 56 weight percent SiO_2. This calc-alkaline character of the rocks in the Coyote Hills is in agreement with the findings of other investigators who have worked in south-central Oregon (Avent, 1969; Walker, 1969a).

Analytical data for the major oxide elements, when plotted on a Harker (1909) variation diagram (Figure 27), do not, in general reflect simple curvilinear trends as depicted in many classic variation diagrams. Although scatter in the trends does exist, this can be attributed, in part, to variations in both the pre-and post-cooling histories, such as crystal fractionation (Kuno, 1968; Carmichael et al., 1974) or subsequent alteration regime(s). As expected, the trends of total Fe as FeO, MgO, CaO, and TiO_2 decrease with increasing

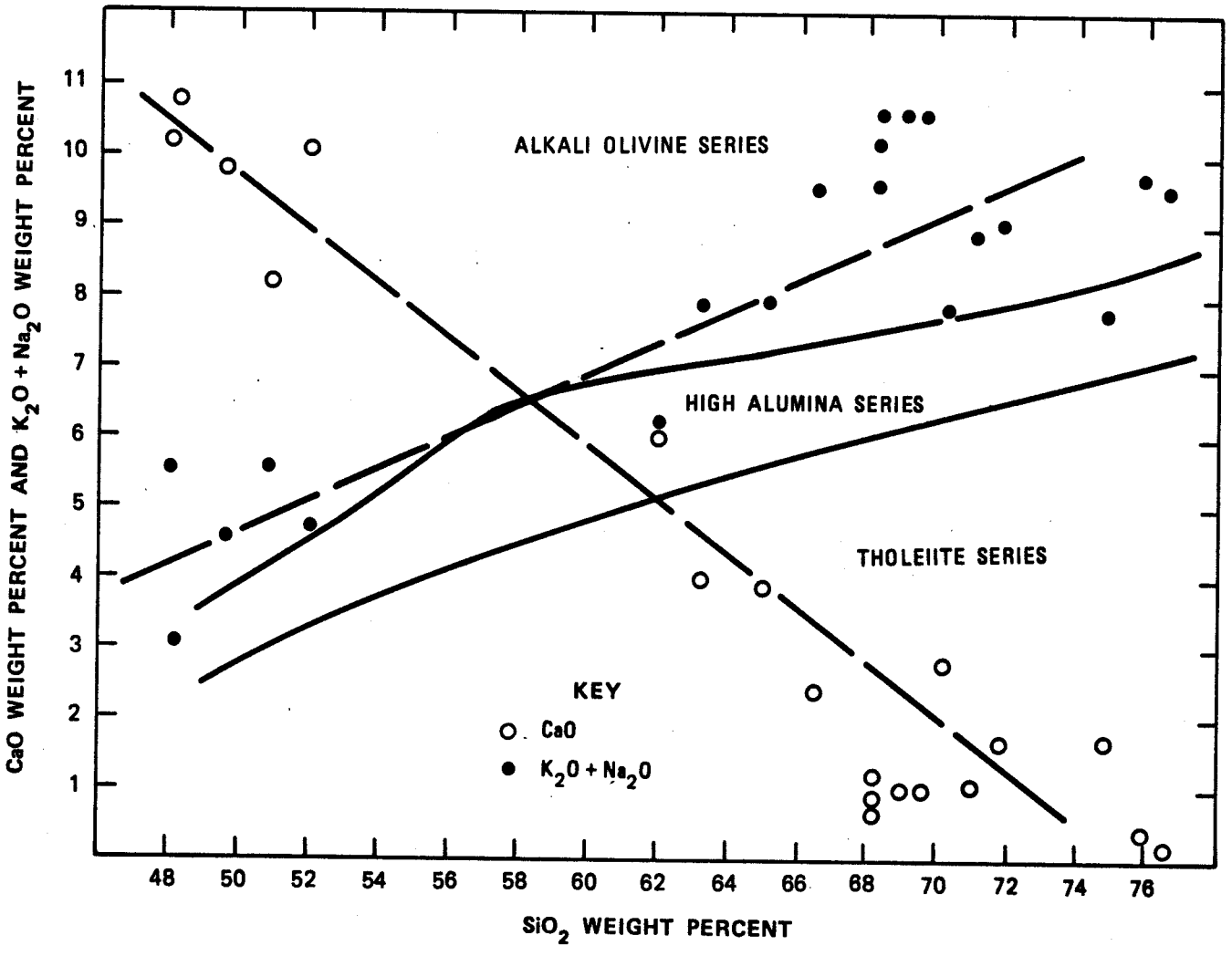

FIGURE 26. Total alkali plotted against total SiO_2 for the volcanic rocks of the Coyote Hills (after MacDonald and Katsura, 1964; Kuno, 1966). Alkali–lime index superimposed on figure (after Peacock, 1931).

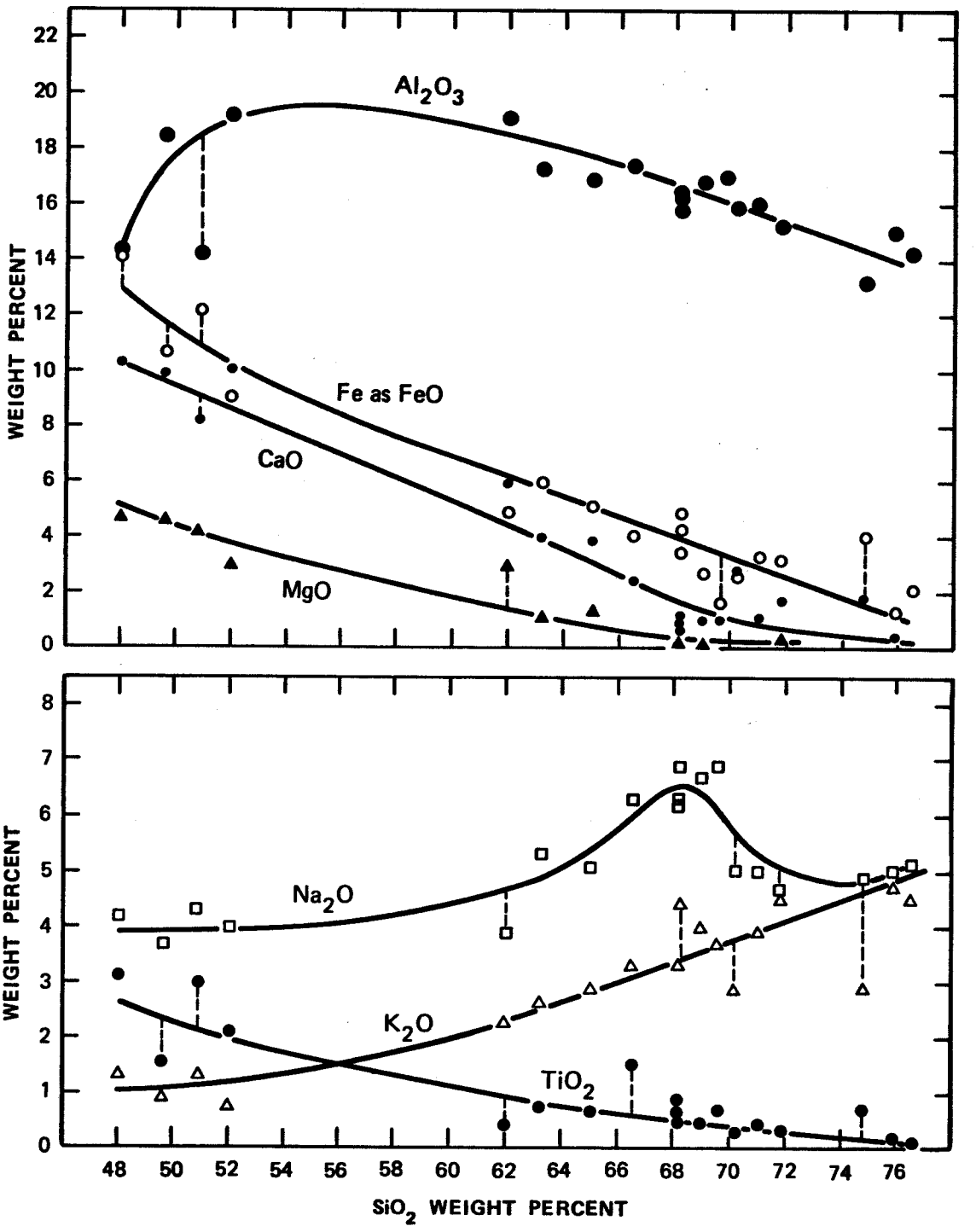

FIGURE 27. Variation diagram for the volcanic rocks of the Coyote Hills (after Harker, 1909).

weight percent SiO_2, whereas the trend of K_2O increases with increasing weight percent SiO_2. Although the data for Al_2O_3 and Na_2O follow expected trends, they are characterized by intervals of anomalous complexity. A gap in the concentration of oxides is present between 53 and 61 weight percent SiO_2. This silica gap includes that of Daly (1925) as described by Chayes (1963) of 53 to 57 weight percent SiO_2. This silica gap in the rocks of the Coyote Hills effectively separates the mafic from the more silicic rock types. Further chemical segregation is indicated by the TiO_2 distribution of the basalts. The older foundation basalts have a TiO_2 content of greater than 1.5 percent, whereas the basalts of post-Steens Basalt age have contents of less than 1.0 percent.

The decrease of Al_2O_3 in the range of 48 to 51 weight percent SiO_2 and the abrupt increase in Na_2O in the range of 66 to 70 weight percent SiO_2 argue against a genesis that involves only simple crystal fractionation. The low initial Al_2O_3 may represent the sporadic settling or rafting of basic plagioclase, i.e., anorthite - bytownite, or aluminous pyroxene in the magma chamber and subsequent extrusion to form the basalt porphyries that are found sporadically throughout the Coyote Hills and adjacent areas (Larson, 1965). The abnormally high Na_2O content may represent a rapid pulse of sanidine ($KAlSi_3O_8$) fractionation with a subsequent enrichment of Na_2O in the liquid portion of the magma. This would effectively result in the crystallization of anorthoclase ($KAlSi_3O_8$-$NaAlSi_3O_8$), which is a common constituent of the silicic flows in the Coyote Hills.

The silica gap that is present in igneous rocks of the Coyote

Hills may be explained as resulting from a discrimination in the eruptive process. For example, for any given temperature and pressure silicic magmas are more viscous than mafic magmas. Conversely, in the presence of volatiles, such as water, viscosity may decrease in the fractionation sequence of basalt through rhyolite because of increasing volatile content. Thus, intermediate magmas may actually be more viscous than mafic or silicic magmas, and they may not reach the surface during the eruptive cycle. A bimodal distribution of lavas, but not magmas, would result from this process (Le Maitre, 1968). An alternate explanation for the apparent silica gap would be an inadequate representation of samples.

The high TiO_2 and less so FeO content of four of the five basalts analyzed would result from a magma with a high oxygen fugacity. This high oxygen content (pressure) would promote the early crystallization of titanium-rich magnetite and/or ilmenite. A high magnetite/ilmenite content (0.5 - 2.0%) was noted both in the field (magnetic attraction) and in petrographic examination.

Chemically, the most primordial rocks found in the Coyote Hills are calc-alkaline alkali-olivine basalts (80%) and high alumina basalts (20%). In terms of their normative compositions, they are alkali basalts (ne and ol normative) and olivine tholeiites (hy and ol normative). The more evolved silicic rocks in the Coyote Hills are also calc-alkaline. They are primarily metaluminus ($Al_2O_3 < CaO + Na_2O + K_2O$ and $Al_2O_3 > Na_2O + K_2O$). Thus, they are somewhat anorthite normative and oversaturated with SiO_2 and contain greater than 10 percent quartz. Na_2O exceeds K_2O and CaO by an average

ratio of 1:1.8 and 1:7.5, for the alkali-olivine and high alumina basalts, respectively. The average Al_2O_3 percent is 15.2 with normative corundum present in two samples of rhyodacite and one sample of rhyolite.

PETROGENESIS

The differentiation trends representative of the rocks from the Coyote Hills are depicted on AFM and NKC ternary diagrams (Figures 28 and 29 respectively). Disregarding the data point representing a post-Coyote Hills era basalt flow (#359), the trends approximate the calc-alkaline line of Nockolds and Allen (1953). On both diagrams it is evident that the distribution of data is bimodal in character. This pattern and the relative compactness of the data points imply the occurrence of two major magmatic events. The bimodal nature of the rocks (see Figure 25) further substantiates this hypothesis.

These two major groups can be subjectively partitioned into five to six subgroups. The relative distance between these subgroups is interpreted to represent unspecified periods of time during evolvement of the initial parental magma, and subsequent derivative magmas. Each of the subgroups, or batches of magma, undoubtedly acquired individual chemical and mineralogical signatures in its history due to variations in crystal fractionation, contamination, magma mixing, and rates of emplacement.

Based on the chemical analyses of four rock samples from the foundation group, the most primitive lithologies found in the Coyote Hills are the calc-alkaline alkali-olivine basalts. In terms of normative minerals, three of the four samples are alkali basalts (ne and ol), whereas the fourth sample is an olivine tholeiite (hy and ol). Analyses of 19 pre-Steens Basalt rocks indicate that these volcanics from the Coyote Hills are of a continental sodic alkali lineage. The average value of K_2O:Na_2O add K_2O/Na_2O for these rocks

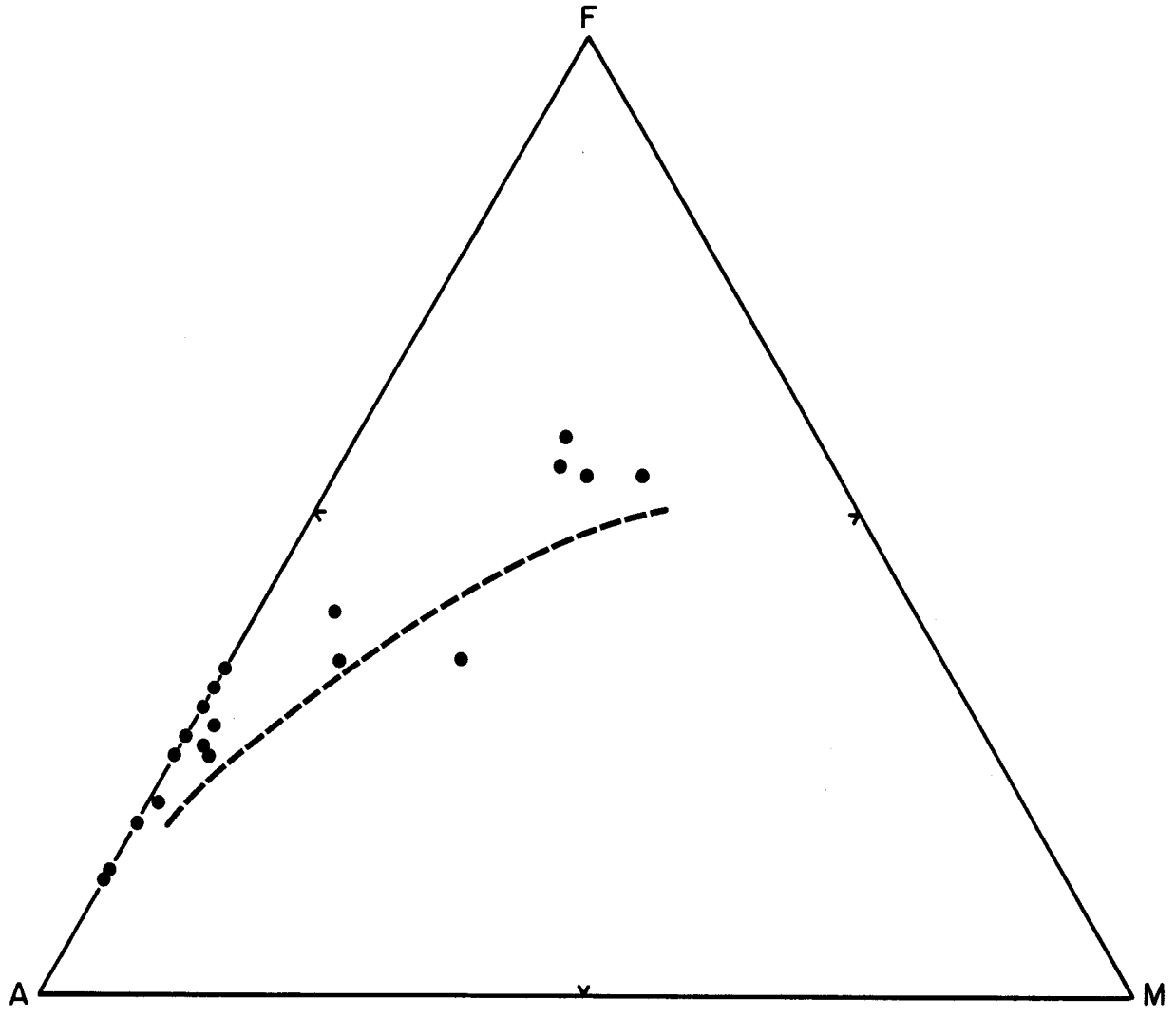

FIGURE 28. Ternary AFM diagram for the igneous rocks of the Coyote Hills. Calc-alkaline fractionation trend of Nockolds and Allen (1953) superimposed on diagram.

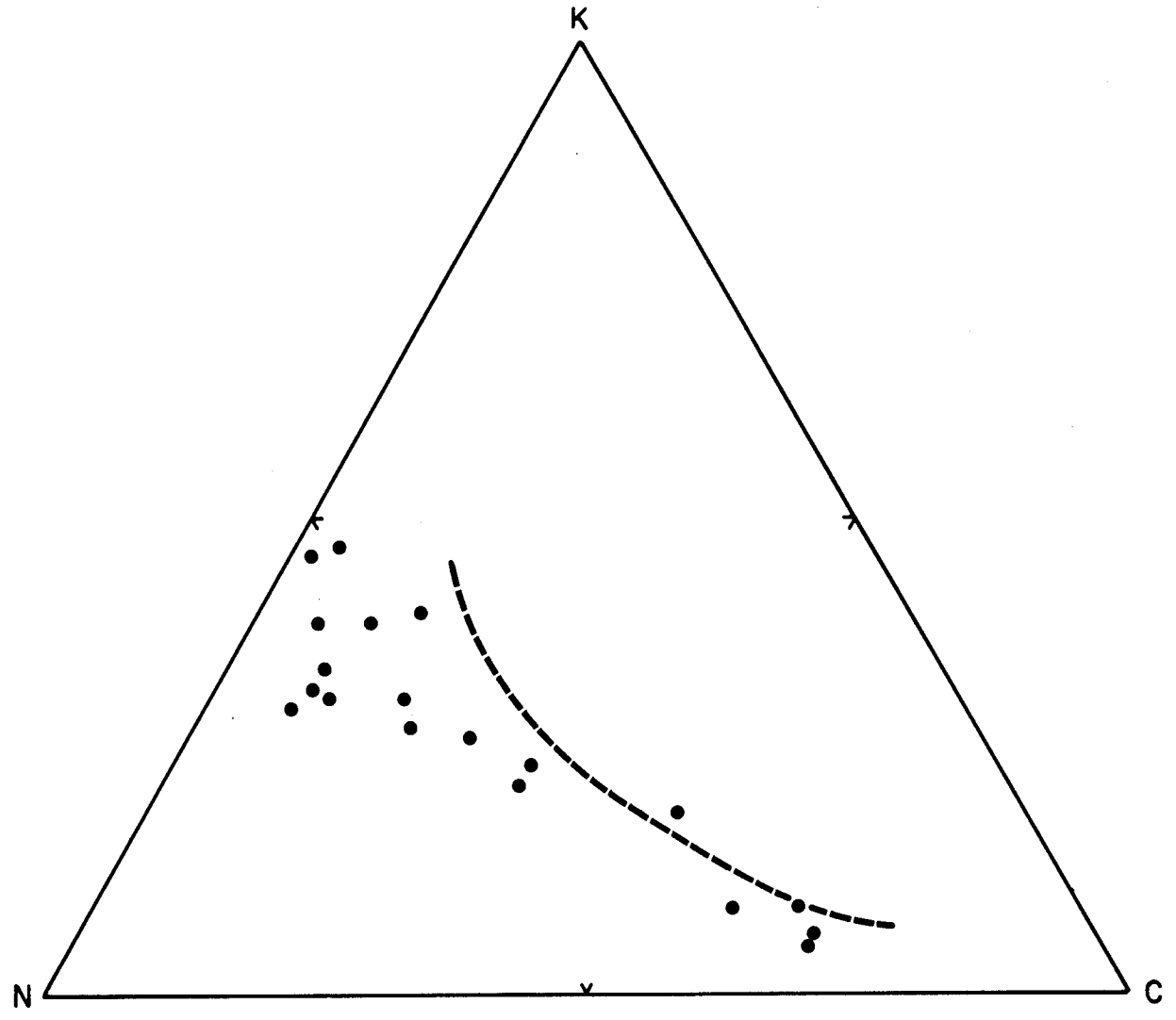

FIGURE 29. Ternary NKC diagram for the igneous rocks of the Coyote Hills. Calc-alkaline fractionation trend of Nockolds and Allen (1953) superimposed on diagram.

is 1:1.8 and 0.55, respectively. The upper value for continental and sodic alkali rocks is 1:2 (Wilkinson, 1974) and 0.5 (Carmichael et al., 1974), respectively.

The fractionation of an olivine-rich, hypersthene-normative, tholeiitic parental magma is dominated by separation of aluminous orthpyroxene ± sub-calcic augite at pressures corresponding to 35 to 70 km depth (Green and Ringwood, 1967a,b). This crystallization of aluminous orthopyroxene from an olivine tholeiitic parental magma results in a decrease in silica and an increase in alkalies in the liquid portion of the magma, and produces a nepheline-normative alkali-olivine basalt magma. Alternatively, partial melting, in the range of 20 to 30 percent, of upper mantle material at depths between 35 to 70 km will yield a residual olivine + aluminous orthopyroxene ± aluminous clinopyroxene and a liquid of alkali-olivine basalt composition (Green and Ringwood, 1968).

Theoretical results in conjunction with high pressure and temperature experiments in basalt and ultramafic materials, both natural and theoretical, are consistent with a depth of origin for alkali basalts approximating the depth of the Mohorovicic discontinuity (Green and Ringwood, 1967) or slightly deeper into the upper mantle (Carmichael et al., 1974).

Alkali basalt provinces are found in areas of high heat flow such as Japan, eastern Australia, and western United States. This spatial geographic-geologic association and the associated high-temperature related features in these areas may indicate a relatively shallow depth of origin compatible with partial melting. The Basin

and Range Province of the western United States is characterized by numerous temperature related anomalies; for example, a relatively thin crust, 28 to 35 km; high temperature gradient, 700 to 1000°C at a depth of 30 km in contrast to 400 to 600°C in the eastern United States; subdued magnetic anomalies; and an accuentuated low velocity zone such as in the asthenosphere (Thompson and Burke, 1974).

The association of calc-alkaline magmas with consuming plate margins is well demonstrated (Kuno, 1966). Furthermore, it is generally accepted that partial melting of mantle or oceanic crustal rocks at depth along subduction zones generates these calc-alkaline magmas (Dickinson, 1968; Green and Ringwood, 1968; Dewey and Horsfield, 1970). The composition of the igneous rocks produced along subduction zones has been shown to vary systematically with respect to both depth to the Benioff Zone, and distance to the trench (Dickinson and Haterton, 1967). However, because such chemical variations are not constant in magnitude with increasing distance from the trench, conclusions concerning the position of the Benioff Zone in the area of the Coyote Hills cannot be derived from these data.

ECONOMIC GEOLOGY

The unincorporated Lost Cabin Mining District (also known as either the Coyote Hill, Camp Loftus, or Windy Hollow Districts) was located on a gold prospect reportedly discovered by the Loftus Brothers in 1906. Shortly thereafter, there was a small prospecting and claim-staking rush in the area. However, interest in the gold potential of this area rapidly declined as available records indicate a complete absence of production.

In 1934, activity in the district increased slightly when Mr. Art Champion recognized the presence of the mineral cinnabar. However, the mercury prospects were not brought into production until 1941-1943. Conflicting reports indicate that between three and seven flasks of mercury were produced at a tenor of 0.15-0.95 percent.

Activity within the district has been dormant since the mid 1940's up until 1978, when a major mining company initiated an integrated exploration program. In contrast to the earlier activities, their target was not gold veins or mercury deposits, but rather large tonnage and low-grade deposits of either base or precious metals.

The area deemed as having the greatest potential for economic mineralization is located in secs. 10-15, and 23 T.35S., R.23E. This area is delineated by a large (13 plus square kilometers) amoeboid-shaped zone of argillic alteration (see Plate 3). Within this zone are anomalous occurrences of both base and precious metals, primarily in the $E\frac{1}{2}$ sec. 15 and the $W\frac{1}{2}$ sec. 14, T.35S., R.23E. Hereafter, this area will be refereed to as the core area of the district.

Although vein gold was the primary precious metal sought by the early prospectors, the veinlets and disseminations present in this district are better classified as epithermal base metal sulfides due to the much larger quantities of these metals. The base metals are chiefly mercury and iron, with subordinate amounts of molybdenum, copper, lead and zinc. They are the principal metallic components of the host sulfide mineral phases that are cinnabar, pyrite, molybdenite (?), chalcopyrite(?), galena(?), and sphalerite(?), respectively. However, molybdenite, chalcopyrite, galena and spalerite were not observed in the field. Thus, it is possible that these metallic components, Mo, Cu, Pb, and Zn, detected as trace elements, are present as solid solution metals in other mineral phases. In general, deposits of the base metal sulfides are found as veins or as disseminations that are spatially associated with and peripheral to much larger mesothermal/epithermal deposits (porphyry-type) of similar mineralogy and metal content.

The veins in this district are typically less than 0.3 centimeters in width and thus will be referred to as veinlets. The dominant trend of these veinlets is northwest, although a subordinate northeast-trend is present. These trends mimic the structural grain of this area. Locally, especially in the core area, the density of the veinlets increases and forms a veinlet controlled stockwork pattern. The contact between the host rock and veinlets is sharp. Small open spaces in the center of the veinlets are not uncommon, and open-space filling and/or crustification are the dominant mineral textures. Typically, the veinlets are composed of mineral crusts, particularly of silica which are

duplicated on both walls and thus render the vein symmetrical. Where vugs and cavities are present in the veinlets small crystals of terminated quartz are present. Frequently, subhedral crystals of pyrite are spaced between the quartz euhedra. These minerals and textures are typical of tensional epithermal environments.

Zonations of vein minerals are not readily apparent due to the paucity of minerals other than quartz and pyrite. This is not unusual as prominent metal zoning is usually not well developed in vein deposits (Stanton, 1972). The absence of such zonations are possible because the veins are such efficient plumbing systems that the fluids are rapidly flushed through before they can fully equilibrate to the rapidly changing chemical and physical conditions of the environment. Furthermore, a poorly defined zonation can be obscured as a consequence of the three-dimensional configuration of the hydrothermal system. Nonetheless, a weak zonation can be demonstrated to exist with respect to the core area and the larger overall area of hydrothermal alteration.

Pyrite, a moderately high temperature mineral, is present as a paragenetically early sulfide phase with major concentrations in the core area. In contrast, cinnabar, a low temperature mineral is present both in the core area, but topographically higher than the major pyrite concentration ans as a discontinuous halo encompassing the larger area of alteration. The ratio of anomalous to non-anomalous trace element values for Mo, Ag, and Hg increase towards the core area whereas those for Cu, Pb, and Zn increases outward in the opposite direction. In addition, field observations show that the density of veinlets, disseminated pyrite and cinnabar, and the ratio of pyrite to quartz in veins

increases towards the core area.

Mineralogy

Three generations of hydrothermal quartz are present in the zone of alteration. Quantitatively, quartz is the most abundant mineral in the veinlets, and it is volumetrically larger than all other minerals combined.

Finely crystalline quartz appears to have been the earliest mineral formed, as deduced from its marginal position in the veins adjoining the country rock. A paragenetically later occurrence is present in small vugs and cavities as minute terminated crystals of quartz. The paragenetically latest occurrence of this mineral is in the form of fine-grained amorphous silica referred to as opalite. These opalized zones are caused by the replacement of the volcanic rocks by silica, which results in an admixture of chalcedony and opal. These opalized zones are found overlying anomalous concentrations of mercury where they form small discontinuous semi-tabular lenses. Thus, it is apparent that silica was an important component of mineralization throughout the duration of hydrothermal activity.

Pyrite is the most ubiquitous and easily observed sulfide in the area of alteration. It is present both as a replacement mineral in the form of subhedral to euhedral dissmenated grains in the country rock and as subhedral crystals in open space vein-fillings. Pyrite is not preferentially associated with other minerals except quartz. It is far more abundant as disseminations outside of the core area

than within. However, as the core area is approached the abundance of disseminated pyrite decreases slightly with respect to vein pyrite.

Deposition of disseminated pyrite was initiated early in the paragenetic history of this area. However, as vein fillings of pyrite are present only between terminated crystals of quartz, this mode of formation is either contemporaneous with or slightly later than the second generation of quartz mineralization.

Cinnabar is the least abundant observed sulfide phase although its presence is nearly as ubiquitous as that of pyrite. It is present primarily in trace amounts as fine disseminations throughout the area of alteration. The greatest concentration of cinnabar is located in and adjacent to two abandoned workings in the NW$\frac{1}{4}$, SW$\frac{1}{4}$, sec. 14 and the S$\frac{1}{2}$, NE$\frac{1}{4}$, sec. 15, T.35S., R.23E.

Gold is reported from veins in and adjacent to Miners Draw (Brooks and Ramp, 1968). The reported occurrence is in small irregular fractures filled with seams of clay, limonite, and locally quartz. Small amounts of gold and copper oxide are said to have been found in some of the seams. Neither gold nor copper oxide was observed either megascopically or microscopically. However, both were detected in trace element analyses of soil and rock (see Plate 3, overlay E and A).

The northwest orientation of the anomalous gold values is coincident with the predominant structural grain that is expressed as faults, fractures, and veinlets. This dominant orientation of the anomalous values and the reported mode of formation would indicate that the gold and copper mineralization is paragenetically earlier than that of cinnabar and probably is contemporaneous with the period

of quartz-pyrite deposition.

Cinnabar was not found in the quartz-pyrite veinlets. However, a fracture containing minor amounts of cinnabar was found that cross-cut a quartz-pyrite veinlet. On this basis, cinnabar is considered to paragenetically post-date the formation of pyrite.

Alteration

Country rocks that border mineral deposits of hydrothermal origin are generally altered by the fluids which transported and deposited the ores. The alteration assemblages produced are dependent on: 1) lithology of the original rock; 2) the composition of the invading fluids; and 3) the temperature and pressure at which the reactions took place. In addition, the physical and thermal environments generally vary as a function of distance from the center of mineralization to produce a zonal distribution of the alteration products. Four broad types of alteration mineral assemblages are recognized. From high to relatively low temperatures, these are the potassic, phyllic, argillic, and proplylitic assemblages, respectively (Creasy, 1959; Burnham, 1962; Meyer and Hemley, 1967).

Argillic alteration was the only type of the four found in the Coyote Hills. The intensity of argillic alteration varies from low and sporadic, through moderate, to high intensity. Intensity is a subjective classification which in this case is based on the visual interpretation of the amount of leaching and bleaching.

One thin section was submitted to Dr. Sid Williams, Phelps Dodge Corporation, Douglas, Arizona, for visual examination to determine

the clay type. Smectite (montmorillonite) was the clay identified. Other alteration minerals present are limonite (hisingerite, canbyite), jarosite, opal, and minor amounts of sericite, most of which presumably formed by supergene process.

The sample collected for clay identification was taken from an area characterized by anomalous mercury, and thus concentrations of it may or may not be representative of this alteration type. Kaolinite is typically present in and adjacent to the core area of a mineralized deposit with montmorillonite located around the periphery. Moreover, kaolinite is a more common derivative of silicic rocks, oxidizing environments, and wet climates. Whereas, in contrast, montmorillonite typically forms in rocks containing calcic feldspars and ferro-magnesian minerals, alkaline environments, areas of poor drainage, and semi-arid climates (Blanchard, 1968).

Montmorillonite can be accounted for in that the climate in and adjacent to the Coyote Hills has been semi-arid since Pleistocene time and the ore solutions containing mercury are thought to have been of an alkaline sulfide affinity (Krauskopf, 1951). However, with the relatively large quantities of pyrite available for supergene oxidation and subsequent development of acid surface waters, kaolnite might be expected to be the dominant clay type. In all, probably both clay groups coexist within the area of alteration.

Trace Element Geochemistry

Differentiation has been defined as a process whereby more than one rock type is formed from a common homogenous magma. This may be accomplished either by fractional crystallization or by fractional

melting. Differentiation leads not only to changes in the abundance of major and minor elements, but also to those of the trace elements as well (Levinson, 1974).

Because of the large degree of inferred differentiation between the various igneous rock types (basalt through rhyolite), of the Coyote Hills, the trace element values for Cu, Mo, Pb, Zn, Au, and Hg from 18 unaltered rock samples were plotted versus SiO_2 content to determine if there were any significant systematic variations among the different phases (Figure 30). As the result of this test were inconclusive, it may be concluded that either the extent of differentiation between the rock phases was insufficient to produce significant changes in the background concentrations of the trace elements, or that approximately similar quantities of the trace elements contained in the oxides, silicates, and sulfides were included in each phase of magma differentiation. (Newhouse, 1936).

In addition to the above trace element-silica variation diagrams, the mean and range of values for these trace elements versus those from other common rock types are given for comparison in Table 15. The mean values for Cu, Pb, and Zn through the rock sequence dacite-rhyolite, in the Coyote Hills, are slightly higher, whereas the converse is true for those through the sequence basalt-andesite. In contrast, the mean values for Mo and Hg are approximately comparable to those for all rock types from the other localities. Comparative values for Au are lacking from the literature.

It is apparent that if any of the various rock types could be categorized as a potential source rock, then the dacites would be

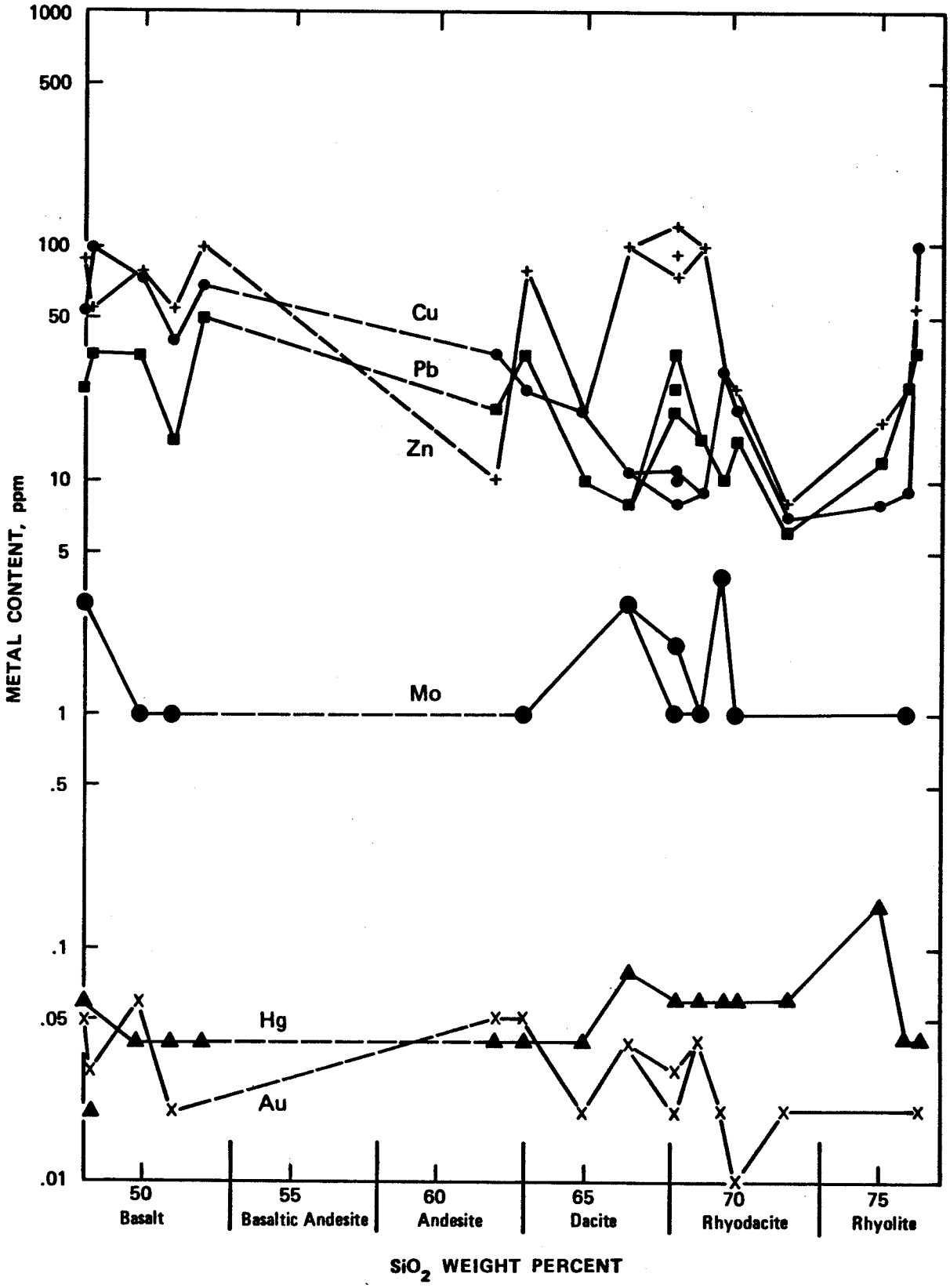

FIGURE 30. Variation diagram showing concentrations of related trace elements versus rock type.

Table 15

Comparison of Selected Trace Element Values from Major Rock Types Found in the Coyote Hills with Other Rock Types

Coyote Hills

	Basalt mean	Basalt range	Andesite	Dacite mean	Dacite range	Rhyodacite mean	Rhyodacite range	Rhyolite mean	Rhyolite range
Cu	68	40-100	35	18	11-25	11	7-20	9	8-11
Mo	1.4	.9-3	.9	1.6	.9-3	1.2	.9-2	1	.9-1
Pb	32	15-50	20	11	8-15	19	6-35	19	12-25
Zn	76	55-100	10	46	18-100	68	8-105	39	18-75
Au	.03	.009-.06	.05	.04	.02-.05	.35	.3-.4	.4	.3-.6
Hg	.04	.02-.06	.04	.05	.04-.08	.06	.06	.08	.04-.16
No. of samples	5		1	3		6		3	

Other Rocks

	Ave. Basalt	Ave. Andesite	Dacite	Rhyolite	Obsidian
Cu	87	44	10	5	5
Mo	1.5	4(?)	1*	1.3*	--
Pb	6	40	20	25	10
Zn	105	85	40	40	30
Au	--	--	--	--	--
Hg	.09	--	.08*	.08*	--
No. of samples	1	25	1	1	1

Source:

Ave. Basalt -Thompson et al., 1970

Ave. Andesite-Thompson et al., 1970

Dacite Jack & Carmichael, 1969

Rhyolite Jack & Carmichael, 1969

Obsidian Jack & Carmichael, 1969

* Turekian & Wedepahl, 1961

All values - ppm

ranked first followed closely by the rhyodacites and rhyolites on the basis of contained metals.

In addition to the trace element analyses of rock samples, those for Cu, Mo, Pb, Zn, Au, and Hg were also determined for 45 samples of soil. The frequency distribution of the trace elements from the soil samples were determined by plotting on probability graph paper the metal concentrations versus the cumulative frequencies of the samples (Figure 31). The diagramatic expression for a simple lognormal sample population plotted on probability graph paper is a straight line. (Lepeltier, 1969). However, it has been shown from theoretical considerations and practical applications that plots derived from cumulative frequencies of multi-modal or complex populations are characteristically expressed as two or more distinct line segments. The breaks in slope, or inflections, between line segments define the separated sample populations (Tennant and White, 1959, Lepeltier, 1969).

Well-defined inflections for each metal are portrayed in Figure 31. The presence of such inflections suggests a minimum of two populations, or complex populations, of metals in the samples. The lower populations represent syngenetic or primary magmatic content of these metals, whereas the upper populations defined by positive or negative inflections are suggestive of an epigenetic overprint of hydrothermal metallization.

As the values protrayed on the frequency distribution diagram are from soil samples, and not from rock samples, complicating inhomogenetics may influence the cumulative frequency curves. Factors contributing to these inhomogenetics are: (1) all samples collected

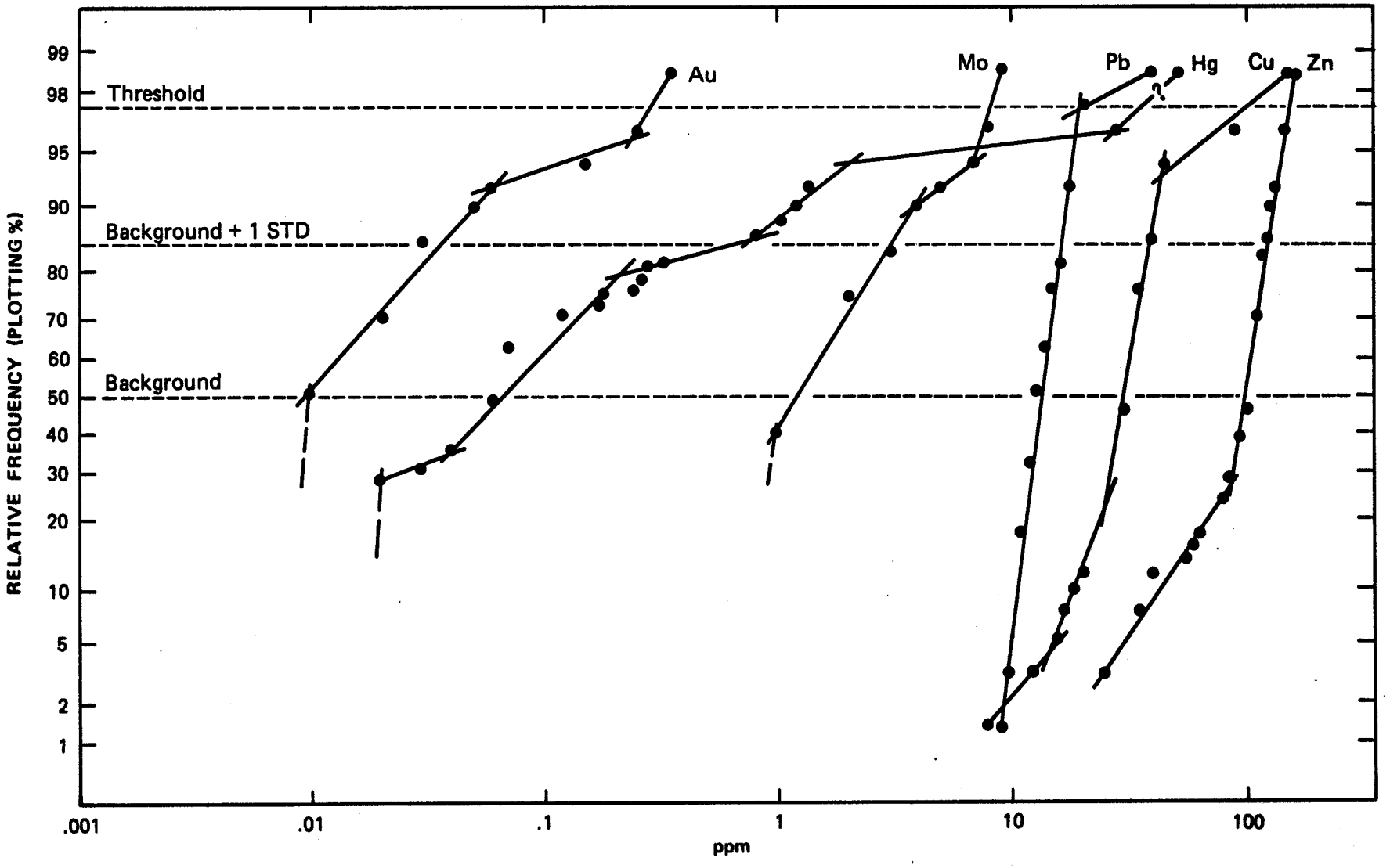

FIGURE 31. Cumulative frequency distribution of Cu, Mo, Pb, Zn, Au, and Hg.

are within the area of alteration; (2) all sample sites are geographic points based on a grid pattern(305 m. by 305 m.) and not on geology; i.e., lithologic units, and (3) no consideration was given to the impact of either primary syngenetic/epigenetic or post-epignetic processes of mineralization. Thus, this sample survey and the manipulation of this basic data can be considered to be only a raw evaluation of the potential of this area.

The Cu, Pb, and Zn data from both the soil and rock samples were plotted on ternary diagrams (Figure 32 and 33) by recalculating the metal contents to 100 percent. In addition, the values from the soil samples are also distingiished on the basis of total metal content. The distribution of values in the soil sample shows a strong preference for the zinc apex, with very minor preference for the zinc-copper boundary. This indicates that of the base metals inferred to be present, copper and especially lead are present in only minor amounts.

The distribution of total metal concentrations for the soil samples is of interest. Background values designated by the symbol ▲ tend to be concentrated around an average value denoted by a solid circle. This point represents 23.6 percent copper, 10 percent lead and 66.4 percent zinc. The clustering of low total metal concentrations represents the final ratios and syngenetic concentrations of copper, lead and zinc in the magma when it crystallized. However, hydrothermal addition of metals did not occur as a constant ratio. Thus, the plotted points of the higher epigenetic values migrate differentially outward from the central field of low syngenetic values. This effect

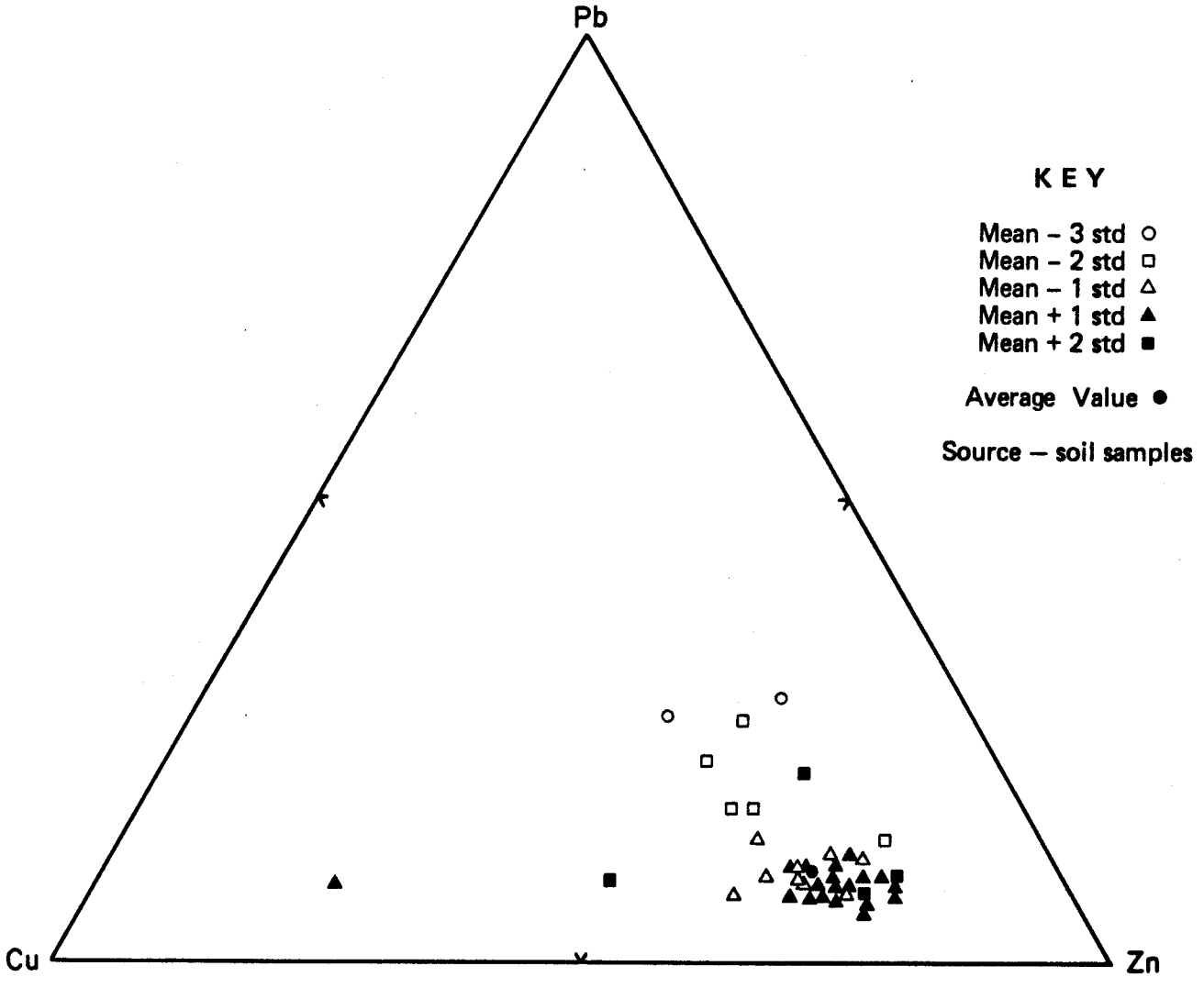

FIGURE 32. Cu–Pb–Zn ternary diagram.

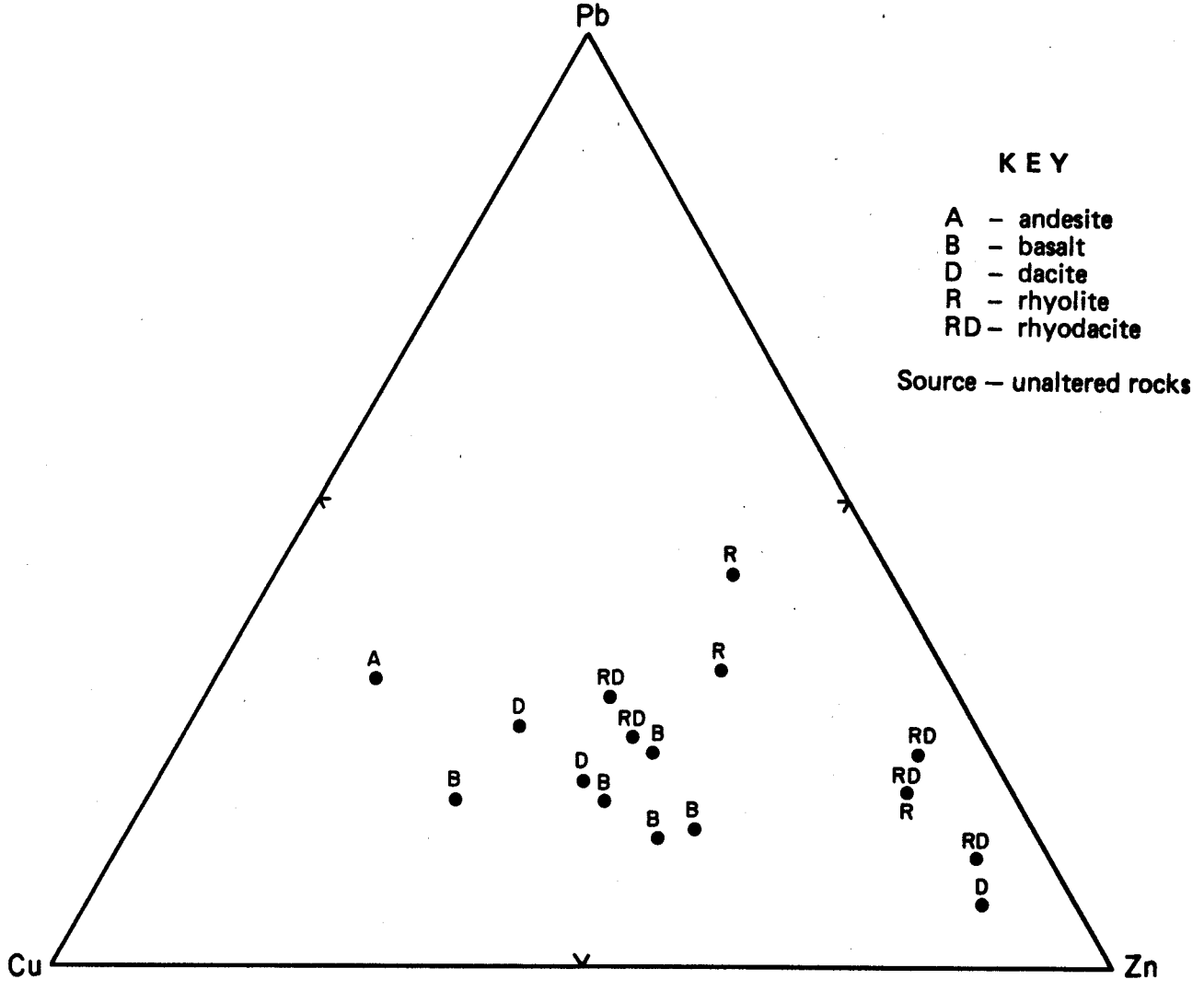

FIGURE 33. Cu–Pb–Zn ternary diagram.

was probably produced and controlled by thermal zoning and by local physical and chemical environments which favored the deposition of one metal in preference to the others. The values denoted by the symbols □ and o are inferred to represent excessively oxidized and leached samples. This population has resulted from low temperature surfical processes whereby the original and introduced metal contents were leached, notably copper and zinc versus lead, to values of less than normal background.

A comparison of the soil and rock sample ternary diagrams (Figure 32 and 33) fingerprints the magma phases via rock types that were most likely responsible for partitioning and expulsion of these three metals, and probably silica, iron, molybdenum, gold, and mercury, into the host rocks. As previously indicated, the dacites followed by rhyodacite and rhyolite appear to be the apparent source phases.

The spatila distributions, of values for Cu, Mo, Pb, Zn, Au, and Hg in soil samples are shown on Plate 3 by overlays A through F. The values for selected rock samples are shown on overlay G. The geochemical data are confined to the primary area of visible alteration, overlay H. Because of the single point distribution pattern, the values were not contoured but, rather, expressed in the form of simple statistics. The overlays for both rock and soil samples show that the metals are both laterally zoned with respect to the core area and are structurally controlled. A vertical zonation, if present at all, is not evident from the distribution of these data.

Values for copper and gold exhibit a primary northwest-southeast trend which is coincident with the dominant structural grain in this

area. The lead values mimic both the dominant (northwest-southeast) and subordinate (northeast-southwest) structural trends. In addition, they form an apparent weak peripheral zone or partial halo southeast of the core area. The spatial distribution of the zinc values is nebulous at best. The zinc values appear to be zoned radially outward from the core area and they overlap those of lead and bridge the gap between the core area and the lead halo to the southeast.

Anomalous values of molybdenum and mercury are primarily restricted to the core area. This spatial coincidence of molybdenum and mercury in a core area is atypical of normal patterns of metal zoning (Emmons, 1936). However, if the zones of vertical metallization, or thermal haloes, were extremely compressed, then the anomalous values for mercury, which are "topographically" slightly higher than those for molybdenum and displaced somewhat to the east, may be considered as forming a supra-ore halo.

A few rock samples collected within the area of alteration were analyzed for Cu, Mo, Pb, An, Au, Ag, and Hg. Except for zinc, all of the metals analyzed have slightly anomalous expressions within the core area.

The mobility of ore metals in a transporting hydrothermal fluid generally follows the sequence Hg-Ag-Pb-Zn-Cu-Au-Sn-Mo-Ni-Fe-Co in order of decreasing mobility (Barnes and Czomanske, 1971; Krauskopf, 1967). Mobility is not related to the solubilities of the ore minerals, but rather to the stabilities of the metals as chloride or sulfide complexes (Stanton, 1972). The northwest to southeast zoning of molybdenum, zinc, and lead duplicates a portion of this ideal sequence.

Copper and gold may, in fact, follow the dominant scheme. However, the structural overprint has obscured this relationship. Mercury is here considered to be paragenetically the latest sulfide to have formed and to spatially occupy the highest, although collapsed, zone of metallization. Thus, mercury also can be considered to follow this ideal scheme of metal zonation.

It is apparent that the core area, area of alteration, and zones of metallization are only partly defined and are not concentric to each other. Nonetheless, this apparent asymmetric spatial relationship may be due to the combined effects of topography and the inferred three-dimensional asymmetry of the core area. The core area is inferred to have the geometric shape of a modified funnel. It is further assumed that the northern boundary plunges at a much steeper angle than the southern boundary. The implications of this three dimensional configuration are apparent, causing a compression of gradients to the north, and can account for the zones of alteration and metallization observed at the surface.

Economic Potential of the Coyote Hills

Mineralization in the Coyote Hills is defined by the following characteristics: (1) a large area comprising 13 square kilometers of hydrothermally altered rocks; (2) alteration dominated exclusively by the argillic type; (3) a core area, partially defined in the $E\frac{1}{2}$ sec. 15 and the $W\frac{1}{2}$ sec. 14, T.35S., R.23E., open to the north and northwest and containing anomalous concentrations of epithermal Mo, Au, and Hg; and (4) quartz-pyrite veinlets prevalent within the core,

whereas disseminated pyrite is present both in and peripheral to the core.

Although the district has not been active since 1943, it is highly unlikely that the potential of this area has been fully appreciated until recently. Factors such as mineralization thus far encountered is spotty, low grade, and restricted to veinlets and fractures, and that the ratio of barren ground to mineralization is quite high, would tend to discourage development in this area. However, a thorough evaluation program was initiated by a major mining company during 1978 which culminated in an ongoing drilling program in 1979.

A much expanded soil and rock sampling program in conjunction with electromagnetic geophysical methods, especially induced polarization or spontaneous potential, would be of great use in evaluating the area for large vein or disseminated type deposits containing both base and precious metals. The area recommended for evaluation would commence with the core and radiate outward with special emphasis given to the terrain north and northwest of the core.

GEOLOGIC SUMMARY

The first significant geologic event recorded in the rocks of the Coyote Hills was the eruption of predominately andesitic volcanism of the late Eocene to early Oligocene Lower Andesite formation. Eruptions of hornblende-bearing andesite and aphanitic basalt flows were interspersed with the deposition of laharic breccias, conglomerates, tuffaceous sandstones and lithic wackes. After an intervening hiatus of several million years, these initial high energy depositional regimes associated with an inferred growing andesitic vent complex(es), gave way to a less energetic, but locally significant, basaltic volcanism to form the Upper Basalt formation of middle to early late Oligocene age. This event consisted predominatly of basaltic andesite flows, flow breccia, and minor amounts of epiclastic derivatives that formed a large shield volcano.

A spectrum of multi-phase silicic volcanism and comagmatic subvolcanic plutonism commenced after a relatively short hiatus. This event, the Coyote Hills rhyolite of late Oligocene to early Miocene age, was emplaced in and upon the shield volcano. Products of this magmatic episode vary in compostion from dacite to rhyolite, and include lava flows, tuffs, dikes, volcanic plugs, laccoliths, a flow dome complex, and a quartz monzonite hypabyssal intrusion. Slight resurgence of a volcanic plug located in sec. 4, T.35S., R.23E. resulted in a series of lahars that formed in the erosionally breached northern side of the shield volcano.

A conjugate northwest and northeast-trending fault and fracture system formed after emplacement of the Coyote Hills rhyolite and as early as late Oligocene to early Miocene time. Discontinuous movement continued along these structural trends to early Pliocene time.

During the late stages of rhyolitic volcanism hydrothermal fluids of magmatic origin ascended along favorable structures in the approximate center of the Coyote Hills. These fluids altered the surrounding country rocks and deposited minor quantities of epithermal gold-silver-copper-molybdenum (?)-lead(?), and zinc (?) in association with veins of pyrite and quartz and disseminations of pyrite and mercury. The association of mineralization with silicic volcanism in time and space leads to the conclusion that the magmatic and hydrothermal processes were genetically related.

Voluminous eruptions of the Steens Basalt lapped onto the lower slopes of the shield volcano during middle Miocene time and buried a complexly eroded topographic surface. Normal faults developed after extrusion of the Steens Basalt but apparently did not appreciably offset the overlying Miocene Plush tuff.

During late middle to early late Miocene time an extensive but locally noncontinuous unit of tuffs and tuffaceous sediments was deposited in a predominately fluival-lacustrine environment. This unit, the Plush tuff, blankets the Steens Basalt and laps onto the shield volcano. Volcanism continued with the eruption of thin widespread flows of olivine basalt. This unit, the Upper basalt overlies the Plush tuff and locally lapped onto the shield volcano.

Continued erosion of the Coyote Hills and adjacent highlands produced a pediment surface to the south and east which was later mantled by a veneer of gravels. Formation of this pediment surface, upon which the major streams of this area have been incised, predates the contemporary period of rejuvenation.

Erosion of the Coyote Hills to date has exposed only the high level portions of the altered and mineralized hydrothermal system. Several lines of evidence suggest that the system continues with depth below the currently exposed level of erosion. These include: 1) the irregular occurrences of high grade alteration which are coincident with zones of structural weakenss; 2) trace element zonation of copper, molybdenum, lead, and zinc than indicate that most of the district lies within the outermost lead-zinc halo; and 3) the partial definition of a core area within the district. In addition, geological and geochemical evidence that includes rock type, alteration patterns, and mineral and trace element zonations, collectively suggest that a large vein or disseminated type deposit containing both base and precious metals may be present at depth.

BIBLIOGRAPHY

Abbott, M.J., 1969, Petrology of the Nadewar Volcano, N.S.W., Australia: Contrib. Mineral. Petrol., J. 20, pp. 115-134.

Albers, J.P., and Robertson, J.F., 1961, Geology and ore deposits of East Shasta Copper-Zinc District Shasta County, California: U.S. Geol. Survey Prof. Paper 338, 107 p.

Anderson, A.L., 1930, The geology and mineral resources of the region about Orofino, Idaho: Idaho Bur. Mines Geol. Pamph., no. 34, 63 p.

Atwater, T., 1970, Implications of plate tectonics for the Cenozoic tectonic evolution of Western North America: Geol. Soc. America Bull., v. 81, no. 12, p. 3513-3535.

Avent, J.C., 1969, Correlation of the Steens-Columbia River Basalts-some tectonic and petrogenetic implications; in Proc. of the 2nd Columbia River Basalt Symposium, Eastern Washington State College Press, p. 135-156.

Bailey, E.B., Thomas, H.H., et al., 1924, Tertiary and post-Tertiary geology of Mull, Lock Aline, and Oban: Geol. Survey Scotland, Mem., 445 p.

Baksi, A.K., York, D., and Watkins, N.D., 1967 Age of the Steens Mountain Geomagnetic Polarity Transition: Jour. Geophys. Research v. 72, p. 6299-6308.

Barnes, H.L., and Czomanske, G.K., 1971 Solubilities and transport of ore minerals, in Geochemistry of hydro thermal ore deposits, Holt, Rinehart, and Winston, Inc., p. 334-381.

Beaulieu, J.D., 1972, Geologic Formations of Eastern Oregon: Oregon Dept. of Geol. and Min. Ind., Bull 73.

Bentley, E.B., 1970, the glacial Geomorphology of Steens Mountain, Oregon: M.S. thesis, Univ. of Oregon, published.

Berg, J.W., and Baker, C.D., 1963, Oregon earthquakes, 1841-1958: Seismological Society of America Bull., v. 53, p. 95-108.

Blackwelder, E., 1914, A summary of the Orogenic Epochs in the geologic history of North America: Jour. of Geology, v. 22, p. 633-654.

Blanchard, R., 1968, interpretation of leeched outcrops: Nevada Bureau of Mines, Bull., 66, 196 p.

Brooks, H.C., 1963, Quicksilver in Oregon: Oregon Dept. Geol. and Min. Indus. Bull. 55, 223 p.

_____, and Ramp, Len, 1968, Gold and Silver in Oregon: Oregon Dept. Geol. and Min. Ind., Bull. 61, 338 p.

Burchfiel, B.C., and Davis, G.D., 1972, Structural framework and evolution of the southern part of the Coredilleran Orogen, Western United States: Am. Jour. of Sci., v. 272, p. 97-118.

Burnham, C.W., 1962, Facies and types of hydrothermal alteration: Econ. Geol., v. 57, p. 768-784.

Carmichael, I.S.E., Turner, F.J., and Verhoogen, J., 1974, Igneous Petrology: McGraw-Hill Book Company, 739 p.

Chayes, F., 1963, Relative abundance of intermediate members of the oceanic basalt-trachyte association: Jour. Geophys. Res., v. 68, p. 1519-1534.

Climatological Data, U.S. Dept. of Commerce, National Oceanic & Atmospheric Administration, Environmental Data Service Annual Summary for 1967-1976.

Cook, E.F., 1954, Mining geology of the Seven Devils region: Idaho Bur. Mines and Geol. Pamph., no. 97, 22 p.

Couch, R., and Johnson, S., 1968, the Warner Valley Earthquake Sequence: Ore. Dept. of Geol. and Min. Inds., in the Ore Bin, v. 30, no. 10, p. 191-212.

Crandall, P.H., 1965, The glacial history of Western Washington and Oregon: in Quaternary of the United States, Princeton Univ. Press, 922 p.

Creasy, S.C., 1959, Some phase relations in hydrothermally altered rocks of porphyry copper deposits: Econ. Geol, v. 54, p. 351-373.

Daly, R.A., 1925, The geology of Ascension Island: Proc. Am. Acad. Arts Sci., 60, p. 1-80.

Dewey, J.F., Horsfield, B., 1970, Plate tectonics, orogeny, and continental growth: Nature, v. 255, p. 521-525.

Dicken, S.N., 1965, Oregon Geography: Eugene, Oregon, 4th ed., 127 p.

Dickinson, W.R., 1968, Circum-Pacific andesite types: Jour. Geophys. Res., v. 73, p. 2261-2269.

_____, and Haterton, 1967, Andesitic volcanism and seismicity around the Pacific: Science, v. 157, no. 3790, p. 801-803.

Donath, F.A., 1962, Analysis of Basin-Range structure, south-central Oregon: Geol. Soc. of America Bull., v. 73, p. 1-16.

Duffield, W.A., and McKee, E.H., 1974, Tertiary stratigraphy and timing of Basin and Range Faulting of the Warner Mountains, northeast California: Geol. Soc. America Abs. with Prog., v. 6, no. 3, p. 168.

Emmons, W.H., 1936, Hypogene zoning in metalliferous lodes: 16th Internat. Geol. Cong. Rept., v. 1, p. 417-432.

Enlows, H.E., and Parker, D.J., 1972, Geochronology of the Clarno igneous activity in the Mitchell Quadrangle, Wheeler County, Oregon: Ore. Dept. of Geol and Min. Inds., in the Ore Bin, v. 34, p. 104-110.

Evernden, J.F., and James, G.T., 1964, K-Ar dates and the Tertiary floras of North America: American Jour. of Sci., v. 262, pp. 945-974.

_____, et al., 1964, K-Ar dates and the Cenozoic Manmalion Chronology of North America: American Journal of Sci., v. 262, p. 145-198.

Fisher, R.V., 1961, Proposed classifications of volcanoclastic sediments and rocks: Geol. Soc. America Bull., v. 72, p. 1409-1414.

_____, 1966, Rocks composed of volcanic fragments and their classification: Earth Science Review, v. 1, p. 287-298.

Franklin, J.F., and Durness, C.T., 1973, Natural vegetation of Washington and Oregon: USDA Forest Service Technical Report, PNW-8, 417 p.

Fuller, R.E., 1931, the geomorphology and volcanic sequence of Steens Mountain in southeastern Oregon: Univ. of Wash. Pub. in Geology, v. 3, no. 1, p. 1-130.

_____, and Waters, A.C., 1929, the nature and origin of the horst and graben structure of southern Oregon: Jour. of Geol., v. 37, p. 204-238.

Green, D.H., and Ringwood, A.E., 1967, An experimental investigation of the gabbro to eclogite transformation and its petrological applications: Geochim. Cosmochim. Acta., v. 31, p. 767-833.

_____, and Ringwood, A.E., 1967, The genesis of basaltic magmas: Contrib. Mineral Petrol., v. 15, p. 103-190.

_____, and Ringwood, A.E., 1968, Genesis of the calc-alkaline igneous rock suite: Contrib. Mineral Petrol., v. 18, p. 105-162.

Greene, R.C., 1973, Petrology of the Welded tuff of Devine Canyon, southeastern Oregon: U.S. Geol. Survey Prof. Paper 797, 26 p.

_____, Walker, C.W., and Corcoran, R.E., 1972, Geologic map of the Burns Quadrangle, Oregon: U.S. Geol. Survey Misc. Geol. Inv. Map I-680.

Haddock, G.H., 1959, Geology of the Congor Peak Volcanic Area, Lake Co., Oregon: Washington State University M.S. Thesis, unpublished, 72 p.

Hamilton, W., 1963, Overlapping of Late Mesozoic Orogens in Western Idaho: Geol. Soc. American Bull., v. 74, p. 779-788.

_____, and Myers, W.B., 1966, Cenozoic tectonics of the Western United States: Reviews of Geophysics, v. 4, no. 4, p. 509-549.

Hamilton, D.L., and Anderson, C.M., 1967, Effects of water and oxygen pressures on the crystallization of basaltic magmas: in Basalts - The Poldervaart treatise on rocks of basaltic composition, v. 1, New York and London, Interscience Publishers, p. 446-482.

Hammit, J.W., 1976, Geology, petrology, and mineralization of the Paisley Mountains plutonic complex, Lake County, Oregon: M.S. Thesis, Oregon State University, Unpublished, 162 p.

Harker, 1904, The Tertiary igneous rocks of Skye: Geol. Survey of U.K. Mem. 1904, 481 p.

Harker, A., 1909, The Natural History of Igneous Rocks: Macmillian NY, 384 p.

Henyey, T.L., and Lee, T.C., 1976, Heat flow in Lake Tahoe, California Nevada, and the Sierra Nevada - Basin and Range transition: Geol. Soc. America Bull., v. 87, No. 8, p. 1179-1187.

Higgins, M.W., 1968, Newberry Caldera field trip: Oreg. Dept. Geol. Min. Ind., Bull. 62, p. 59-77.

Jack, R.N., and Carmichael, I.S.E., 1969, The chemical fingerprinting of acid volcanic rocks: Short Contributions to Calif. Geol., Special Rpt. 100, p. 17-31.

Jackson, K.C., 1970, Textbook of lithology: McGraw-Hill Book Company, 552 p.

Kistler, R.W., Evernden, J.F., and Shaw, H.R., 1971, Sierra Nevada plutonic cycle: Part 1; Origin of composite granitic batholiths: Geol. Soc. American Bull., v. 82, p. 853-868.

Krauskopf, K.B., 1951, Physical chemistry of quicksilver transportation in vein fluids: Econ. Geol., v. 46, p. 498-523.

_____, 1967, Introduction to geochemistry: McGraw-Hill Book Company, 721 p.

Kuno, H., 1965, Fractionation trends of Basaltic Magmas in lava flows: J. Petrology, v. 6, pt. Z, pp. 302-321.

_____, 1966, Laterial variation of basalt magma type across continental margins and island arcs: Bull. volc., v. 29, p. 195-222.

_____, 1968, Origin of andesite and its bearing on the island arc structure: Bull., volc., v. 32, p. 141-176.

_____, et al, 1957, Differentiation of Hawaiian Magmas: Jap. J. Geol. Geogr., v. 28, pp. 179-218.

Lanphere, M.A., Irwin, W.P., and Hotz, P.E., 1968, Isotopic age of the Nevada Orogeny and older plutonic and metamorphic events in the Klamath Mountains, California: Geol. Soc. of America Bull., v. 79, p. 1027-1052.

Larson, E.E., 1965, The structure, stratigraphy, and paleomagnetics of the Plush Area, southeastern Lake County, Oregon: Ph.D. dissertation, University of Colorado, Unpublished, 166 p.

Lawrence, R.D., 1976, Strike-slip faulting terminates the Basin and Range Province in Oregon: Geol. Soc. of America Bull., v. 87, p. 846-850.

Le Maitre, R.W., 1968, Chemical variation within and between volcanic rock series - A statistical approach: Jour. Petrol., v. 9, p. 220-252.

Leeman, W.P., and Rogers, J.J.W., 1970, Late Cenozoic Alkali-Olivine Basalts of the Basin-Range Province, U.S.A.: Contrib. Mineral. Petrol., v. 25, pp. 1-24.

Lepeltier, C. 1969, A simplified treatment of geochemical data by graphical representation: Econ. Geol, v. 64, p. 538-550.

Levinson, A. A., 1974, Introduction to exploration geology: Applied Publishing Ltd., 614 p.

Lipman, P.W., Prostka, H.J., and Christiansen, R.L., 1971, Evolving subduction in the Western United States, as interpreted from igneous rock: Geol. Soc. America, Abstr., v. 3, no. 2, p. 148.

Loney, R.A., 1968, Flow structure and composition of the southern coulee, Mono Craters, Calif. - a pumiceous rhyolite flow, in Coats, R.R., et al., Studies in volcanology: Geol. Soc. Am. Mem. 116, p. 415-440.

Lydon, P.A., 1968, Geology and lahars of the Tuscon Formation, Northern California: Geol. Soc. America Mem. 116, p. 441-475.

MacDonald, G.A., 1972, Volcanoes: Prentice-Hall, Inc., 510 p.

_____, and Katsura, T., 1964, Chemical compositions of Hawaiian lavas: Jour. Petrology, v. 5, pt. 1, p. 82-133.

MacKenzie, D.E. and Chappell, B.W., 1972 Shoshonite and calc-alkaline lavas from the highlands of Papua, New Guinea: Contr. Mineralogy and Petrology, v. 35, p. 50-62.

MacLeod, N.S., 1978, personal communication.

_____, Walker, G.W., and McKee, E.H., 1975, Geothermal significance of an eastward increase in age of upper Cenozoic rhyolitic domes in southeastern Oregon: Open-File Report (Preliminary) no. 75-348, 22 p.

McBirney, A.R., 1968, Petrochemistry of Cascade andesite volcanoes: Oreg. Dept. Geol. Min. Ind., Bull. 62, p. 101-107.

Manson, J., 1967, Geochemistry of basaltic rocks - major elements; in Basalts - the Poldervaart treatise on rocks of basaltic composition, v. 1; New York and London, Interscience Publishers, p. 215-269.

Merriam, J.C., 1901, A contribution to the geology of the John Day basin: Univ. of Calif. Pub. Bull. Dept. Geol. Sciences, v. 2, p. 269-314.

Meyer, C. and Hemley, J.J., 1967, Wall rock alteration; in Geochemistry of hydrothermal ore deposits; Holt, Rinehart and Winston, Inc. Inc., p. 167-235.

Muntzert, J.K., 1969, Geology and Mineral Deposits of the Brattain District, Lake County, Oregon: Oregon State University M.S. Thesis, unpublished, 72 p.

_____, and Field, C.W., 1909, Geology and mineral deposits of the Brattain district, Lake County, Oregon: Geol. Soc. America Spec. Paper 121, Abs. for 1968, p. 616-617.

Newhouse, W.H., 1936, Opaque oxides and sulfides in common igneous rocks: Geol. Soc. America Bull., v. 47, no. 1, p. 1-52.

Noble, D.C., et al., 1972, Highly differentiated subalkaline rhyolite from Glass Mountain, Mono County, Calif.: Geol. Soc. Am., Bull. v. 83, no. 4, p. 1179-1184.

Nockolds, S.R. and Allen, R., 1953, The geochemistry of some igneous rock series: Geochim et Cosmochim. Acta, U. 4, p. 105-142.

_____, 1954, Average chemical compositions of some igneous rocks: Geol. Soc. America Bull., v. 65, p. 1007-1032.

Nolan, T.B., 1943, The Basin and Range Province in Utah, Nevada, and

California: U.S. Geol. Survey, Professional Paper 197-D, 195 p.

Peacock, M.A., 1931, Classification of igneous rock series: Jour. Geol., v. 39, p. 54-67.

Peck, D.L., 1961, John Day Formation near Ashwood, north-central Oregon: U.S. Geol. Survey Prof. Paper 424-D, p. 153-156.

Peterson, N.V., 1959, Preliminary geology of the Lakeview Uranium Area, Oregon: Ore. Dept. of Geol. and Min. Inds., in the Ore Bin, v. 21, no. 2, p. 11-16.

_____, and McIntyre, J.R., 1970, The reconnaissance geology and mineral resource of eastern Klamath County and western Lake County, Oregon: Ore. Dept. of Geol. and Min. Industries Bull. 66, 70 p.

Piper, A.M., Robinson, T.W., and Park, C.F., Jr., 1939, Geology and ground-water resources of the Harney Basin, Oregon: U.S. Geol. Sur. Water-Supply Paper, no. 841 189 p.

Roberts, J.L., 1970, The intrusion of magma into brittle rocks: in Mechanisms of Igneous Intrusion, Gallery Press, Liverpool, 325 p.

Rock-Color Chart, 1979: Geol. Soc. Am., 10 p.

Russell, I.C., 1884, A geological reconnaissance in southern Oregon: U.S. Geol. Survey 4th Annual Report, p. 431-473.

Russell, I.C., 1903a, Preliminary report on artesian basins in southwestern Idaho and southeastern Oregon: U.S. Geol. Survey Water-Supply and Irrigation Paper, no. 78, 53 p.

_____, 1903b, Notes on the geology of wouthwestern Idaho and southeastern Oregon: U.S. Geological Survey Bull. 217, 83 p.

Russell, R.J., 1928, Basin Range structure and stratigraphy of the Warner Range, northeastern California: Univ. of Calif. Pub. in Geol. Sciences, v. 17, p. 387-496.

Scholz, C.H., Barazongi, M., and Skar, M.L., 1971, Late Cenozoic evolving of the Great Basin, western United States as an ensialic inter-arc basin: Geol. Soc. America Bull., v. 82, no. 11, p. 2979-2990.

Smith, R.L., and Bailey, R.A., 1968, Resurgent cauldrons; in Studies in Volcanology: Geol. Soc. America Mem. 116, p. 613-662.

Smith, W.D., 1927, Contribution to the geology of south-eastern Oregon (Steens and Pueblo Mountains): Jour. of Geol., v. 35, p. 421-440.

Stanton, R.L., 1972, Ore Petrology: McGraw-Hill Book Company, 713 p.

Streckeisen, A., 1967, in Hyndman, D.W., 1972, Petrology of igneous and metamorphic rocks: McGraw-Hill Book Company, 533 p.

Taubenneck, W.H., 1966, An evaluation of tectonic rotation in the Pacific Northwest: Jour. of Geophy. Research, v. 71, no. 8, p. 2113-2120.

Taylor, E.M., 1977, personal communication.

_____, 1978, personal communication.

Tennant, C.B., and White, M.L., 1959, Study of the distribution of some geochemical data: Econ. Geol., v. 54, p. 1281-1290.

Thompson, G., Bookston, D.C., and Pasley, S.M., 1970, Trace element data for USGS reference silicate rocks: Chem. Geol., v. 5, no. 3, p. 215-221.

Thompson, G.A., and Burke, D.B., 1974, Regional geophysics of the Basin and Range Province: Annu. Rev. Earth and Plant. Sci., v. 2, p. 213-238.

Travis, P., and Gettings, M., 1974, in Wells, R.E., 1975, The geology of the Drake Peak Rhyolite Complex and the surrounding area, Lake Co., Oregon: M.S., Thesis, University of Oregon, unpublished, p. 13.

Turekian, K.K., and Wedepahl, K.H., 1961, Distribution of the elements in some units of the earth's crust: Geol. Soc. of America Bull. 72, no. 2, p. 175-192.

Varne, R., 1968, The Petrology of Moroto Mountain, Eastern Uganda, and the Origin of Nephelinites: J. Petrol., v. 9, pp. 169-190.

Walker, G.W., 1960, Age and correlation of some unnamed volcanic rocks in south-central Oregon: U.S. Geol. Survey Prof. Paper 400-B, p. 298-300.

_____, 1963, Reconnaissance geologic map of the eastern half of the Klamath Falls (AMS) Quadrangle, Lake and Klamath Counties, Oregon: Mineral Investigations Field Studies Map MF 260.

_____, 1965, and Repenning, C.A., 1965, Reconnaissance geologic map of the Adel Quadrangle, Lake, Harney, and Molheur Counties, Oregon: Misc. Geol. Investigations Map I-446.

_____, 1969a, Some comparisons of basalts of southeast Oregon with those of the Columbia River Group: in Proceedings of the Second Columbia River Basalt Symposium, Eastern Washington State College, p. 223-238.

_____, 1969b, Possible fissure vent for a Pliocene ash-flow tuff, Buzzard Creek area, Harney County, Oregon: U.S. Geol. Survey Professional Paper 630-C, p. C8-C17.

_____, Dalrymple, G.B., and Lanphere, M.A., 1974, Index to potassium-argon ages of Cenozoic volcanic rocks of Oregon: U.S. Geol. Survey Misc. Field Studies, Map MF-S69.

_____, 1977, Geologic map of Oregon east of the 121st Meridian: Miscellaneous Investigations Series Map I-902.

Waring, G.A., 1908, Geology and water resources of a portion of south-central Oregon: U.S. Geol. Survey Water Supply-Paper, no. 220, 86 p.

_____, 1909, Geology and water resources of the Harney Basin region, Oregon: U.S. Geol. Survey Water Supply-Paper, no. 231, 93 p.

Waters, A.C., 1961, Stratigraphic and lithologic variations in the Columbia River Basalt: Am. Jour. Sci., . 259, pp. 583-611.

Watkins, N.D., 1963, Behavior of the geomagnetic field during the Miocene Period in south-eastern Oregon: Nature, v. 197, no. 4863, p. 126-128.

_____, 1964, Structural implications of paleomagnetism in Miocene lavas of north-eastern Oregon, south-eastern Washington, and west-central Idaho: Nature, v. 203, no. 4947, p. 830-832.

_____, 1965, A palaeomagnetic observation of Miocene geomagnetic secular variation in Oregon: Nature, v. 206, no. 4987, p. 879-882.

_____, and Larsen, E.E., 1966, Combined paleomagnetic and petrological delineation of faults in Miocene basalts of Oregon: Geol. Mog., v. 103, no. 2, p. 166-178.

_____, and Baksi, A.K., 1974, Magnetstratigraphy and oroclinal folding of the Columbia River, Steens and Owyhee Basalts in Oregon, Washington, and Idaho: Am. Jour. Sci., v. 274, p. 148-189.

Wells, R.E., 1975, The geology of the Drake Peak rhyolite Complex and the surrounding area, Lake County, Oregon: M.S. Thesis, University of Oregon, unpublished, 130 p.

Wilkinson, JPG., 1974, The mineralogy and petrology of alkali basaltic rocks (With comments); in the Alkaline Rocks, Petrology and Petrology, p. 67-95: John, Wiley & Sons, London.

Williams, H., 1932, The history and character of volcanic domes: Univ. Calif. Berkeley Pub. Bull. Dept. Geol. Sci., v. 21, p. 51-46.

Wilson, J.T., 1970, Some possible effects if North America has

overridden part of the East Pacific Rise: Geol. Soc. America Abs. with Programs, v. 2, no. 7, p. 722-723.

Zoback, M.L., and Thompson, G.A., 1978, Basin and range rifting in northern Nevada; clues from a mid-Miocene rift and its subsequent: Geology, v. 6, no. 2, p. 111-116.

APPENDICES

APPENDIX 1

Concentrations of Cu, Mo, Pb, Zn, Au, and Hg in Soil Samples

Sample No.	Cu ppm	Mo ppm	Pb ppm	Zn ppm	Au ppm	Hg ppb
1	30	1	13	80	.01	60
2	35	1	11	90	.02	80
3	110	2	13	35	.03	280
3A	90	3	18	100	.15	800
4	40	2	18	110	.03	20
5	25	1	14	80	.01	40
6	30	2	11	100	.01	20
7	30	1	14	110	.02	20
8	25	5	14	110	.01	20
8A	30	2	13	95	.03	20
9	25	2	15	95	.06	20
9A	35	3	40	115	.35	1200
10	45	1	18	115	.03	20
11	35	1	15	125	.01	20
12	35	2	18	115	.02	320
12A	30	2	15	115	.01	175
13	30	2	18	110	.01	40
14	35	2	14	115	.01	20
15	30	1	16	100	.01	20
16	35	1	20	160	.01	20
17	35	1	14	90	.03	20
18	30	1	15	65	.01	180
19	35	1	12	80	.01	260
20	45	2	12	110	.01	1040
21	8	4	13	25	.02	240
21A	17	9	20	40	.25	2000
22	45	1	10	85	.03	60
23	35	2	13	90	.05	60
23A	16	8	15	25	.02	>50000
23B	25	3	16	55	.02	28000
24	35	1	11	110	.01	1360
25	35	2	9	120	.01	80
26	30	2	11	110	.01	120
27	40	1	12	110	.01	80
28	35	2	13	125	.01	140
29	30	4	15	135	.02	80
30	20	7	12	40	.01	60
31	13	4	11	60	.01	140
32	40	1	12	115	.01	80
33	35	1	13	110	.01	30
34	35	2	12	130	.01	80
35	25	2	11	110	.02	60
36	30	1	11	110	.02	20
36A	19	3	15	35	.03	80
37	40	1	12	145	.05	60

APPENDIX 2

Concentrations of Cu, Mo, Pb, Zn, Au, Ag, and Hg in Selected Rock Samples

Sample No.	Cu ppm	Mo ppm	Pb ppm	Zn ppm	Au ppm	Ag ppm	Hg ppm
A	30	4	10	30	.01	.4	60
B	8	3	35	8	.01	.3	39200
C	12	5	45	10	.09	4.1	2800
D	9	1	30	8	.03	.4	2400
E	10	1	40	8	.04	1.0	640
F	16	1	12	30	.02	.5	60